UNIVERSITEIT VAN PRETORIA
UNIVERSITY OF PRETORIA
YUNIBESITHI YA PRETORIA

Estimating a dynamically adjusted carrying capacity output for Limpopo Province using seasonal forecasts and remote sensing products

by

P. Maluleke

Student number 14448778

Supervisor: Prof. Willem A. Landman

Co-supervisor: Dr. Johan Malherbe & Dr. Emma Archer van Garderen

Dissertation submitted

in partial fulfilment of the requirements

for the degree of Master of Science

in the Department of Geography, Geoinformatics and Meteorology,

Faculty of Natural & Agricultural Sciences,

University of Pretoria,

South Africa

May 2016

Declaration

I understand what plagiarism is and I am aware of the University's policy in this regard.

I declare that this dissertation is my own original work. Where other people's work has been used (either from a printed source, Internet or any other source), this has been properly acknowledged and referenced in accordance with departmental requirements.

I have not used work previously produced by another student or any other person to hand in as my own.

I have not allowed, and will not allow, anyone to copy my work with the intention of passing it off as his or her own work.

SIGNATURE STUDENT:

SIGNATURE SUPERVISOR:

Abstract

Rangelands are extremely important for livestock grazing purposes in South Africa. Grazing should thus be regulated in order to conserve grass, shrubs and trees thereby ensuring sustainability of rangelands. In South Africa, the existing national grazing capacity estimate was developed in 1993 and updated in 2005 using National Oceanic and Atmospheric Administration Advanced Very High Resolution Radiometer (NOAA-AVHRR) satellite data. Largely due to changing land use practices (as well as changing data availability), there exists a clear need to create a new estimate, making use of current available data. For Limpopo, a province shown to be prone to recent land degradation, droughts and climate change, developing such an updated carrying capacity (CC) product (adjusted monthly according to monitoring data and seasonal forecasts) may help support more sustainable agricultural practices.

The main objectives of the study are to update current CC products and to create deviation maps from CC for several years with relevant data. For estimation of the CC product, input data have included Satellite Pour l'Observation de la Terre (SPOT) VEGETATION Dry Matter Productivity (DMP), vegetation map of 2009 and downscaled coupled model data (ECHAM4.5–MOM3-DC2). A tree density product of 2003, observed rainfall and secondary ground truth data are also used.

Study results show that Remote Sensing (RS) and Geographic Information System (GIS) technology, Earth Observation System (EOS) data and products, climate data and ground truth data are successfully used in a series of steps, processes with modelling to ultimately estimate grazing capacity. It is clear that rainfall is a primary determinant of DMP. The Coupled General Circulation Model (CGCM) shows that the December-January-February (DJF) rainfall season is important as a predictor season for the November through to April (NDJFMA) DMP growing season for the Limpopo Province. This model can discriminate high and low DMP (and GC) seasons. This study shows that the DMP product can, with certain assumptions, be used as a proxy for grass biomass. There is a strong drive towards the application of seasonal forecasts in agriculture. This project demonstrates the development of a tailored forecast, an avenue that should be explored in enhancing relevance of forecasts to agricultural production.

Keywords: DMP, Remote Sensing, Limpopo Province, grazing capacity, seasonal forecasts

Preface

Carrying capacity is a vital component in agricultural activities particularly for a province like Limpopo because of its varying climate. Limpopo Province capitalizes on subsistence farming including livestock and crop production. However, some of these subsistence farming practices are not sustainable and can negatively influence the rangelands resulting in land degradation. This dissertation addresses land degradation, its causes and possible remediation methods. The latter is accomplished by estimating grazing capacity; which looks at cattle farming and stocking rates. The grazing capacity concept implies that livestock should be allocated grazing land according to the land's productivity and capacity. It is important to note that the words "carrying capacity" and "grazing capacity" are used interchangeably throughout the dissertation.

There is an indisputable link between precipitation and agricultural production and it is therefore crucial to analyze this relationship for the purpose of this study. In order to study this relationship, seasonal forecasts along with satellite data as well as field data are employed. The Limpopo Province experiences summer rainfall and high skill of predictability has been shown by coupled global circulation models.

The work done in this dissertation involves a fusion of modelling, downscaling of seasonal forecasts hindcasts to DMP data, GIS and RS technology. The hypothesis to be tested in this study is: "Is it possible to use seasonal forecasts and RS products to estimate a dynamically adjusted carrying capacity output for Limpopo Province?" The following steps will be followed to address the hypothesis:

(i) Obtain satellite data and products
(ii) Collect available field data for selected sites for the Limpopo Province
(iii) Obtain historical rainfall data and seasonal hindcasts
(iv) Create grazing capacity maps based on data for several historical years
(v) Estimate grazing capacity anomalies

There are five chapters in this dissertation. In Chapter 1 an introduction to the carrying capacity concept in South Africa is given. Chapter 2 looks at the literature review covering the history of remote sensing and geographic information systems in the region, as well as seasonal forecasts and their varied application in the agricultural sector of South Africa. Lastly, current trends in the above mentioned subjects are also reviewed. The study area and data collection – types of products, tools, data sources, and application – are covered in Chapter 3. Chapter 4 covers the results and processes towards estimating grazing capacity. Then finally, Chapter 5 brings the

dissertation to a closure by giving conclusions, thereby giving recommendations that can further improve grazing capacity, seasonal forecasts, operational use and livestock productivity.

Acknowledgements

- I would like to thank the Agricultural Research Council - Institute for Soil, Climate and Water (ARC-ISCW) and National Research Foundation (NRF) for funding – and supplying resources for my studies
- I would also like to thank ARC-ISCW staff, especially Agrometeorology and Geoinformation for their advice on data sources and technical issues
- I would also like to thank Catherine Odendaal-Etsebeth for generously sharing the office space with me and giving me support
- I would like to acknowledge my supervisor Prof. Willem Landman for his continued guidance and keen supervision
- I would like to express my thanks to Dr. Johan Malherbe and Dr. Emma Archer for their relentless support by giving input and assistance
- I would also like to appreciate all the contribution from Dr. Tony Palmer, Agricultural Research Council - Range and Forage Institute for his advice on methodology and supplying biomass field data
- I would also like to thank the following people for providing me with field data:
    - Dr. Izak Smit for Kruger National Park biomass data
    - Mr. Christians Harmse for Rustenburg and Molopo biomass data
    - Mr. Jock McMillan for Mabula biomass data
- My family, for their consistent love and faith in me
- My best friend, Nhlamulo Chauke for always listening to all my moaning and cheering me on

“Commitment means crashing through all quitting points.”

Ed Young.

Contents

List of figures

List of tables

List of appendices

Abbreviations, Acronyms and Glossary

ARC-ISCW	Agricultural Research Council - Institute for Soil, Climate and Water, Pretoria, South Africa
ARC-RFI	Agricultural Research Council - Range and Forage Institute, Grahamstown, South Africa
ANPP	Above Ground Net Primary Production
AVHRR	Advanced Very High Resolution Radiometer
CC	Carrying Capacity
CSIR	Council for Scientific and Industrial Research, South Africa
CCA	Canonical Correlation Analysis
CCAM	Conformal-Cubic Atmospheric Model
CGCM	Coupled General Circulation Model
CPC	Climate Prediction Center, USA
CPT	Climate Predictability Tool
dbf	database files
Dekad	10-day period encompassing either the first ten days (1^{st}-10^{th}), second ten days (11^{th}-20^{th}), or remainder of the month (21^{st}-end)
DJF	December-January-February
DMP	Dry Matter Productivity
ECHAM4.5 –MOM3-DC2	The Global Climate Model developed by the Max Planck Institute for Meteorology, one of the research organizations of the Max Planck Society. It was created by modifying global forecast models developed by European Centre for Medium-Range Weather Forecasts (ECMWF) to be used for climate research
ECMWF	European Centre for Medium-Range Weather Forecasts
ERDAS	Earth Resources Data Analysis
EOS	Earth Observation System
EOTM	Earth Observatory Thematic Mapper
FMA	February-March-April
GC	Grazing Capacity
GCM	General Circulation Model
GDP	Gross Domestic Product
GIS	Geographic Information System
hPa	hectopascal is a standard measurement unit of pressure

IRI	International Research Institute for Climate and Society
JFM	January-February-March
KNP	Kruger National Park
Landsat	NASA's Landsat satellite
MLR	Multiple Linear Regression
MODIS	Moderate Resolution Imaging Spectroradiometer
MSS	Multispectral Mapper
MVC	Maximum Normalized Difference Vegetation Index Value Composite
NASA	National Aeronautics and Space Administration, USA
NDJ	November-December-January
NDJFMA	November-December-January-February-March-April
NDVI	Normalized Difference Vegetation Index
NGO	Non-governmental Organization
NOAA	National Oceanic and Atmospheric Administration
NPP	Net Primary Production
PAR	Photosynthetically Active Radiation
PCR	Principal Components Regression
PROBA-V	is a small satellite on board the French SPOT-4 and SPOT-5 Earth Observation missions
RFE	Rainfall Estimate product
RS	Remote Sensing
R^2	Coefficient of determination
SADC	Southern African Development Community
SANBI	South African National Biodiversity Institute
SAWS	South African Weather Service
SPOT -VEGETATION	The French Satellite Pour l'Observation de la Terre. SPOT was launched on 24 March 1998. The VEGETATION instrument onboard SPOT-VEGETATION is funded by the European Union, Belgium, France, Italy and Sweden and led by French space agency Centre National d'études spatiales
TM	Thematic Mapper (of Landsat)
WUE	Water use efficiency

CHAPTER 1

INTRODUCTION

1.1 Background

In South Africa, livestock production comprises a key contribution to the agricultural gross domestic product (GDP) of the country, making the sustainable usage of rangelands of paramount importance (De Leeuw & Tothill, 1990; Stroebel *et al*., 2008; Palmer & Bennet, 2013). If livestock numbers are not monitored, overgrazing may result. Unsustainable grazing may lead to severe impacts on the environment, such as land degradation, erosion and depletion of non-renewable natural resources (De Leeuw & Tothill, 1990; Pickup *et al*., 1994; Calvao & Palmeirim, 2004; Zika, 2008; Kurtz *et al*., 2010). Land degradation can be defined as the long-term state where the land loses ecosystem function and productivity, i.e. can no longer produce crops or sustain livestock. The causes for the latter state are disturbances from which the land cannot recover unaided. Several factors contribute to land degradation; including erosion, soil compaction, bush encroachment, salinization, as well as, and linked to human activities – dating back to previous land policies – and overgrazing (Hoffman *et al*., 1999; Archer, 2004; Vanderpost *et al*., 2011). Current and former communal grazing areas in the provinces of KwaZulu-Natal, Eastern Cape and Limpopo have suffered effects of sharing land for settlement, farming and grazing – later often resulting in inappropriate land use practices. While it is sometimes difficult to indicate the key causes of land degradation, it remains increasingly problematic and a threat to food and livelihood security, hence optimal utilization of rangelands is vital (Pickup *et al*., 1998; Kurtz *et al*., 2010).

Carrying capacity (CC) is defined as the number of herbivores/livestock that the natural rangeland can support without the addition of external feeding sources that can potentially result in degrading the environment (De Leeuw & Tothill, 1990; Hayward *et al*., 2007). It is clear that the CC of a rangeland should be estimated relative to the number of livestock in it – ideally before any livestock is introduced therein – in order to be able to manage and monitor its sustainability, acknowledging limitations on such measurement (Roe, 1997; Archer, 2004). The latter has, however, not always been the case in South Africa as farmers and pastoralists in certain areas used to overstock rangelands (Wessels *et al*., 2007a). The assumptions behind this notion generally considered climate vagaries to be solely responsible for land degradation, hence overlooking the contribution made by humans and animal activities (De Leeuw & Tothill, 1990; Wessels *et al*., 2007b). In the past, estimation of CC used to be time consuming and costly.

Nowadays, however, various techniques of estimating CC exist, depending on the specific biome, long-term climate in location and soil texture (Pickup *et al*., 1998; Xia & Shao, 2008). It is important to note that the use of technology has not, however, rendered null the need for field work in order to collect data. It is true that grazing capacities may be estimated without making use of biomass data, but it is advisable to use concrete biomass data as an indicator of production (Morgenthal *et al*., 2004). Field data undoubtedly serve as an important verification tool in remote sensing (RS) studies.

1.2 Problems to be solved

Figure 1 supports the fact that rangelands in the Limpopo Province are extensively degraded – so much so that the province has been perceived as one of the most degraded in South Africa (Hoffman *et al*., 1999; Wessels *et al*., 2007a,). Limpopo Province further experiences multiple challenges as well as limitations when it comes to livestock farming, grazing practices and regulations. The impetus behind this study is to assist the provincial government of the Limpopo Province in raising awareness about rangeland grazing capacity (GC) and also by providing a monitoring time-management tool. The CC product is intended to assist decision makers to outline and apportion grazing land according to vegetation productivity in the different seasons of the year. The latter should contribute to managing land degradation, since the intensity of land use can exceed the productive potential (Hoffman *et al*., 1999).

Furthermore, the CC product should provide sound guidance to livestock farmers and grazers on rangeland maintenance, monitoring of grazing particularly how to adjust their grazing schedules – which should ultimately support rehabilitation of land that had previously been degraded due to overgrazing. With the CC product in place, local government relief projects will be able to regulate compensation funds in cases of droughts or veld fires according to GC guidelines that will be implemented. It is envisaged that this product will ultimately enable government, decision support systems and farmers to devise better grazing practices, subsequently rehabilitating natural resources (which can take many years). A CC system would be of great utility to have in place as it would be updated monthly as a predictive tool with projection for future months, making it possible for farmers and herders to manage and graze their livestock cautiously, and to engage in adaptive management.

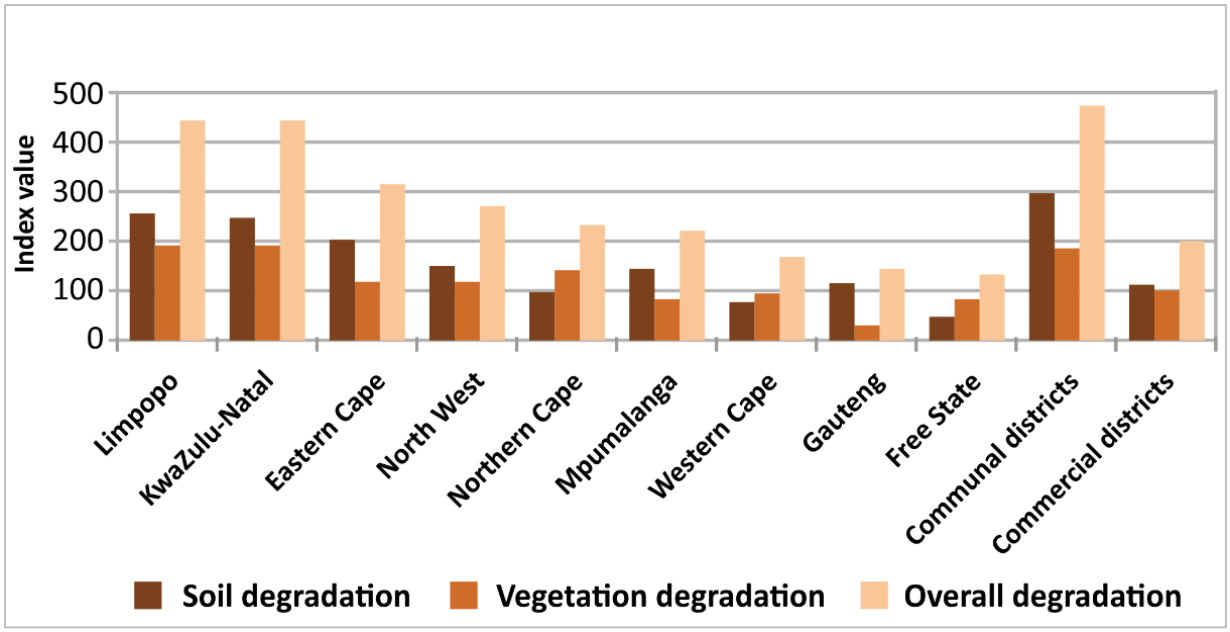

Figure 1: Land degradation in the Limpopo Province is higher than other provinces in South Africa (Hoffman *et al*., 1999).

This study focuses on the Limpopo Province as it is a semi-arid region, making it susceptible to land degradation (Hoffman *et al*., 1999). The Limpopo Province has high variability in forage thus overgrazing can easily occur, moreover unreliable rainfall contributes to the great variability in forage throughout the province. The study commenced in January 2014 with collection of Satellite Pour l'Observation de la Terre (SPOT) VEGETATION Dry Matter Productivity (DMP) dataset for 12 years (1998/99-2009/10), as well as biomass field data. CC over the Limpopo Province is strongly linked to seasonal rainfall totals, and, since seasonal forecast skill over the area is relatively high compared to other areas over South Africa, (Figure 2), employing seasonal forecasts over the region should lead to positive and useful results to improve agricultural management and operations (Landman *et al*., 2012; Malherbe *et al*., 2014).

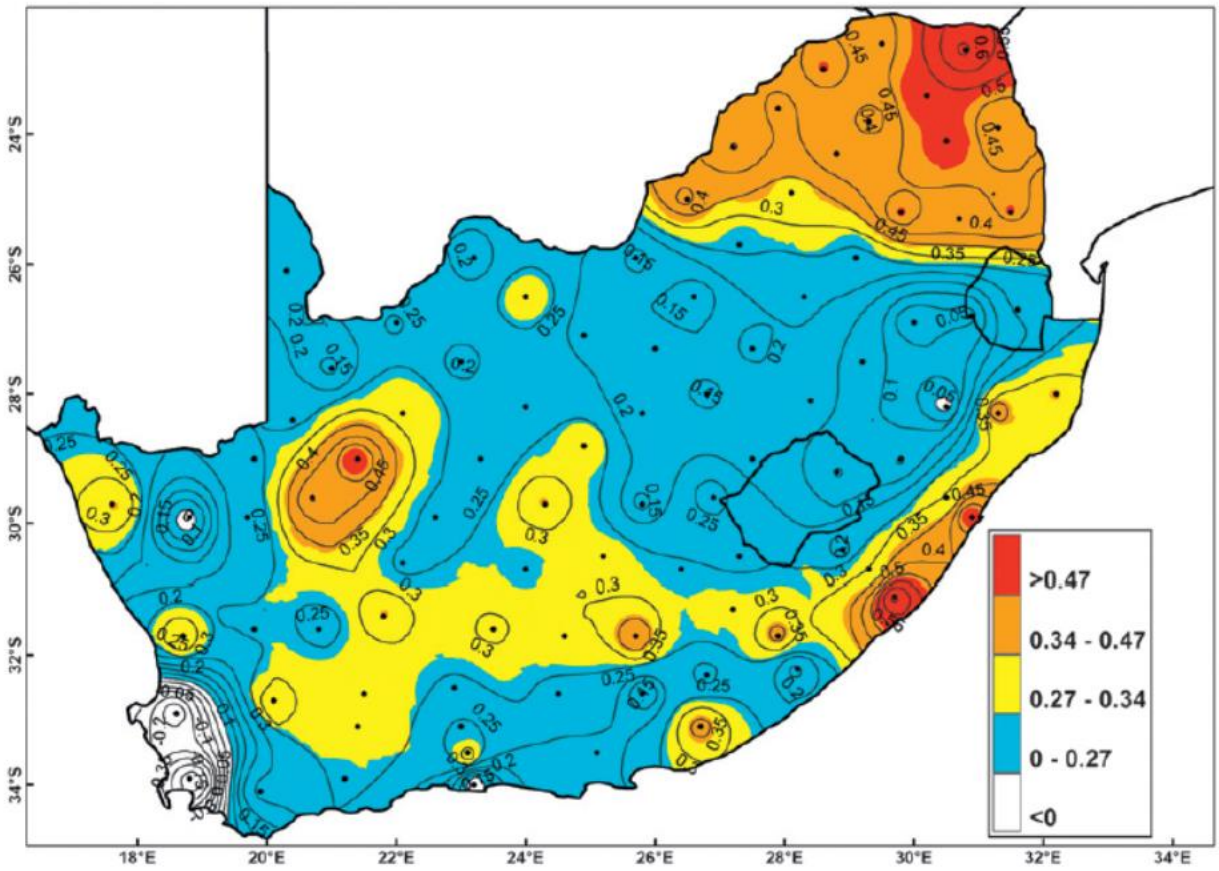

Figure 2: Map showing high skill of seasonal rainfall predictability over Limpopo Province. The Limpopo Province is the area on the top-right corner highlighted in Orange. The map shows Kendall's tau correlations between observed and coupled model precipitation as obtained from downscaling to rainfall districts for December-January-February (DJF) totals (Landman *et al*., 2012).

1.3 Research questions

This study will address the following questions:

- What is the potential to update the existing national CC map for Limpopo Province on both monthly and annual basis?
- What is the possibility of developing an updated skillful operational CC product for Limpopo Province?

The objectives can be outlined as follows:

Objectives

- To update current CC products for Limpopo Province.
- To create CC deviation maps for several years with relevant data.
- To screen current and future available monitoring data.
- To develop an operational method to update baseline CC monthly according to:

(i) Progress of current CC season.

(ii) Forecast for current CC season.

CHAPTER 2

LITERATURE REVIEW

2.1 Introduction to Remote Sensing and Geographic Information Systems

The use of satellite technologies such as RS first appeared in the 1960s, and was later applied in vegetation monitoring (Gallo & Daughtry, 1987; Hayes & Decker, 1998; Fraser *et al*., 2000; Lamb, 2000). The debut of RS technology coupled with GIS technology has provided significant research opportunities – thus today, RS and GIS applications have advanced into different fields of science. These products are numerous and may be customized for various tasks to provide desired results. The demand for new methods and algorithms in both science and communities is driving emerging techniques.

Climatological data, particularly precipitation, and RS products such as the Normalized Difference Vegetation Index (NDVI), derivatives of the NDVI etc. have been used in a wide range of resource monitoring applications. These include (but are not limited to) forecasting crop yield (Smoliak, 1956; Murphy, 1970; Shiftlet & Dietz, 1974; Wight *et al*., 1984; Benedetti & Rossini, 1993; Moran *et al*., 1997; Reynolds *et al*., 2000; Calvao & Palmeirim, 2004; Frost, 2006), monitoring rangelands (Townshend, 1986; Baret & Guyot, 1991; Nicholson *et al*., 1998; Azzali & Menenti, 2000, Anyamba *et al*., 2001; Myneni *et al*., 2002; Hunt *et al*., 2003; Wessels *et al*., 2006) and identifying rangeland degradation (Archer, 2004; Wessels *et al*., 2007a; Vanderpost *et al*., 2011). The use of RS technology has seen improved results and efficiency in various research projects, particularly environmental monitoring (Townshend, 1992; Goodchild, 1994; Hayes & Decker, 1998; Jianlong *et al*., 1998; Xie *et al*., 2008; Han *et al*., 2013). Another benefit of using RS and GIS methods is that less input data, i.e. number of parameters, are required, which may not be the case with most crop models (Joshi *et* al., 2004; Becker-Reshef *et al*., 2010).

There are, however, shortcomings in using NDVI. Soil background, clouds and atmospheric particles such as aerosols may affect the quality of these derivatives of satellite images. Nonetheless, they are still widely used because they are less intricate to work with, long-term datasets are available (Bartalev *et al*., 2003; Gibson, 2006; Xie *et al*., 2008), and they are sensitive to change and applicable to large scale studies (Xie *et al*., 2008). The type and intensity of image degradation by atmospheric constituents vary spatially. Studies have shown positive results for the use of RS and GIS technologies for yield estimates, resulting in increased confidence towards improved crop production (Hanson *et al*., 1983; Jianlong *et al*., 1998; Becker-Reshef *et al*., 2010). When crop yield is estimated a few months prior to harvest, decisions can be made based on

whether there will be a surplus or shortage of food (e.g. Reynolds *et al*., 2000; Mkhabela *et al*., 2005; Sivakumar, 2006). RS and GIS technologies have been utilized to estimate grassland yield in China (Jianlong *et al*., 1998). As mentioned earlier, grassland yield estimates can be useful – if timely and accurate – in livestock production. A combination of RS and ground truth data was shown to be useful for estimating and monitoring grassland yield at a large scale (Jianlong *et al*., 1998). As mentioned previously, yield estimates may be used by decision makers to advise livestock farmers on grazing periods, systems and/or routines.

2.2 The application of seasonal forecasts in agriculture

Maize is an important staple crop in most rural areas of sub-Saharan Africa, making yield forecasts for the maize crop vital (Sileshi *et al*., 2008; You *et al*., 2009; Malherbe *et al*., 2014; Wetterhall *et al*., 2015). The application of RS products, specifically NDVI, varies greatly, with substantial research concentrating on the use of the index in agriculture such as for estimating maize yield (Unganai & Kogan, 1998; Verdin *et al*., 1999; Tadross *et al*., 2005; Frost, 2006). For example, the potential usefulness of NDVI in making maize yield forecasts in Swaziland was evaluated (Mkhabela *et al*., 2005). In the study, three agroecological regions (Lowveld, middleveld and Lubombo plateau) showed a positive linear relationship between maize yield and accumulated average NDVI. However, for the Highveld region, where cloud contamination of imagery can play a major role, the correlation proved poor. The study further aimed to establish the best lead-time for making a reliable forecast to alleviate food insecurity (Mkhabela *et al*., 2005; Mkhabela *et al*., 2011). The findings further showed that maize forecasts may be issued 2-3 months prior to harvest, providing government, non-government organizations (NGOs) and other food security stakeholders with sufficient time (in this case) to plan for maize imports, should a shortage occur.

The combination of climate data and RS constitutes a rapidly evolving technology applicable to a wide range of fields. Meteorological variables, especially rainfall, play a very important role in the planting and growth stages of the maize crop. The use of climate data, models and seasonal forecasts thus make a conspicuous contribution towards improving the quality of crop yield forecasts. The relationship between seasonal rainfall characteristics and maize yields has been explored in several studies focusing on the maize crop in South Africa (Unganai & Kogan, 1998; Verdin *et al*., 1999; Tadross *et al*., 2005; Tsubo *et al*., 2005; Frost, 2006; Walker & Schulze, 2006; Rockstrom *et al*., 2009; Tadross *et al*., 2009; Malherbe *et al*., 2014). Spatial rainfall and Moderate Resolution Imaging Spectroradiometer (MODIS) products were used to improve maize crop yield

estimates by considering the seasonal NDVI curve with respect also to the planting date (Frost, 2006).

In the past, seasonal forecasts were not extensively used in agriculture for many reasons, one of them being their lack of applicability (Landman *et al*., 2009; Goddard *et al*., 2010; Haigh *et al*., 2015). This has, however, changed recently, with a growing trend of research being done on improved modelling, communication as well as accessibility of seasonal forecasts and climate data to users (Ziervogel *et al*., 2014; Malherbe *et al*., 2014; Haigh *et al*., 2015; Wetterhall *et al*., 2015). One impetus behind this increased interest is addressing food security, by providing useful seasonal forecasts – coupled with crop and rangeland modelling – to decision makers and extension officers (Murphy, 1993; Reynolds *et al*., 2000; Goddard *et al*., 2010; Thornton *et al*., 2011).

The need for seasonal forecasts in crop modelling to assist with the added-value and tailor-made part of expanding of seasonal climate forecasts to be useful for farmers cannot be emphasized enough. It should be noted, however, that climate models also have caveats which may affect results, depending on the desired product/output (Mkhabela *et al*., 2005; Sivakumar, 2006; Semenov & Stratonovitch, 2010; Landman & Beraki, 2012). Training would thus be beneficial for decision makers and users in climate and crop modelling, sparking interest in employing probabilistic seasonal forecasts in agricultural production, as well as improving their efficiency (Moeletsi *et al*., 2013). Maize yield and stream flows were, for example, successfully estimated over north-eastern South Africa with the use of SINTEX-F coupled model (Malherbe *et al*., 2014), and results show the potential of using seasonal forecasts in an agricultural field operationally.

As mentioned previously, significant need exists to make use of seasonal forecasts for food production and climate risk management, to assist farmers advance their methods of planting, i.e. planting dates, irrigation scheduling, marketing and trade of their products (Marletto, 2005; Sivakumar, 2006; Goddard *et al*., 2014; Ziervogel *et al*., 2014). The latter would, ideally, ultimately inspire progression from short- and mid-range weather forecasts to employing long-range climatic projections (Marletto, 2005; Goddard *et al*., 2014; Wetterhall *et al*., 2015). If the latter can be achieved in small-scale farming, progressing to commercial farming, food production would, under certain circumstances, stabilize according to Marletto, (2005) and Goddard *et al*. (2014) (Figure 3). Research has further shown that multi-models make better seasonal forecasts than single models, during both El Niño and La Niña years (Mason *et al*., 1999; Landman & Beraki, 2012; Malherbe *et al*., 2014).

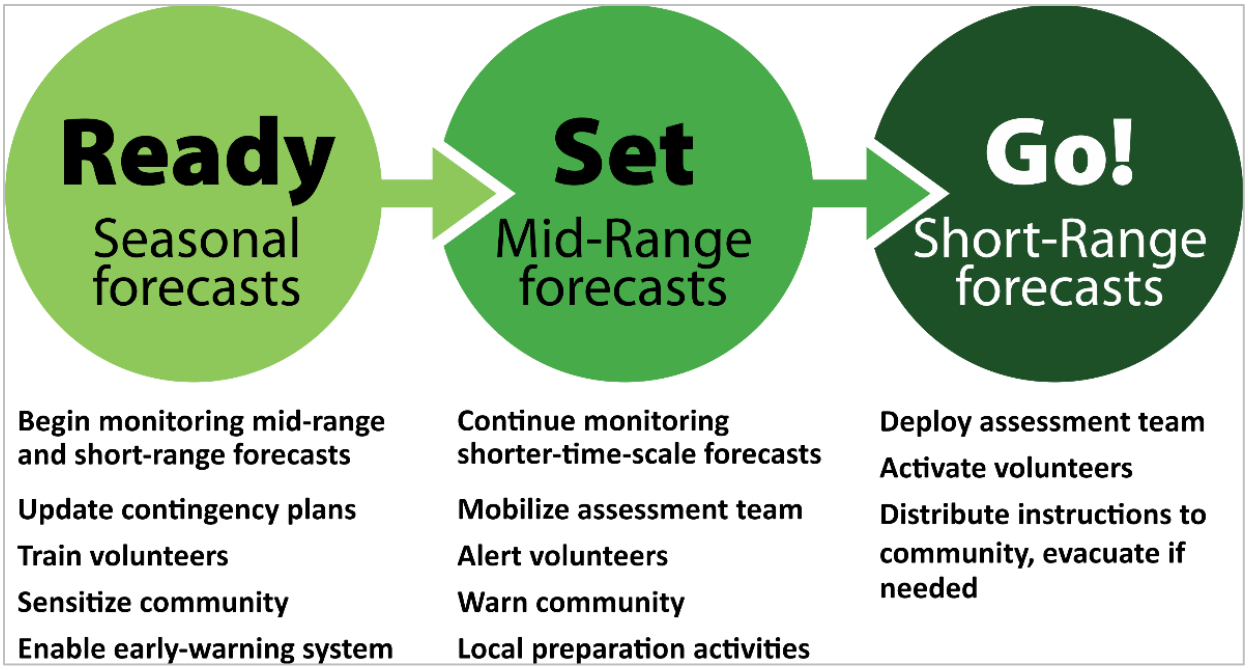

Figure 3: Schematic flow on how climate models can be made accessible to users for increased crop and livestock production (Goddard *et al*., 2014).

Tailored forecasting can improve the significance and use of seasonal forecasts in agricultural production (Sivakumar, 2006; Goddard *et al*., 2010; Zuma-Netshiukhwi *et al*., 2013). Tailored forecasting refers to forecasts which focus on specific needs, i.e. aviation, insurance, livestock farming or rangeland management. Research focusing on tailored forecasts to support the livestock sector has limited focus as compared to the crop sector in South Africa (Landman, 2014). The incorporation of available historical climate and commodity production information in the making of seasonal forecasts could contribute to enhanced application by meeting users' needs. For example, seasonal forecasts for grazing would focus on location and species composition of grasses in South Africa as well as the growth cycles, i.e. July-June. These forecasts would be more useful in estimating deviations from previously determined GC, with concomitant potential impacts on livestock production and, therefore, livestock production farmers may be inclined to employ these forecasts in agricultural risk management (Malherbe *et al*., 2014).

2.3 Use of vegetation indices in rangeland degradation monitoring

Whether land degradation is attributed to human practices or precipitation variability remains an ongoing dispute. As mentioned earlier, NDVI – and other vegetation indices – have been employed in many studies to determine what the causes of land degradation are and what solutions exist for this problem (e.g. Azzali & Menenti, 2000; Archer, 2004; Wessels *et al*., 2007a;

Vanderpost *et al*., 2011; Palmer & Bennet, 2013). These studies concluded that anthropogenic influences, such as management practices of rangelands, play a major role in land degradation. Precipitation variability is also, however, responsible for land degradation (Pickup *et al*., 1998; Evans & Geerken, 2004; Pachavo & Murwira, 2013). Grazing practices and their effects on vegetation cover in the Karoo were determined using 12 years of NDVI data (corrected for rainfall), highlighting the role of anthropogenic activities in land degradation (Archer, 2004).

The cumulative NDVI from both Advanced Very High Resolution Radiometer (AVHRR) and MODIS for 6 years (2000-2005) in the Limpopo Province of South Africa were used to show that land degradation resulting from higher stocking rates has significant effects on long-term vegetation productivity (Wessels *et al*., 2007a). This result was achieved by dividing the area into land capability units in order to separate the severity of land degradation within each rangeland with respect to different soils, topography and climate. Rangeland degradation (in some cases) can be the dominant factor for interannual vegetation variability in rangelands (Paudel & Andersen, 2010).

Inappropriate anthropogenic practices such as deforestation and overgrazing can affect rangelands negatively, ultimately lowering production capacity of the land. The importance of anthropogenic influences such as unsustainable farming practices in land degradation instead of climate variability was demonstrated for Botswana (Vanderpost *et al*., 2011). Conclusions were based on comparison of findings over protected versus communal areas, which showed extremely degraded conditions in the communal areas (e.g. Palmer & Bennet, 2013). Conversely, droughts, climate variability and climate change also affect natural vegetation production in rangelands (Smoliak, 1986).

Rangelands basically sustain livestock by providing abundant forage of good quality. Forage production (expressed as grass biomass and Above Ground Net Primary Production (ANPP) in many studies) from rangelands directly affects livestock production (Trollope *et al*., 1990; Du *et al*., 2004; Xiao *et al*., 2004; Flombaum & Sala, 2007; Guevara *et al.*, 2009; Montès, 2009; Palmer & Yunusa, 2011; Pachavo & Murwira, 2013). In an epitome rangeland (other factors negligible), high forage production would mean that livestock production increases – forage production can, however, be negatively affected by land degradation. For example, ANPP was estimated in the Northern Cape Province, showing that water use efficiency (WUE) was lower than previous

estimates reflecting the degraded state of rangeland in the dwarf shrublands and arid savanna of the Riemvasmaak Rural Area of Northern Cape (Palmer & Yunusa, 2011).

Land that is degraded may take many years to be restored (Hoffman *et al*., 1999; Archer, 2004) – nonetheless this does not mean that efforts should not be made towards land restoration. GC is strongly linked to land management – if the GC of land is estimated and updated monthly, guidelines on available and unavailable pasture may be given to farmers. There are existing national long-term GC products for South Africa for 1993 and 2005 expressed in hectares per large stock unit (ha/LSU). The 2005 GC product was estimated using National Oceanic and Atmospheric Administration Advanced Very High Resolution Radiometer (NOAA-AVHRR) satellite derived data, thereby indicating that the map could be updated for succeeding years (Morgenthal *et al*., 2004).

Apart from GC products, other technologies and land assessment procedures are in place across the globe for rangeland management, and these include a combination of land cover maps and continuous assessment of above ground biomass (Lamb, 2000; Bartalev *et al*., 2003; Kurtz *et al*., 2010). Satellite (remotely sensed spectral, NDVI) data, biomass ground truth data, ancillary crop and soil information are also used for monitoring purposes. Many studies have recommended the use of the land cover classification system towards supporting rangeland farmers and advisory services (Jianlong *et al*., 1998; Reynolds *et al*., 2000; Kurtz *et al*., 2010; Wessels *et al*., 2012). There is also a great need for an operational rangeland system which can be updated in real time.

2.4 Current trends in RS, GIS products and climate models

Current research trends in the integration of RS products and climatological data have yielded promising results, as shown above. Precipitation is one of the many meteorological variables that affects growth of crops, therefore it is not unexpected that NDVI and precipitation variability will show a high correlation (Nicholson *et al*., 1990; Di *et al*., 1994; Richard & Poccard, 1998; Verdin *et al*., 1999; Kawabata *et al*., 2001; Wang *et al*., 2003; Zhang *et al*., 2003; Wessels *et al*., 2012). The following are the most popular products used in RS studies: National Aeronautics and Space Administration (NASA)'s Landsat satellite, vegetation indices from satellite imagery from the following sensors; NOAA-AVHRR, MODIS, SPOT-VEGETATION, PROBA-V, Multispectral Mapper (MSS), Thematic Mapper (TM) and Earth Observatory Thematic Mapper (EOTM). Ground truth data play a very important role as a verification tool (e.g. Gallo & Daughtry, 1987;

Marsh *et al*., 1992; Goetz *et al*., 1999; Marletto, 2005; Paudel & Andersen, 2010; Nutini *et al*., 2011).

The development of climate models (statistical and dynamical) for research has seen immense improvement in understanding how sea-surface temperatures influence the livelihoods of human beings and the environment. As a result, these models are readily used in many South African institutions today such as the South African Weather Service (SAWS), the Council for Scientific and Industrial Research (CSIR) and the University of Cape Town for seasonal forecasting research (Landman, 2014). Single-models such as the Conformal-Cubic Atmospheric Model (CCAM) and the ECHAM4.5–MOM3-DC2 coupled model as well as multi-model ensembles have been used successfully in many studies for seasonal forecasting, predicting extreme climate phenomena and projections for climate change scenarios (Landman *et al*., 2009; Semenov & Stratonovitch, 2010; Engelbrecht *et al*., 2011; Barnston *et al*., 2012; Landman & Beraki, 2012; Robertson *et al*., 2013; Malherbe *et al*., 2014).

SPOT-VEGETATION satellite has become popular in research because of its multi-spectral bands and daily image capturing abilities (Gallo & Daughtry, 1987; Fraser *et al*., 2000; Lupo *et al*., 2001; Xiao *et al*., 2002; Kamthonkiat *et al*., 2005; Tucker *et al*., 2005; Nutini *et al*., 2011). The NOAA-AVHRR, SPOT-VEGETATION and PROBA-V satellite imagery datasets in particular are being used for research purposes focusing on monitoring of vegetation condition by the Agricultural Research Council - Institute for Soil, Climate and Water (ARC-ISCW). These products have been successfully used in several studies for the following objectives: estimating crop yields, assessing and monitoring rangelands, classifying landcover, producing land degradation maps, managing rangeland systems and making yield forecasts (Shiftlet & Dietz, 1974; Townshend, 1992; Pickup *et al*., 1994; Leconte & Brissette, 2004; Frost, 2006; Prasad *et al*., 2006; Wardlow *et al*., 2007; Funk & Budde, 2009). Figure 4 is a product of PROBA-V satellite showing vegetation activity – approximation for biomass productivity – in South Africa.

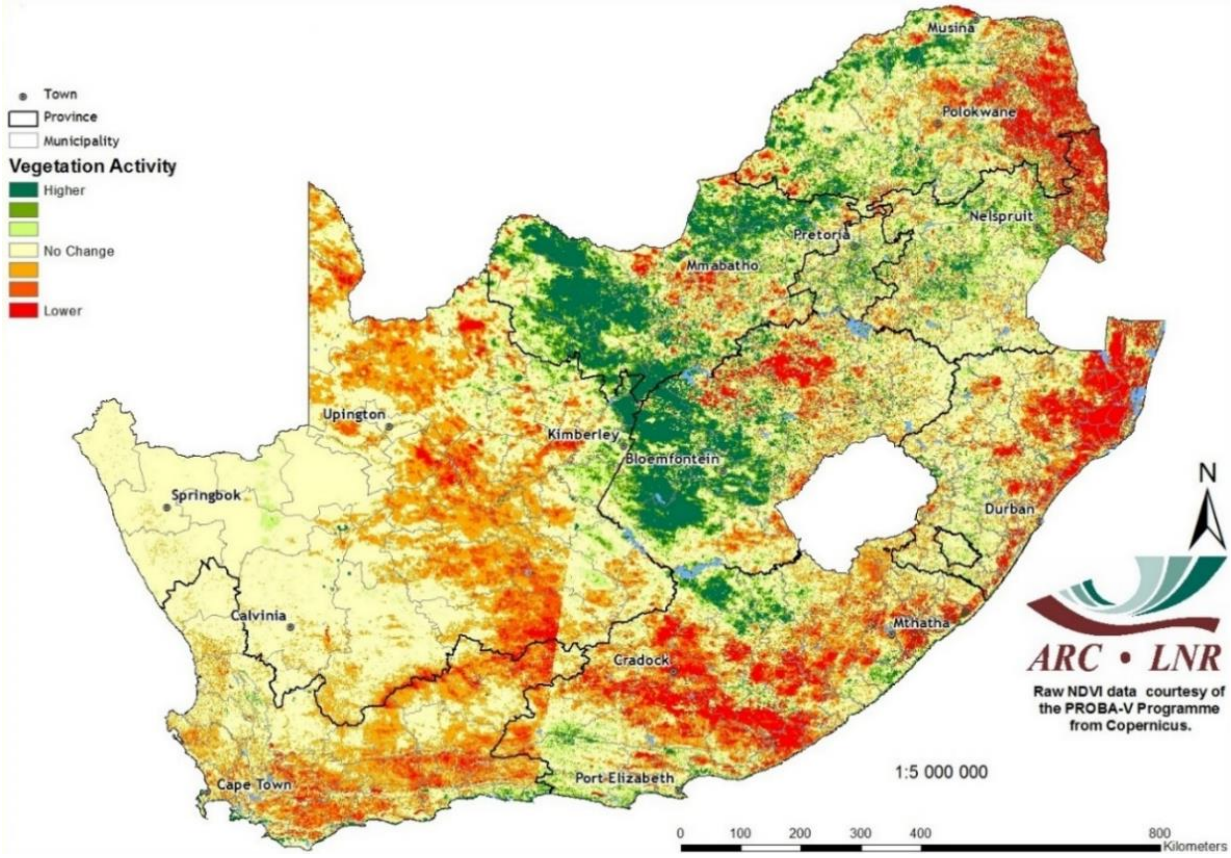

Figure 4: Vegetation activity for 1-10 January 2015 compared to 1-10 December 2014 covering South Africa from Umlindi Newsletter, 2015 (http://www.arc.agric.za).

The SPOT-VEGETATION DMP product dataset is going to be used by the Southern African Development Community (SADC) (in partnership with the ARC-ISCW) in creating a GC output for the SADC region (Malherbe, 2015). The above literature shows the potential application of seasonal forecasts, RS and GIS products in the agricultural environment. The current study therefore aims to show the application of RS products and seasonal forecasts in the agricultural field by developing an operational dynamic CC product for the Limpopo Province. Further on, the study aims to bridge the existing gap of seasonal forecast tailored for livestock production by estimating a product that will be updated monthly.

2.5 Synopsis

This chapter reviews CC estimation techniques, data/products that are employed as well as the results obtained. Limitations and gaps regarding RS and seasonal forecasts application in the agricultural sector discovered in these studies are highlighted as well as how this current study aims to bridge those gaps. RS and GIS techniques involve the use of numerous satellite imagery such as NOAA AVHRR NDVI, MODIS NDVI, SPOT-VEGETATION DMP to mention a few. Further, application of seasonal forecasts in agriculture is explored, encompassing yield estimates, forecasts and risk management. It is further shown that a fusion of satellite data, biomass ground truth data, ancillary crop as well as soil information has been most successful in supporting rangeland farmers and advisory services. Lastly, current trends in RS, GIS products and seasonal forecasts in South Africa are briefly discussed.

CHAPTER 3

STUDY AREA AND METHODOLOGY

3.1 Area of study

The Limpopo Province is located in the most northern parts of the Republic of South Africa, north of 22-25˚ S and west of 26-32˚ E (Figure 5). The region is generally semi-arid, covers approximately 129 910 km^2 of land and the landscape ranges from mountainous to flat land and the climate is hot and dry. In summer, the days and nights can be extremely hot with average maximum temperatures of 27˚C, but winter is mild with average minimum temperatures of 20˚C (Schulze & McGee, 1978). Limpopo is a summer rainfall region, with an annual rainfall of less than 350 mm in the lower lying areas, while the higher lying Drakensberg escarpment receives more than 1000 mm in certain places. Most parts of Limpopo are rural, supporting extensive livestock farming and ranching operations with irrigated crops (Vogel *et al*., 2010). The latter increases rangelands' vulnerability to overgrazing, causing land degradation to worsen in many parts of the province. However, it should be noted that overgrazing is mainly prevalent in the north-eastern parts of the Limpopo Province. Therefore, an operational CC system developed for Limpopo Province may be able to provide forecasts for grazing conditions and assist government with policy making, monitoring and managing of rangelands.

Figure 5: Map of Limpopo Province (http://www.mapsharing.org.za/).

Limpopo Province falls largely under the Savanna biome, as shown in Figure 6, which is the biggest of all biomes in South Africa. The topography is characterized by undulating plains, i.e. flat plains to mountainous slopes. The Savanna biome is a summer rainfall area with semi-arid conditions and varying rainfall patterns (Buckle, 1996). Erratic rainfall can affect vegetation growth and production (rainfall is a primary determinant of forage growth) for grazing to livestock and game available in the area. Domestic animals that graze include mainly cattle with goats on a limited scale in the south-western parts. The dominant veld type has been identified as the Mopane veld (Acocks, 1988). Various trees, shrubs and grass types have been identified in the Mopane veld (Van Oudtshoorn, 1999).

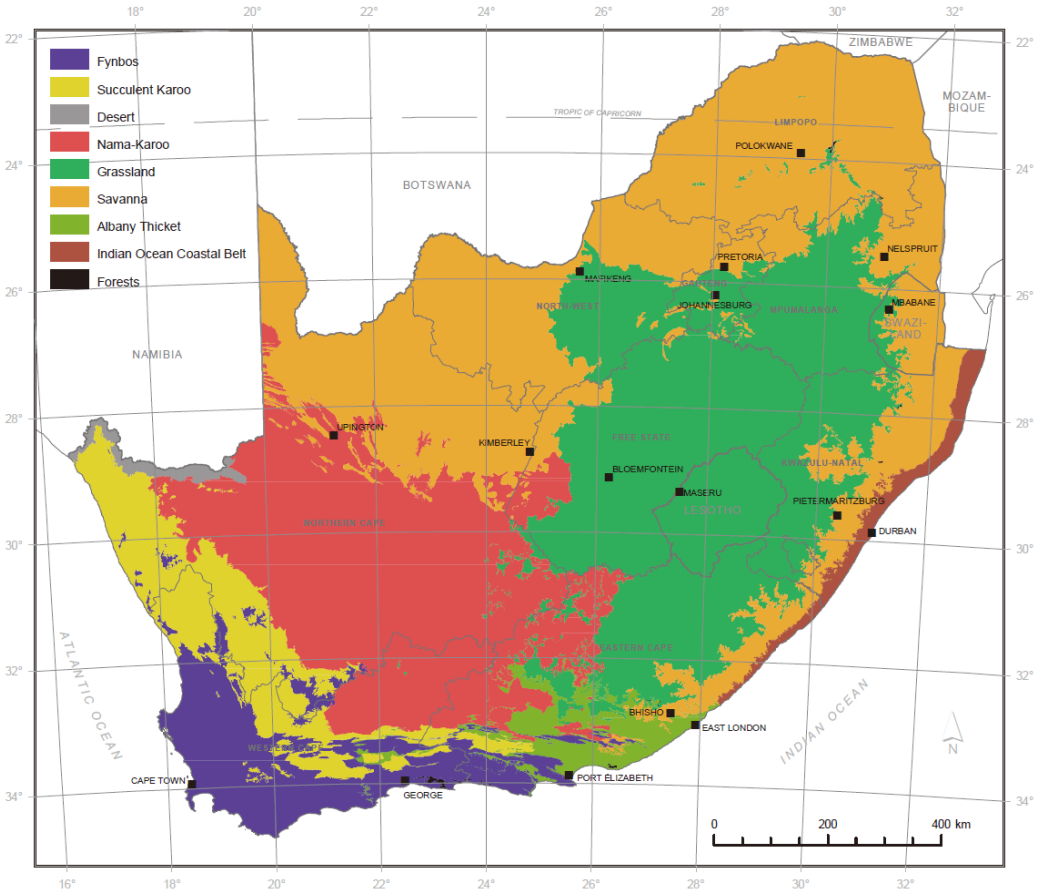

Figure 6: The different biomes found in South Africa (Rutherford *et al*., 2006).

Examples of trees and shrubs include: *Colophospermum* mopane (Mopane), *Acacia tortilis* (Umbrella Thorn), *Adansonia digitata* (Baobab), *Acacia nigrescens* (Knobthorn) and *Kirkia acuminate* (Seringa), the common grasses include: *Aristida congesta* (Tassel Three-awn), *Enneapogon cenchroides* (Nine-awned grass), *Cenchrus ciliaris* (Blue Buffalo grass) and *Stipagrostis uniplumis* (Silky Bushman grass) (Van Oudtshoorn, 1999). Bush encroachment by the Sickelbush (*Dichrostachys cinerea*) is a common problem in this area, which reduces availability of grass feed for livestock. Forage has different growth stages and cycles – grass in particular grows in the July-June season. In this study, the growth season of grass tailors for both summer and winter DMP imagery of the vegetation cover. Livestock graze on natural vegetation and it is therefore important that forage is monitored and conserved – this can be supported by estimating GC and supplying forecasts for future months.

Grazing routines in the Limpopo Province, in certain areas, may not be in place or monitored – compounding problems of degradation. Land degradation is a major challenge as it limits farmers

from grazing large areas because as livestock continue to graze on the same land the problem is exacerbated, and most farmers thrive on crop and livestock farming. It is therefore important that GC for the Province be estimated in order to assist in scheduling grazing patterns for farmers, planning for future seasons – based on forecast model outputs and looking into options of land restoration programmes. How the latter is implemented requires a tactful approach for farmers and local municipalities, including capacity building.

3.2 Data collection

A set of methods including GIS and Earth Observation System data (EOS), seasonal climate forecasts and secondary ground truth data are employed to calculate CC for the Limpopo Province. The calculations are based on satellite data per growing season for the years 1998/99-2009/10 (12 seasons). Products that are used in this study include; SPOT-VEGETATION DMP based (http://proba-v.vgt.vito.be/), seasonal hindcasts (re-forecasts) from ECHAM4.5–MOM3-DC2 coupled model (http://iri.columbia.edu/resources/data-library/), gridded observed rainfall from ARC-ISCW, tree density product_2003 (ARC-ISCW databank), vegetation map of 2009 (http://bgis.sanbi.org/vegmap/map.asp), MODIS Net Primary Production (NPP) (http://www.nasa.gov/) and grass biomass field data. The 1993 map (Figure 7) was estimated using various grazing capacity information such as field data, however, the 2005 (Figure 8) update was estimated using NOAA-AVHRR (http://www.noaa.gov/) and MODIS satellite data.

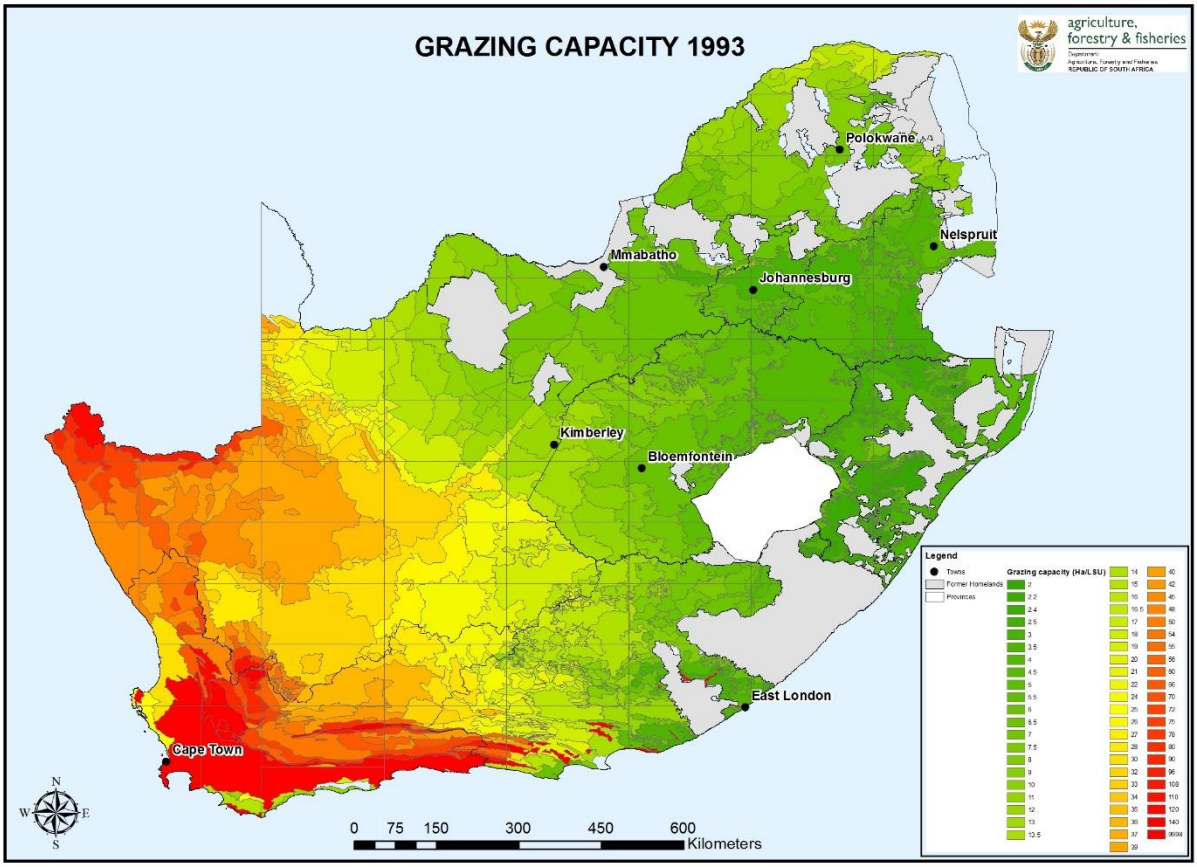

Figure 7: 1993 National GC potential map for South Africa (Department of Agriculture, Forestry and Fisheries, 1993).

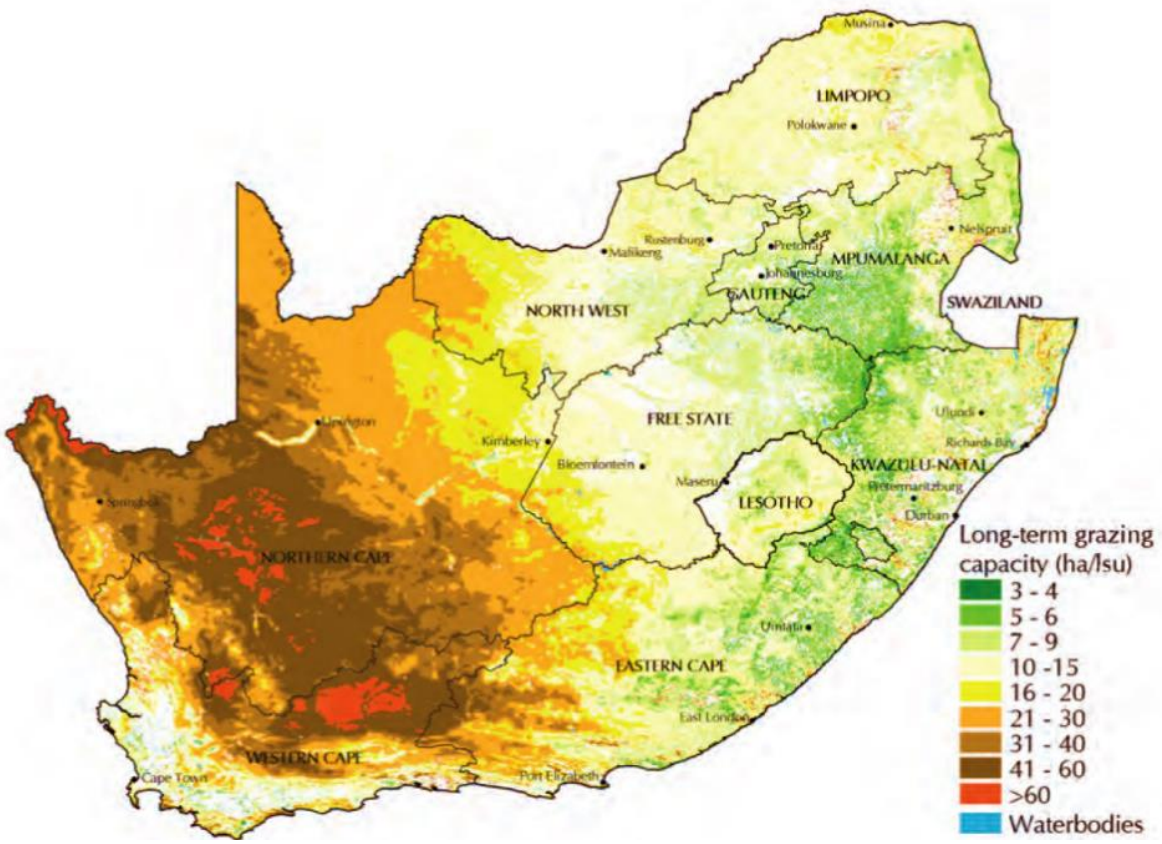

Figure 8: 2005 National GC map for South Africa; as an upgrade to the 1993 product (Morgenthal *et al*., 2004).

The data are analyzed using the following tools: Earth Resources Data Analysis System–IMAGINE (ERDAS version 14.00) software (http://www.hexagongeospatial.com/), Excel 2013, and the Climate Predictability Tool (CPT; http://iri.columbia.edu/). The tree-density product, vegetation map, grass biomass data and veld types are used to adjust the Dry Matter Productivity to estimate grass biomass for a final estimate of CC as shown on the flowchart of methodology (Figure 9).

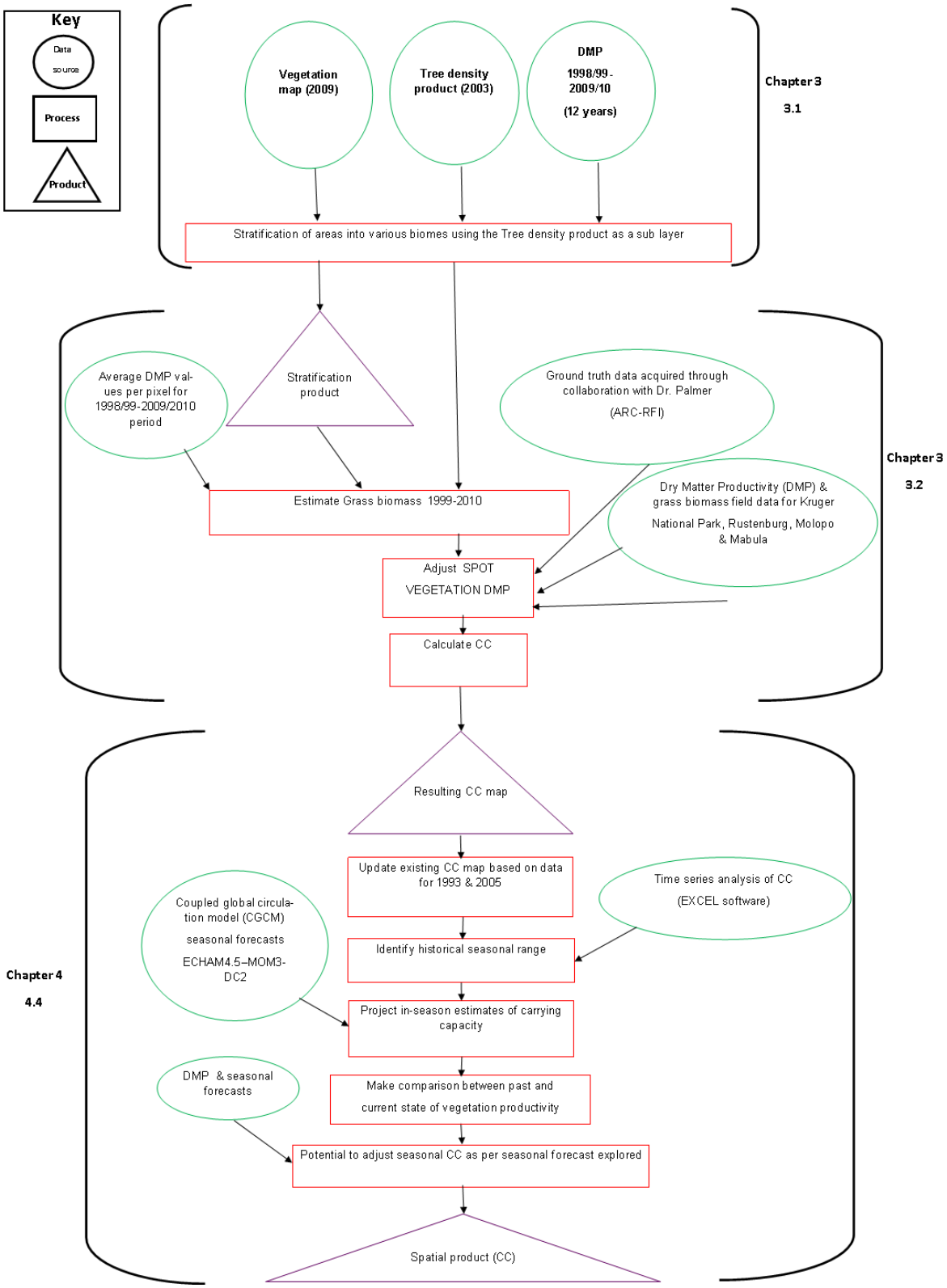

Figure 9: Flow diagram showing the processes and products involved in estimating GC.

3.2.1 Earth Observation System data

The data are acquired in different formats and scales, therefore, data quality control is imperative. The latter leads to the deletion of certain data points due to missing and/or incomplete data. The following tools: Excel 2013, ArcMap 10.3, ArcView 3.1, CPT and ERDAS software are employed in analyzing the data and ultimately for estimating GC. In ArcMap, all datasets (both vector and raster) that are used are converted to the WGS-1984 projection for uniformity and better display, particularly for output as maps.

3.2.1.1 SPOT-VEGETATION DMP data

SPOT-VEGETATION DMP for 12 years (1998/99-2009/10) are obtained from the PROBA-V website (http://proba-v.vgt.vito.be/) in January 2014. DMP satellite imagery are produced from a combination of RS and meteorological data from the European Centre for Medium-Range Weather Forecasts (ECMWF). The meteorological data considered in these estimations are solar shortwave radiation and temperature based on the eminent Monteith (1972) model (Nutini *et al*., 2011). Each satellite image represents the maximum value of DMP per month. The SPOT satellite captures high quality global images using the VEGETATION sensor which was launched in 1998, developed by a collaboration between France, European Commission, Belgium, Italy and Sweden (Fraser *et al*., 2000). Although the resolution of SPOT-VEGETATION is 1 km, the sensor has numerous advantages such as high temporal resolution and multi-spectral bands (Fraser *et al*., 2000; Xiao *et al*., 2002; Bartalev *et al*., 2003). The data obtained consist of S10 DMP dekads (10 day composites) for each month, i.e. 1-10 days; 11-20 and 21 to the last day of the month.

DMP represents the total biomass production of vegetation across an area. It should be noted however that DMP only reflects the above-ground dry matter biomass and the Disc Pasture Meter method also estimates the above-ground biomass, thereby endorsing the use of biomass field data for validation purposes. Moreover, DMP only indicates the quantity of vegetative growth and does not take into account the quality of harvested biomass. As a result, DMP should be considered as an indicator of potential production but not the actual marketable product (ENDELEO, 2009). The DMP dataset is in a raster format, Figure 10 shows the DMP map for 2008/09 that is drawn in ArcMap. The Spatial Analyst tool in ArcMap 10.3 is used to get the maximum of the 3 dekads DMP per month, resulting in the Maximum DMP Value composite (MVC) per year. The latter is done to reduce cloud and atmospheric noise owing to the coarse resolution of the data (Kamthonkiat *et al*., 2005; Tucker *et al*., 2005). DMP data are analyzed in ArcMap 10.3 using the Spatial Analyst tool, and maximum DMP composites are calculated per

year. The data are subsequently analyzed in Excel. ERDAS software is used to estimate GC – based on the average of the DMP values per pixel for the 1998/99-2009/10 period. Further 12-month composites for each annual growing period of grasses (e.g. July 1998-June 1999) are also calculated, resulting in 12 years of DMP composites. All these datasets are converted to database files (dbf) so that they can be compatible with Excel 2013 and checked for contamination or missing values to minimize the potential of inconsistencies in results. Spatial subsets are created for the Limpopo Province.

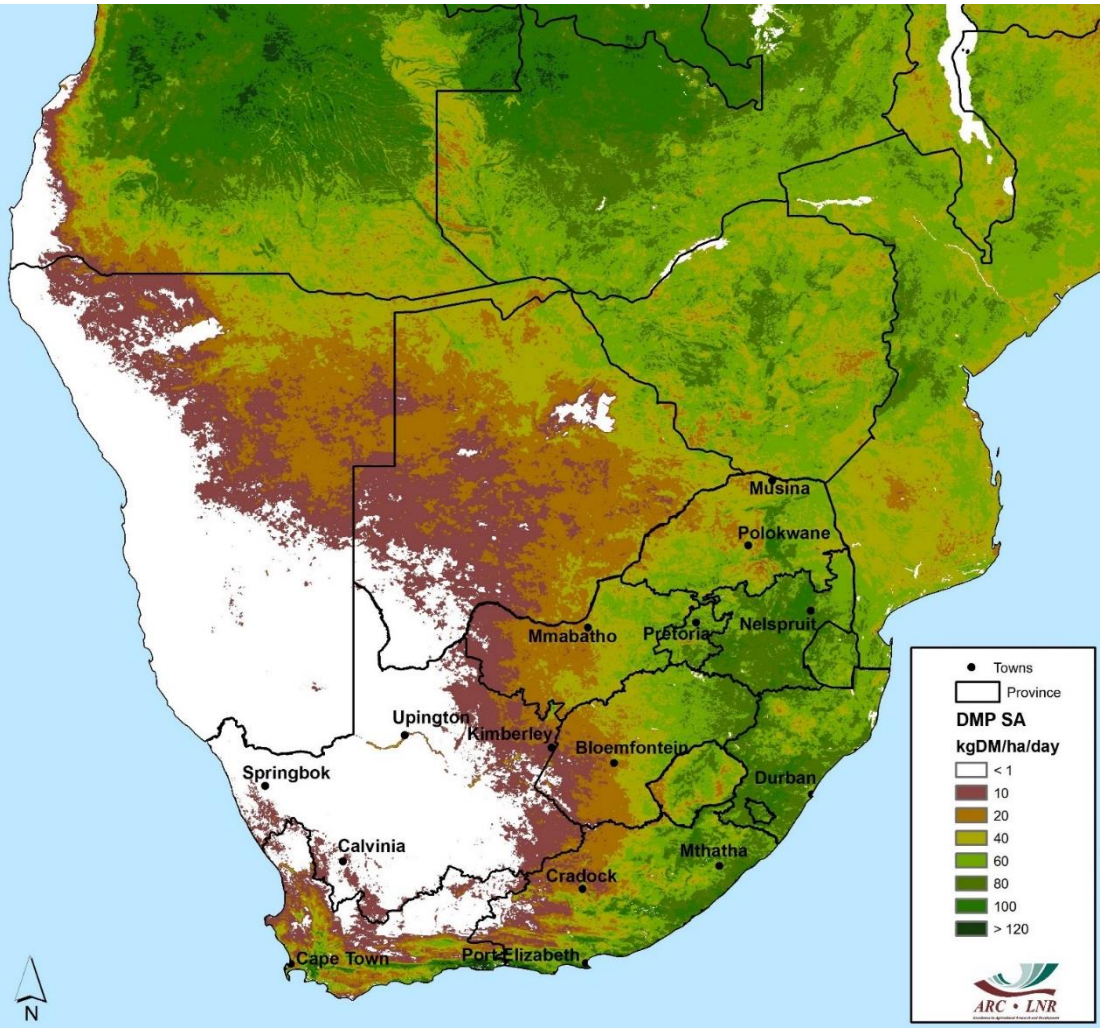

Figure 10: DMP raster image for southern Africa for the year 2008/09.

Rainfall influences crop production (Zambatis *et al*., 2006), thus in years with below normal rainfall or droughts, production decreases, whereas in good years with normal or above normal rainfall, production increases. However, it should be noted that the time when the rainfall is received is also crucial, regarding vegetation growth seasons. Given that the rainfall season in the Limpopo Province is November through April (NDJFMA). DMP maximum composites for this period are

also calculated resulting in 12 years of composites. In ArcMap, the Spatial Analyst tool-Extraction tool is used to extract the DMP composite data for an even grid of points for the Limpopo Province for the year 2008/09 (Figure 11).

Since dry matter production is primarily determined by rainfall in semi-arid areas, it is necessary to run tests that analyze the relationship between these two variables in order to establish whether or not rainfall can be used as a predictor for the DMP product in the Limpopo Province. The CPT is used to achieve this objective through Canonical Correlation Analysis (CCA); where the predictor is coupled model rainfall data and the predictand is the DMP product data. After several test runs, the CPT gives acceptable results in the form of graphs, diagrams, maps and tables.

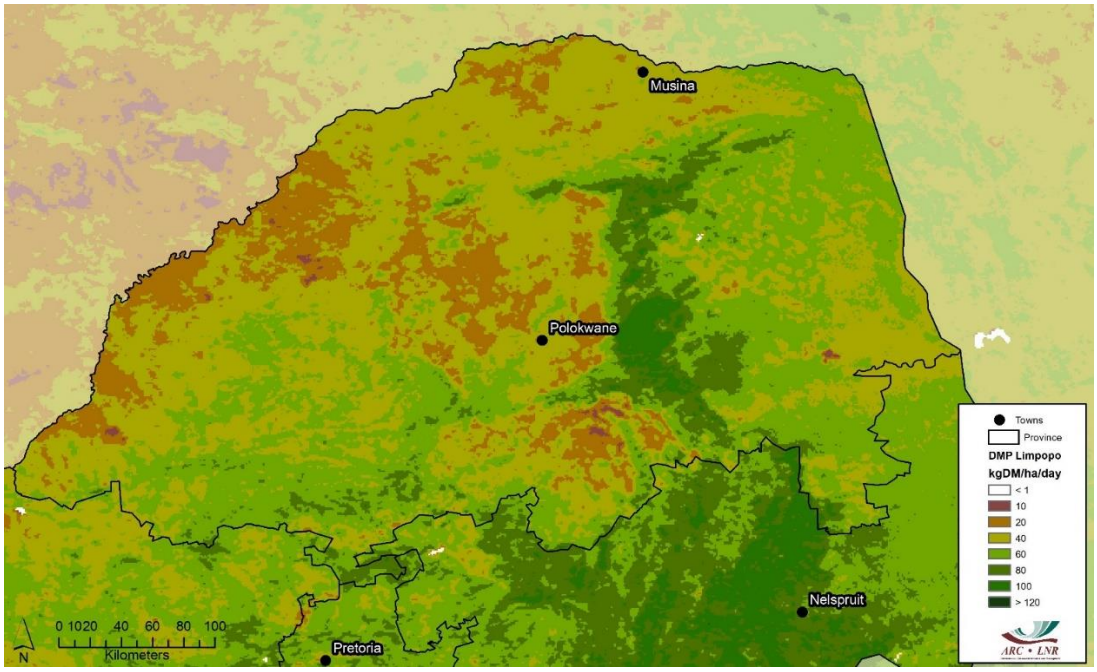

Figure 11: DMP image extracted for the Limpopo Province for the year 2008/09.

3.2.1.2 MODIS data

MODIS NPP data from 1999/00-2010/11 are obtained from the MODIS website (http://www.nasa.gov/). The spatial resolution of MODIS is 250 m. These data are used in this study because the 2005 GC map is produced using MODIS NPP data (Morgenthal *et al*., 2004; Pachavo & Murwira, 2013). Therefore, a comparison between SPOT-VEGETATION DMP and MODIS NPP is made in order to validate the prospect of using the DMP data product in this study.

This MODIS NPP product is a raster dataset, as can be seen in Figure 12. In ArcMap, the Spatial Analyst-Extraction tool is therefore used to extract NPP data to the Limpopo shapefile. Maximum composites of MODIS NPP data (11 years) are created in ArcMap 10.3 using the Spatial Analyst tool. The CPT downscaling tool is used to analyze the linear association between NPP and DMP. The results are further analyzed in Excel 2013.

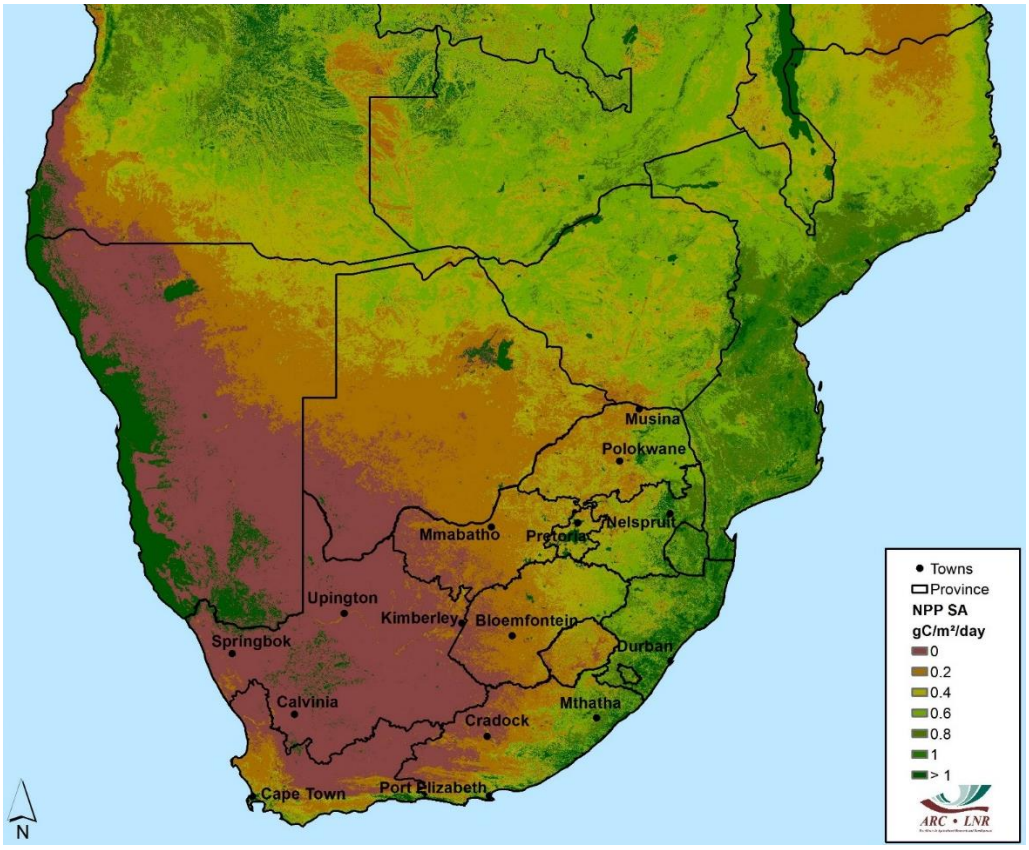

Figure 12: MODIS NPP raster image for southern Africa for the year 2008/09.

3.2.1.3 Tree density product of 2003

The tree density product of 2003 that is used is obtained from ARC-ISCW databank. The tree density map has been successfully used in research to refine rangeland GC ratings calculated with the use of NDVI data (Hansen *et al*., 2003). The tree density product comprises a map showing tree density distribution across South Africa (Figure 13). The map is produced from MODIS imagery by a consortium of institutions from Maryland in the United States of America using a global tree cover dataset (Hansen *et al*., 2003).

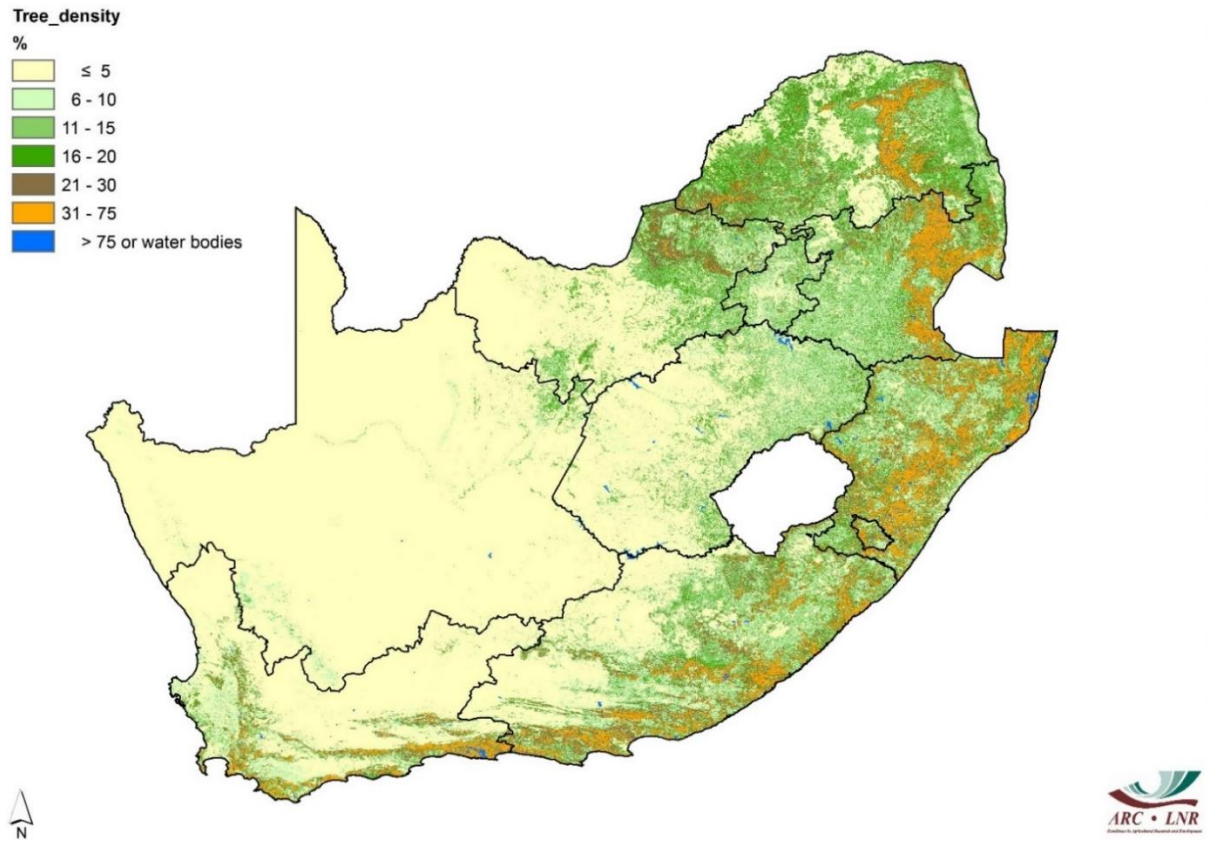

Figure 13: Tree density map of 2003 showing the distribution of trees across South Africa.

The tree density product is a raster dataset and is used as a sub-layer in ArcMap. The Spatial Analyst tool-Zonal statistics is used to calculate the tree density percentage. Further, data are stratified into various tree density categories, namely low (0-10%), medium (10-20%), high (20-30%) and extremely high tree density (30% and above). The choice of range of tree density values is influenced by the fewer tree species in the Limpopo Province in comparison with South Africa as a whole. The Geoprocessing tool is thus used to intersect the output tree density table with the vegetation map output. The output is later opened in Excel for further analysis and contains the following data: identification number (ID no), date, site no, Latitude, Longitude, grass biomass, DMP, veld types and tree density percentage per point (Appendix 1). The tree density percentage is useful for indicating areas with many trees as well as areas with less, since grass biomass will be analyzed relative to tree density across the Limpopo Province. The influence of tree density on grass biomass production varies according to percentage for example; low tree density would have minimum or no influence whereas high tree density would potentially impede biomass production. However, it should also be noted that various tree species may influence biomass production differently.

3.2.1.4 Vegetation map of 2009

The vegetation map of 2009 is obtained from the South African National Biodiversity Institute (SANBI) website (http://bgis.sanbi.org/vegmap/map.asp). This vegetation product comprises a map showing various vegetation types across South Africa.

The vegetation map is used for stratification of the DMP and Grass biomass data into various veld types in the Limpopo Province. The map is a raster dataset. Firstly, the data are added into ArcMap and the attribute table is analyzed to display the data contained in the map. The data contain columns of latitude, longitude, DMP, Grass biomass, biome, veld type and group ID. The Spatial Analyst tool is used to extract the data to the Limpopo shapefile to get corresponding positions and their veld types. This is done so that each veld type can be treated separately as each contains unique vegetation types. The output table shows veld types found in the Limpopo Province, namely Mopane, Lowveld, Azonal forests, Alluvial, Zonal & Intrazonal forests and Central bushveld (Table 1). This output table is intersected with the DMP product for each year separately. The intersect tables are later combined into one table with all the points, making it easier to analyze each grass biomass point, DMP dataset and corresponding veld type. The table is utilized to analyze the relationship between grass biomass and DMP for each veld type respectively.

Table 1: Various veld types found in the Limpopo Province.

ID	Latitude	Longitude	DMP (kgDM/ha/day)	Grass biomass (kg/ha)	Veld type	Group ID
332	-24.07	31.62	49724	1387	Mopane	87
29	-25.42	31.48	92187	4668	Lowveld	7
409	-22.42	31.24	76736	8018	Azonal forests	17
319	-23.15	31.49	34479	276	Alluvial	23
490	-22.66	30.99	63449	3502	Zonal & Intrazonal	13
63	-25.55	27.34	55035	675	Central bushveld	6

3.2.2 CPT

The CPT version 14.7.4 software is obtained from the International Research Institute for Climate and Society (IRI) website (http://iri.columbia.edu/). CPT is a statistical prediction and downscaling software which offers the following options: Principal Components Regression (PCR), CCA, Multiple Linear Regression (MLR) and General Circulation Model (GCM) verification. The CCA option is used in this study because it analyzes linear relationship between two variables – in this case DMP and low level circulation (850 hPa) of the coupled model. CCA further measures linear combinations of the two variables with maximum correlation, which meets the objective required from CPT.

The file requires input data in the form of a predictor (typically an output from a climate model) and a predictand (in this case DMP). The domains of interest are selected next in order to represent the predictor domain (Figure 14) and the predictand domain, i.e. the Limpopo Province. Statistical downscaling from the climate models to observed DMP data is performed with the CPT in order to represent verification statistics and to identify modes of seasonal-to-interannual co-variability between the predictor and predictand fields during the 12-year period.

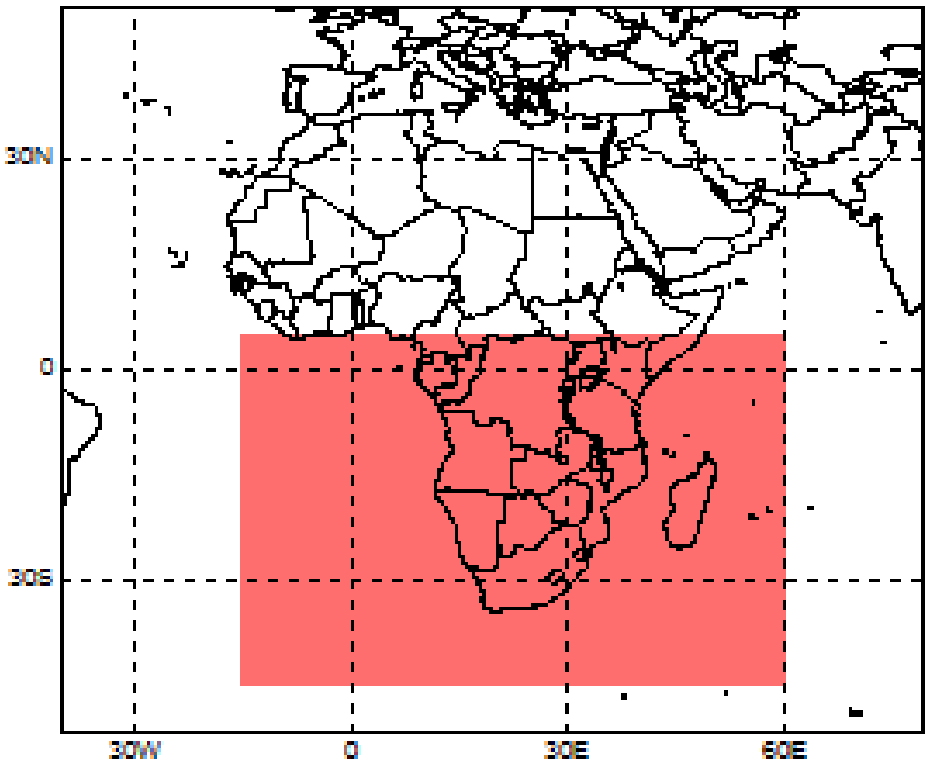

Figure 14: Domain from which model data are used to do downscaling.

3.2.3. Forecast verification

It is vital that the model's forecasts are verified, for validation of forecast quality. These results will enable the performance and accuracy of the proposed method to be analyzed. The CPT allows for the comparison of the skill of different models. In this study, probabilistic forecast verification tests are run retroactively for a 12-year period (1998/99-2009/10) to validate CPT output results. The initial training period for cross-validation is 6 years, extended by 1 year after each integration.

Verification attributes of discrimination and reliability are respectively estimated with relative operating characteristic (ROC; Mason & Graham, 1999; Mason & Graham, 2002) and reliability (Hamill, 1997, Wilks, 2006) diagrams in order to test the discrimination and reliability attributes of the forecasts. Further, the tests generate probability forecasts using error variances which are then verified (Landman *et al*., 2014). If the ROC score is 1.0, then perfect discrimination is achieved, however if the ROC scores are ≤ 0.5, the forecasts lack sufficient skill. The level of confidence in the probabilistic forecasts is seen in the reliability diagrams. When the slope of a reliability regression line lies above (below) the diagonal line of perfect reliability, the forecasts are said to be underconfident (over-confident). However, if the regression line lies perfectly on the diagonal line then perfect reliability of the forecasts is achieved. ROC and reliability diagrams are defined and interpreted in more detail in Troccoli *et al*. (2008), Barnston *et al*. (2010) and Wilks (2011) among others.

3.2.4 Rainfall data

Observed daily rainfall data for the period 1998/99-2009/10 are obtained from the ARC-ISCW, Agroclimatology division's data bank. Subsequently, rainfall grids are created using the Spatial Analyst tool in ArcView 3.1 from 10-day intervals data for 700-800 automatic weather stations in the Limpopo Province. The rainfall data are complimented with the National Oceanic and Atmospheric Prediction Centre's Climate Prediction Centre (NOAA-CPC) satellite rainfall estimate (RFE) product. The rainfall values are extracted for the corresponding number of years as the DMP, which is 1998/99-2009/10. These data are tested in CPT with rainfall as predictor and DMP as predictand. Further data analysis is done with Excel 2013.

3.2.5 Coupled model data

Climate model hindcasts of precipitation and circulation (850 hPa geopotential heights) data are obtained from the data library of the IRI. A coupled model, ECHAM4.5–MOM3-DC2 is used in this

study (see reference in Landman *et al*., 2012). The data are obtained for the corresponding DMP annual maximum composites.

3.2.6 Grass biomass field data

Ground truth data for 12 years (1998/99-2009/10) are obtained through collaboration with Dr. Tony Palmer, a specialist scientist from the Agricultural Research Council - Range and Forage Institute (ARC-RFI) who has been involved in the development of a previous CC product across South Africa. Grass biomass field data are used for the following places: Kruger National Park (KNP) for 5310 sites; Rustenburg for 116 sites; Molopo for 49 sites and Mabula game reserve for 48 sites (Figure 15). From the field data collected, only data for the Limpopo Province are used to do calculations in this study, while data for Rustenburg and Molopo are used for calibration purposes. The field data are collected using the Disc Pasture Meter method (kg/ha). The Disc pasture method is only used when measuring grass length or height, therefore the results are limited to grazers due to the field data obtained. The DPM is widely used for veld management purposes.

Ground truth data are received in Excel files with columns for average Disc measurements, date, latitude and longitude, and later converted into a GIS friendly format in ArcMap 10.3. The Spatial Analyst tool in ArcMap 10.3 is used to extract the DMP values at the ground truth points (represented by site numbers) to a shapefile for the Limpopo Province. The output is saved as a DBF table and the tables for all sites, i.e. Kruger National Park, Rustenburg, Molopo and Mabula are merged. The table is opened in an Excel spreadsheet and a regression between DMP and grass biomass for all the years is calculated. The Geoprocessing tool is used to intersect the data with the vegetation and tree density maps, whereby stratification according to group veld types is done in order to get regression equations between Grass biomass and Dry matter productivity for each veld type. Linear regression graphs are used to calculate the coefficient of determination (R^2) per veld type. The above mentioned steps are required in order to obtain equations for the veld types, which are ultimately used in calculating GC per veld type.

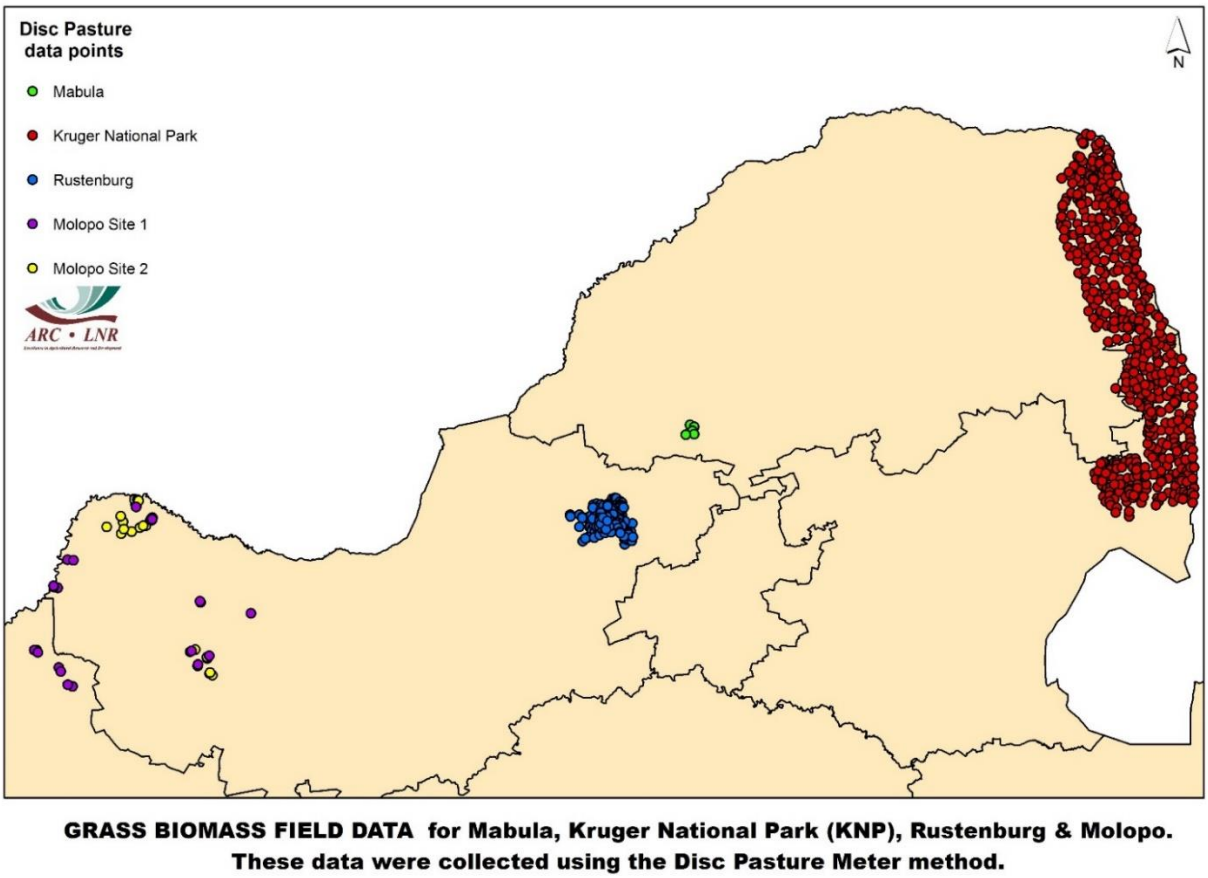

Figure 15: Field data sites for Mabula (n=48), Kruger National Park (n=5301), Rustenburg (n=116) and Molopo (n=49).

3.2.7 Modelling using the ERDAS software

In the ERDAS software, the objective is to calculate a GC estimate per veld type for each year in the 12-year period (1998/99-2009/10). The input data used in these calculations are tree density, veld type and DMP. Equations are developed with the ERDAS software in a GIS model for use in calculations. In order to calculate a GC estimate; an adjusted grass biomass is calculated first and the output is later used as input data towards calculating a DMP product estimate. The DMP product is used as a first estimate of biomass productivity. All these products are ultimately used as inputs towards estimating GC, per veld type. The first model for calculating an estimate of grass biomass is built for each year in the 12-year period. Moving forward, average DMP for all the years, i.e.1998/99-2009/10 is calculated. The mean DMP value is used as an input towards calculating an estimate of DMP for the 12-year period. These DMP estimates are ultimately used as inputs in a formula to calculate GC (Morgenthal *et al*., 2004). Lastly GC anomalies are

calculated for each year using a model in ERDAS. GC is calculated by using the following equation:

$$GC = \frac{365 \times 10}{DM \times 0.35}$$

Whereby:

365 =Days of the year

10 = Dry mass requirement per day for a large stock unit (LSU) (Kg dry mass/day)

DM = Dry biomass (kg/ha)

0.35 =Utilization factor

3.3 Synopsis

In chapter 3, data collection is tackled in different steps showing the types of products used, tools, sources and their application. These datasets/products include EOS data, field data, vegetation map, tree density and the ECHAM4.5–MOM3-DC2 coupled model output. The tools that are used for analyzing the data are as follows: ArcMap, Excel, CPT and ERDAS software. This chapter also shows specifications for choosing detailed dataset. A brief overview of forecast verification is given highlighting the use of ROC and reliability diagrams.

Secondary ground truth data are being used for validation in this study because there are limited funds to collect field data. The relationship between grass biomass and DMP data is determined by using linear regression where R^2 values are calculated per veld type. The veld types that show highly significant R^2 values indicate a positive relationship between DMP and ground truth data, while those with low R^2 values show a poor relationship for that specific veld type. The vegetation map product (2009) is the most recent available product at the time of this study and is useful to delineate the various vegetation types in Limpopo.

GC varies in different locations (veld types), thus the vegetation map serves the purpose of showing the types of vegetation found at all DMP points. Subsequently the tree density product is used for stratification purposes and calculating tree density per veld type. Veld types with higher tree density will have less grass for grazing due to shade and competition for sunlight or radiation. Finally, in the ERDAS software GIS models are built to calculate GC with the following inputs: Tree density product, veld type and DMP for each year (1998/99-2009/10), for each growing season (NDJFMA). The outputs are CC deviation maps which give confidence in forecasting GC for NDJFMA seasons in the Limpopo Province.

CHAPTER 4

RESULTS AND DISCUSSION

4.1 SPOT-VEGETATION DMP and CPT data analysis

4.1.1 Spearman's correlation tests

The main objective of this chapter is to explore if there is skill in forecasting CC for the Limpopo Province; which is potentially achieved by exploring the relationship between DMP and coupled model rainfall using the Spearman's rank correlation. Whether a hypothesis is approved or disproved may be decided with the aid of the Spearman's rank correlation which is a robust and resistant alternative to the Pearson or ordinary correlation.

Figure 16 shows the Spearman's rank correlation, reflecting the skill of the model (coupled model DJF rainfall data as a predictor for DMP). It shows whether the correlation between the variables is high or low based on the values -0.8 (inversely/negatively correlated) to 0.8 (highly positively correlated). The results indicate positive correlations between forecast seasonal rainfall and the DMP product over the Limpopo Province, especially over the drier areas where grazing is prevalent, i.e. north-eastern parts of the Limpopo Province. The low correlation at the escarpment is a result of the quality of the RS products. The results, however certainly show that rainfall can be used to predict DMP in the Limpopo Province. These results show potential use of a forecast model to predict CC, considering that DMP is one of the primary input parameters for calculating CC.

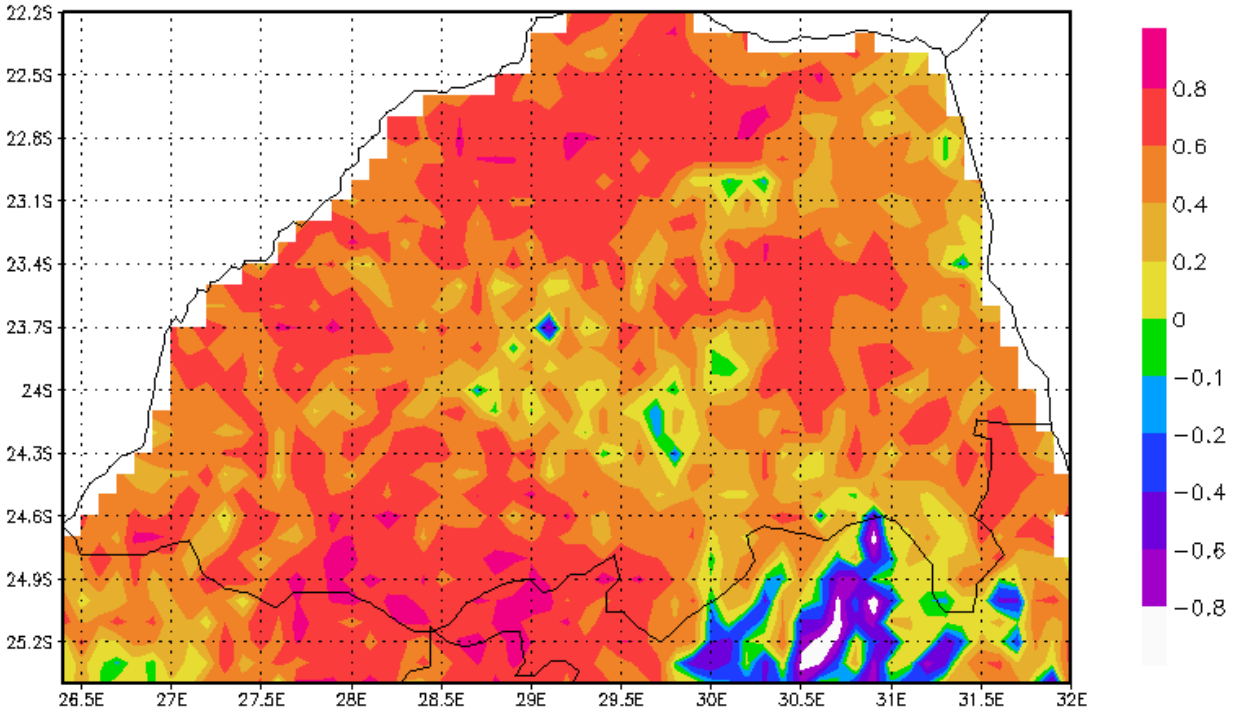

Figure 16: Spearman's rank correlations for the coupled model DJF rainfall data used as predictor downscaled to NDJFMA DMP values over the Limpopo Province spanning the 12-year period.

One of the aims of the research is to use seasonal forecasts to estimate the expected CC product every month. To dynamically update CC within a season, best lead-times for rainfall seasons must be identified. Therefore, further tests are run with the CPT using the coupled model rainfall and DMP data at a 1-month lead time, which means that for DJF, the data are downloaded in November and the same rule applies to all other 3-month, 4-month and whole season periods. Ultimately, eight rainfall (and DMP composites) seasons are identified as follows: November-December-January (NDJ), November-December-January-February (NDJF), NDJFMA, DJF, December-January-February-March (DJFM), January-February-March (JFM), January-February-March-April (JFMA) and February-March-April (FMA) to allow for optimal correlation windows.

Subsequently, the coupled model data for these eight seasons are downloaded and accumulated – as well as DMP composites for the respective seasons calculated in ArcMap. Other variables than rainfall are explored for predicting DMP such as coupled model regional circulation (850 hPa geopotential heights) data. The coupled model geopotential heights (850 hPa) are shown to resolve DMP response, as the results show a similar level of skill to the coupled model rainfall, especially in areas with high grazing activities. Results show largely positive correlations between downscaled regional circulation (850 hPa) and DMP. Yet again, this validates the potential use of

low level circulation predicted by a coupled model to in turn predict CC. Further tests are run in the CPT to investigate which of the 8 coupled model geopotential heights (850 hPa) seasons best predict the DMP product (also considering 8 DMP seasons). After analyzing the output results from the CPT, four of the eight seasons show substantial positive results, namely NDJ, DJF, JFM and FMA. However, of the four model data seasons, DJF is identified to give high skill in predicting NDJ, DJF, JFM and FMA DMP seasons (Figure 17).

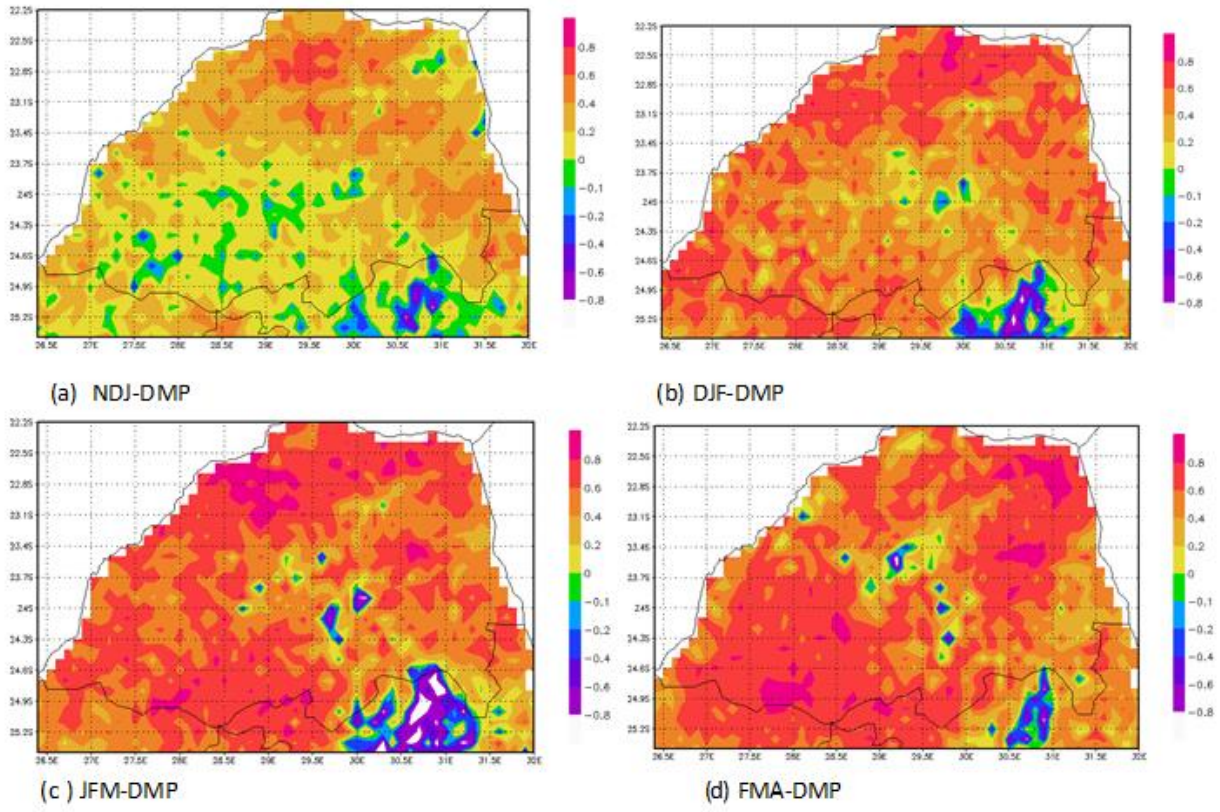

Figure 17: Spearman's rank correlations for the coupled model DJF 850 hPa geopotential heights downscaled to DMP values considering four 3-month seasons (a) Coupled model vs NDJ-DMP, (b) Coupled model vs DJF-DMP, (c) Coupled model vs JFM-DMP and (d) Coupled model vs FMA-DMP over the Limpopo Province spanning the 12-year period.

4.1.2 ROC and Reliability diagrams

The main goal of this section is to demonstrate how skillful the DJF coupled model geopotential heights (850 hPa) hindcasts are in predicting DMP seasons over the Limpopo Province by testing the 4 growing seasons (NDJ, DJF, FMA and JFM). Figure 18 for NDJ season shows above-normal scores of 0.55, which means that there is 55% chance for above-normal DMP events to occur. Below-normal ROC scores are 0.58, which means that there is 58% chance for the below-normal events to occur. Lastly is the near-normal category, which shows less than 50% chance of near-normal events happening. Therefore, the results show good discrimination of above- and below-normal DMP seasons by the ECHAM4.5–MOM3-DC2 model.

Figure 19 for DJF season shows that for the above-normal category, ROC scores are 0.61 which means there is a high chance for above-normal DMP conditions during DJF. The below-normal category shows ROC scores of 0.72, which shows an even higher chance of below-normal conditions occurring during DJF. Near-normal category shows less than 50% chance of near-normal DMP conditions occurring. The CGCM is unable to discriminate near-normal DMP seasons from other seasons.

Figure 20 for JFM season shows that the above-normal ROC scores are 0.56, while ROC scores for below-normal category are 0.66. And lastly near-normal events are less than 50% which means that there is little skill in the ECHAM4.5–MOM3-DC2 model predicting near-normal DMP seasons. However, the CGCM is able to discriminate above- and below-normal DMP seasons from other seasons.

Finally, Figure 21 for FMA season shows that the above-normal ROC scores are 0.70, showing a high chance of above-normal events happening. The below-normal ROC scores are 0.78, showing an even higher chance of below-normal events occurring. However, less than 50% chance for near-normal category can be seen. Therefore, it can be seen that above- and below-normal categories are discriminated with great skill, however below-normal category shows the highest skill of prediction during this season.

Above- and below-normal DMP conditions are crucial for farmers in the Limpopo Province therefore the diagrams below can assist in giving guidelines for example, if the forecasts show above-normal DMP conditions, the farmers can know how many livestock should be grazed on a portion of grazing land. Below-normal conditions can mainly be seen during drought conditions when rainfall is less than what is needed for natural vegetation to grow, so these results can be utilized to give advisories during times of droughts. For example, in the 2014/15 El Niño period,

these results could have been used to guide livestock farmers on grazing patterns as well as grazing their livestock close to water sources. It is important to note that for all the above figures, near-normal conditions are not well discriminated by the ECHAM4.5–MOM3-DC2 DJF model. Studies show that near-normal conditions are not easily captured by models and are therefore not reported in most studies (Van den Dool & Toth, 1991).

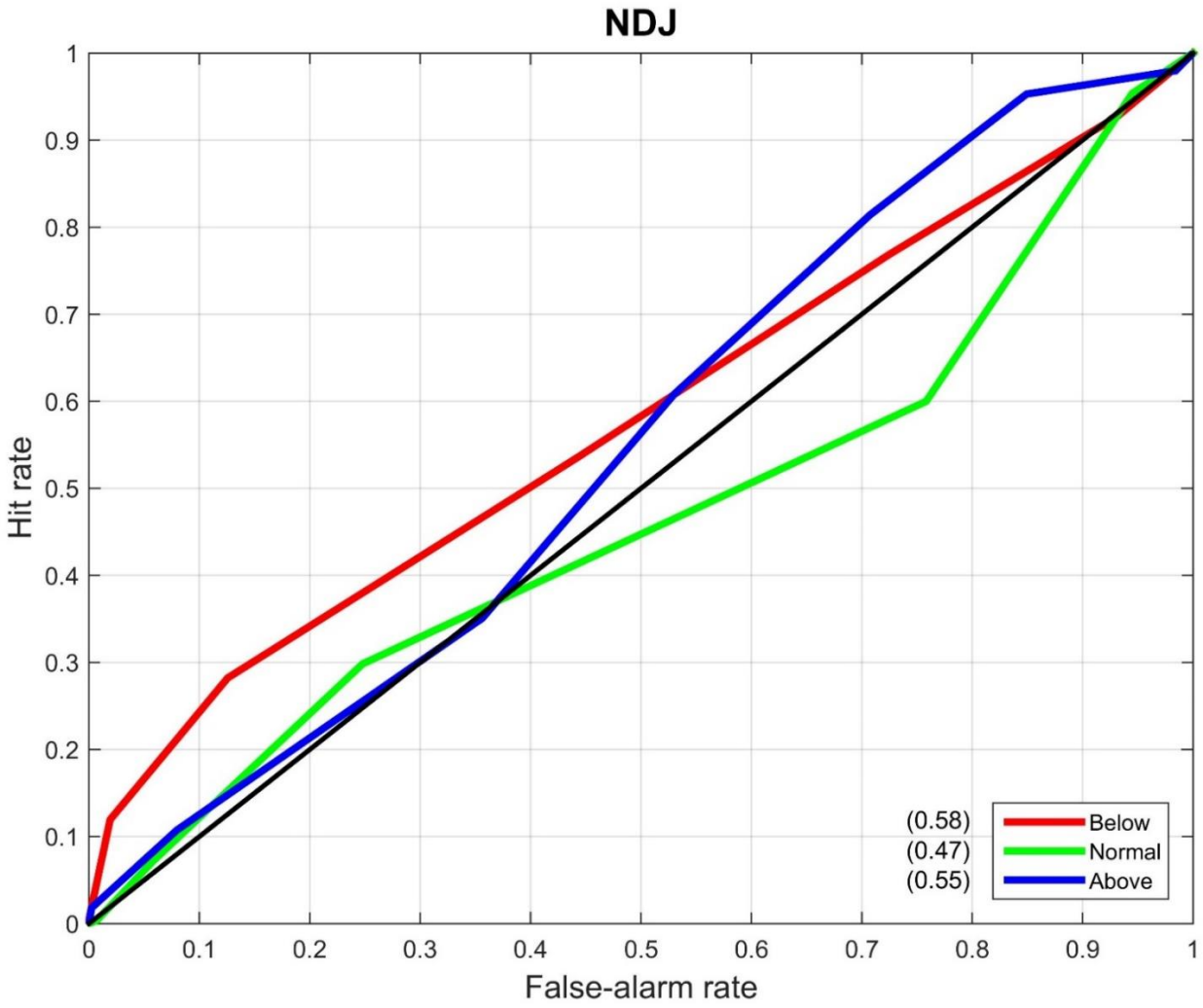

Figure 18: ROC curves obtained by retroactively predicting DMP probabilistically over 12 years (1998/99-2009/10) for the NDJ season for above-, below- and near-normal tercile values of the climatological record. The areas underneath the respective curves are shown in parenthesis on the Figure. The x axis shows False-alarm rate, while the y axis shows Hit rate.

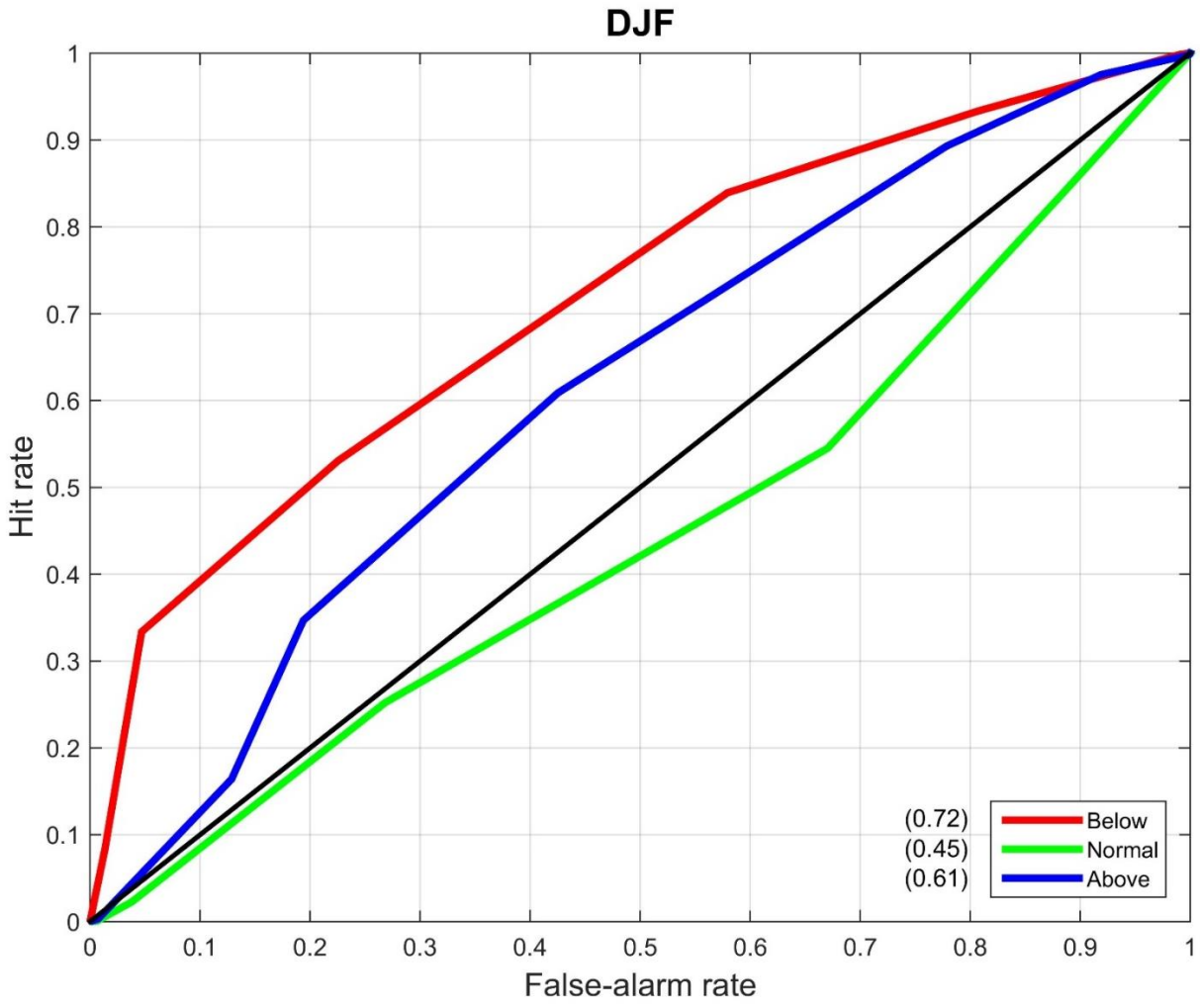

Figure 19: ROC curves obtained by retroactively predicting DMP probabilistically over 12 years (1998/99-2009/10) for the DJF season for above-, below- and near-normal tercile values of the climatological record. The areas underneath the respective curves are shown in parenthesis on the Figure. The x axis shows False-alarm rate, while the y axis shows Hit rate.

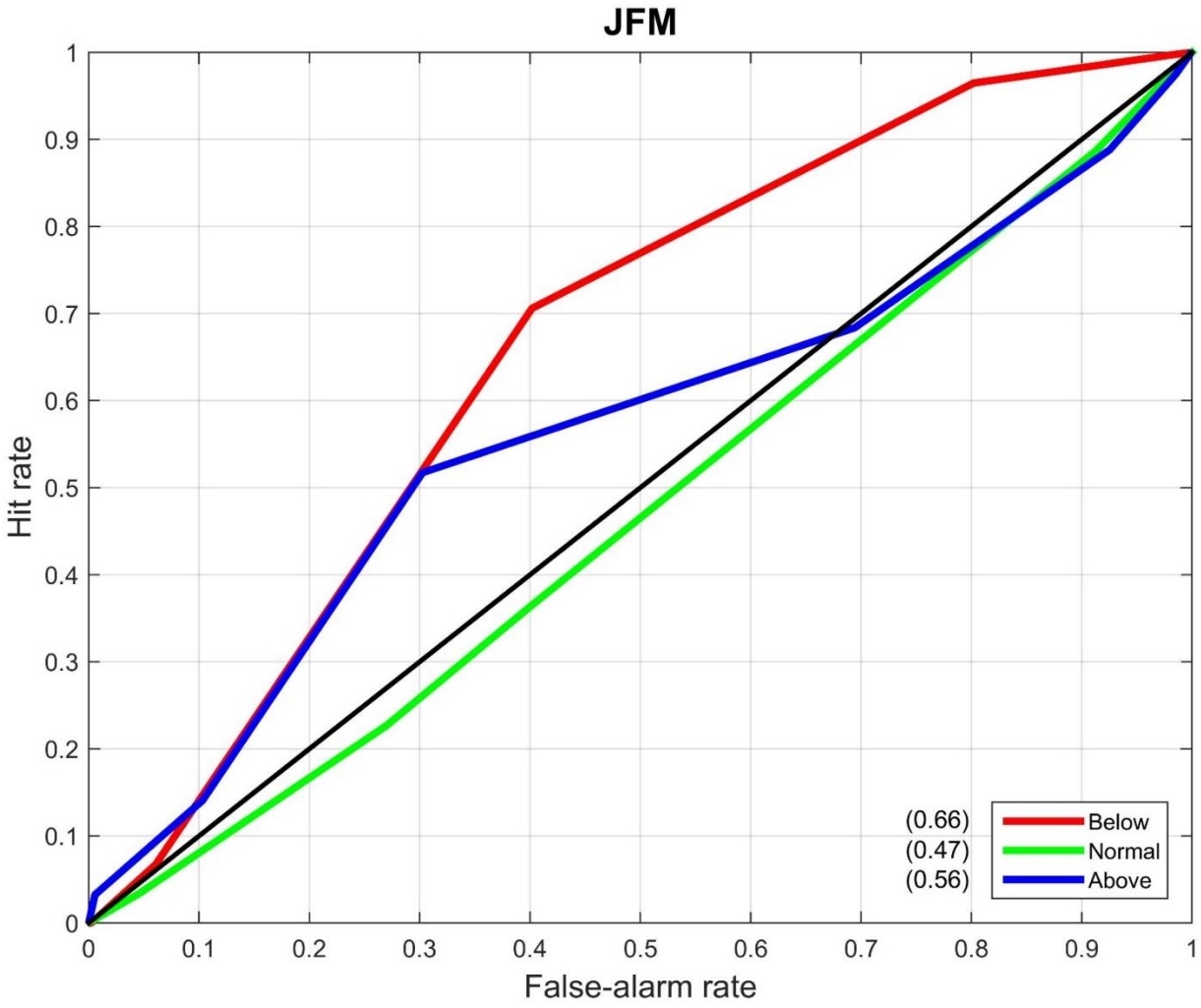

Figure 20: ROC curves obtained by retroactively predicting DMP probabilistically over 12 years (1998/99-2009/10) for the JFM season for above-, below- and near-normal tercile values of the climatological record. The areas underneath the respective curves are shown in parenthesis on the Figure. The x axis shows False-alarm rate, while the y axis shows Hit rate.

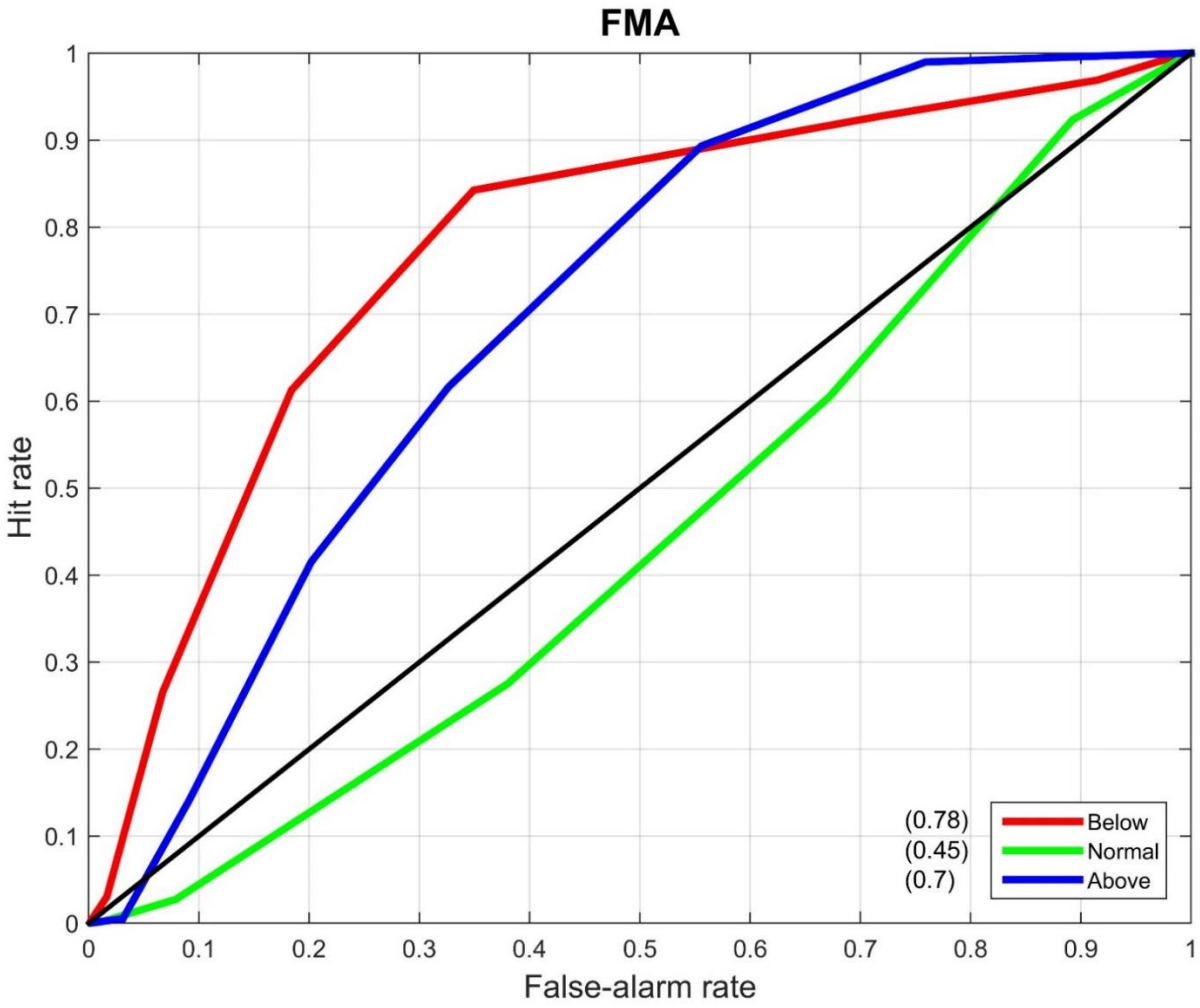

Figure 21: ROC curves obtained by retroactively predicting DMP probabilistically over 12 years (1998/99-2009/10) for the FMA season for above-, below- and near-normal tercile values of the climatological record. The areas underneath the respective curves are shown in parenthesis on the Figure. The x axis shows False-alarm rate, while the y axis shows Hit rate.

In Figure 22, considering the NDJ DMP season, High DMP regression line shows over-confidence, which means the model is not reliable in predicting high DMP conditions during this season. The low DMP regression line shows underconfidence between 0-43%, thus showing better reliability in the model for predicting low DMP conditions in this season.

In Figure 23, considering the DJF season, high DMP regression line is underconfident for only about 19%, but is over-confident between 20-100%. The regression line for low DMP shows over-confidence between 0-60%, but shows underconfidence for only a small portion (about 40%). Therefore, model shows low reliability in predicting both high and low DMP conditions in this season.

In Figure 24, during JFM, high DMP regression line shows over-confidence (34%) which means low reliability in the model predicting high DMP conditions in this season. However, the low DMP regression line shows underconfidence between 35-75%. There is high reliability in the model for predicting low DMP conditions in this season.

Lastly, during the FMA season (Figure 25), regression lines for both high and low DMP are lying close to the perfect diagonal. However, the high DMP line shows over-confidence, while the low DMP line shows underconfidence for about 42% and over-confidence between 43-100%. There is therefore low reliability in the model for predicting both high and low DMP conditions in this season. Reliability diagrams show over-confidence for high DMP seasons and underconfidence for low DMP seasons during the NDJ and JFM seasons, whereas low reliability in the model is demonstrated during the DJF and FMA seasons for both high and low DMP conditions.

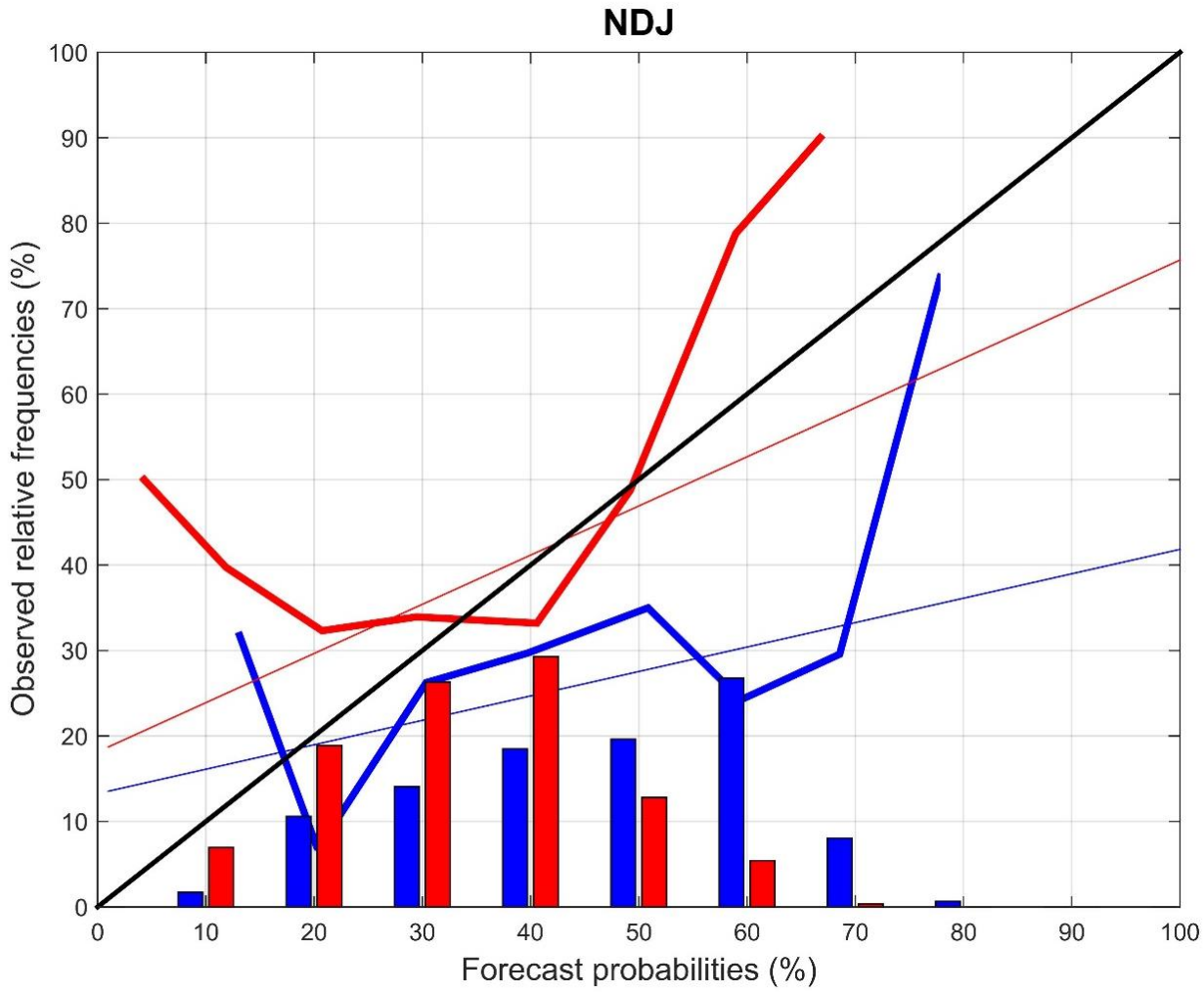

Figure 22: Reliability diagram and frequency histogram for above- (66th tercile) and below- (33rd tercile) normal DMP values for NDJ obtained by downscaling the coupled model's low level circulation. The thick blue (red) curve and the blue (red) bars represent high (low) DMP category. The thin blue (red) line is the weighted least squares regression line of the high (low) DMP reliability curve.

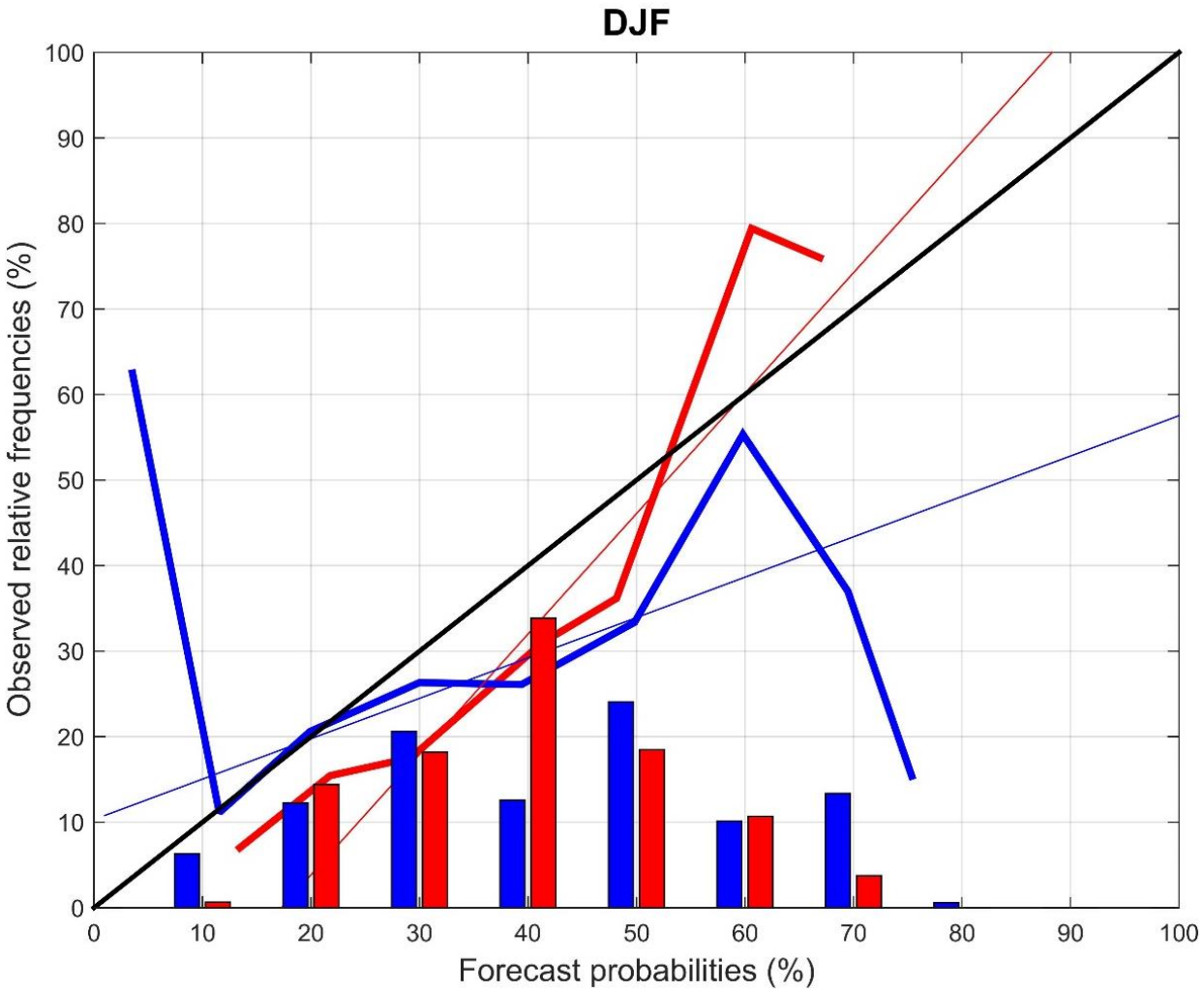

Figure 23: Reliability diagram and frequency histogram for above- (66th tercile) and below- (33rd tercile) normal DMP values for DJF obtained by downscaling the coupled model's low level circulation. The thick blue (red) curve and the blue (red) bars represent high (low) DMP category. The thin blue (red) line is the weighted least squares regression line of the high (low) DMP reliability curve.

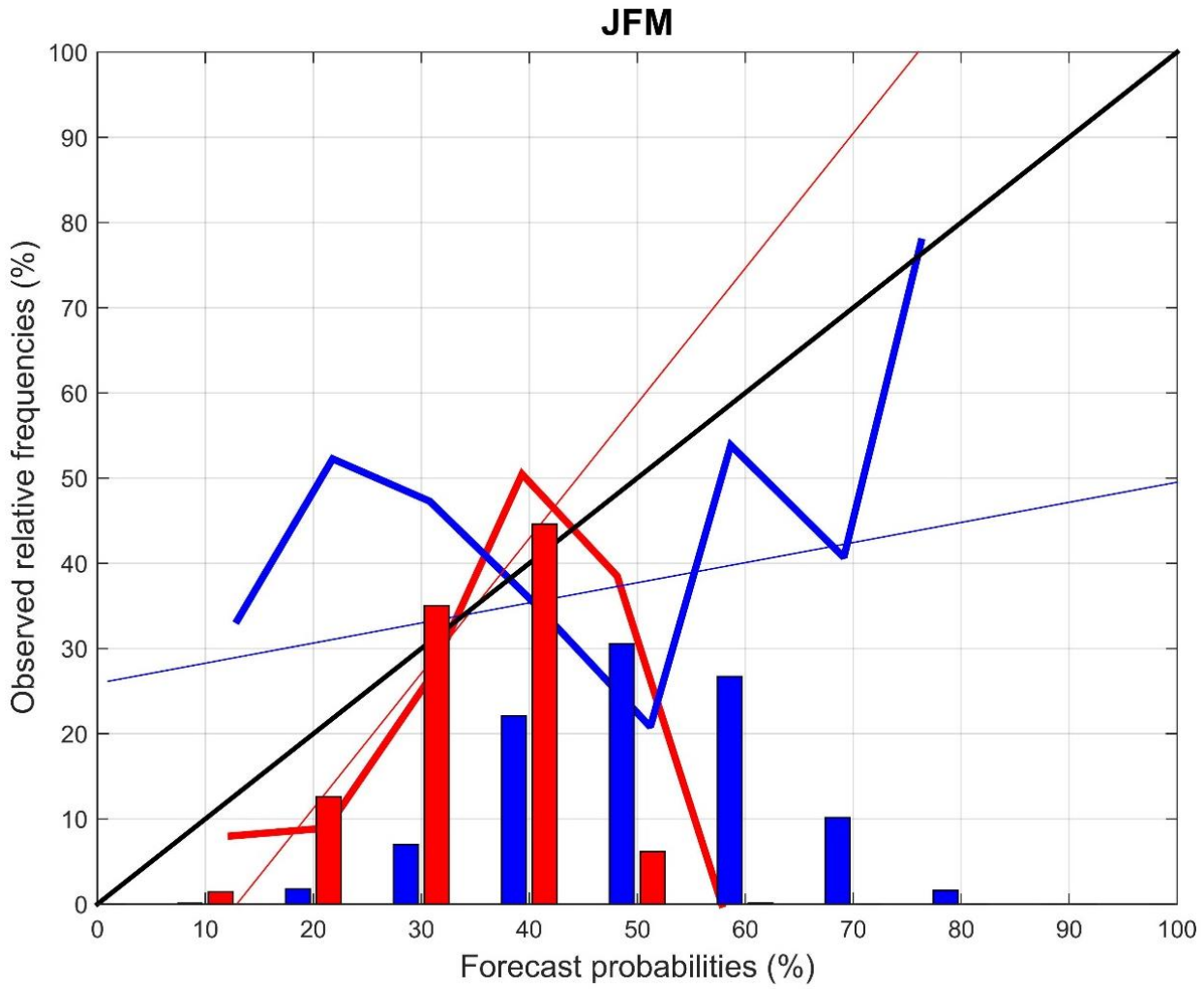

Figure 24: Reliability diagram and frequency histogram for above- (66th tercile) and below- (33rd tercile) normal DMP values for JFM obtained by downscaling the coupled model's low level circulation. The thick blue (red) curve and the blue (red) bars represent high (low) DMP category. The thin blue (red) line is the weighted least squares regression line of the high (low) DMP reliability curve.

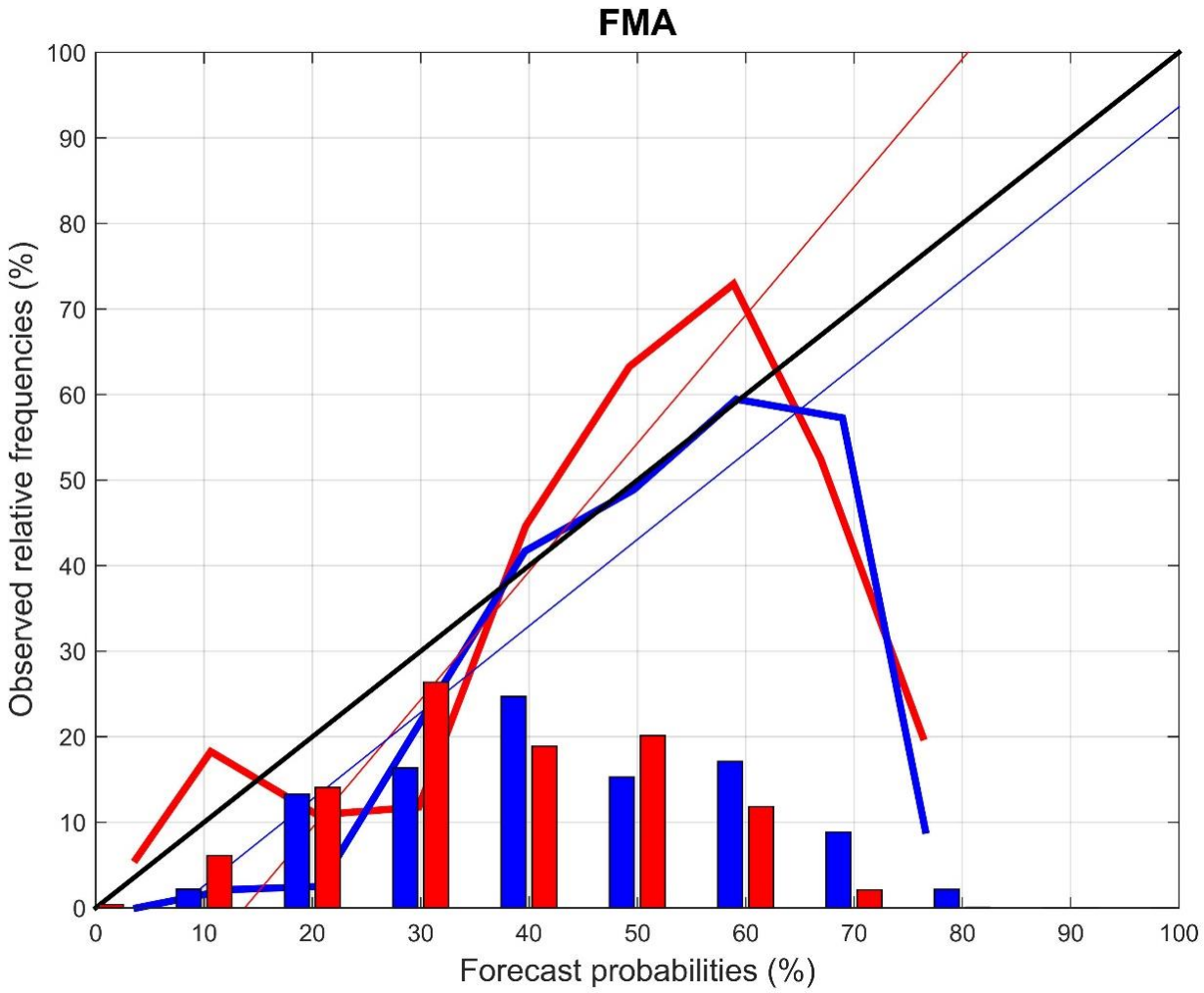

Figure 25: Reliability diagram and frequency histogram for above- (66th tercile) and below- (33rd tercile) normal DMP values for FMA obtained by downscaling the coupled model's low level circulation. The thick blue (red) curve and the blue (red) bars represent high (low) DMP category. The thin blue (red) line is the weighted least squares regression line of the high (low) DMP reliability curve.

4.1.3 Coupled model and accumulated DMP correlation tests

More tests are run using the CPT where an accumulated value of the DMP 3-month seasons is used to analyze what the outcome would be and positive results are found, leaving coupled model DJF low level circulation (850 hPa) as the best predictor of NDJFMA DMP product (Figure 26).

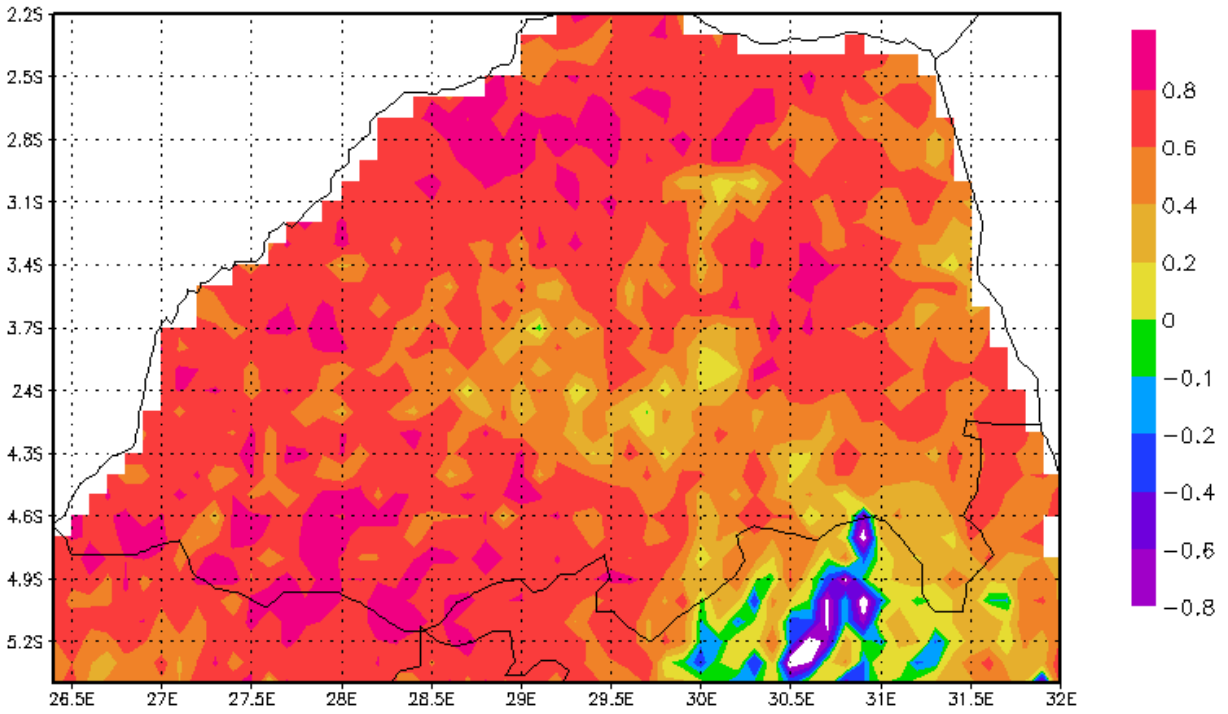

Figure 26: Spearman's rank correlations for the coupled model DJF 850 hPa geopotential heights downscaled to NDJFMA DMP values over the Limpopo Province spanning the 12-year period.

Subsequently verification tests are run to demonstrate that DJF low-level circulation is a good predictor of NDJFMA DMP – thus showing that it is possible to predict DMP with the coupled model data (850 hPa geopotential heights). In the ROC diagram, above- and below-normal curves lie more to the upper left corner showing good skill – coupled model can discriminate below- and above-normal DMP seasons from other seasons in the Limpopo Province (Figure 27). However, the normal curve lies on the right of the no skill line showing lack of skill of coupled model in predicting DMP in near-normal DMP seasons. Therefore, forecasts for both above-and below-normal conditions can be issued with confidence to farmers.

The reliability diagram in Figure 28 shows over-confidence for the high DMP regression line, while the low DMP regression line shows underconfidence for about 44% and over-confidence between 45-100%. The model shows better reliability in predicting below-normal DMP conditions during the NDJFMA season.

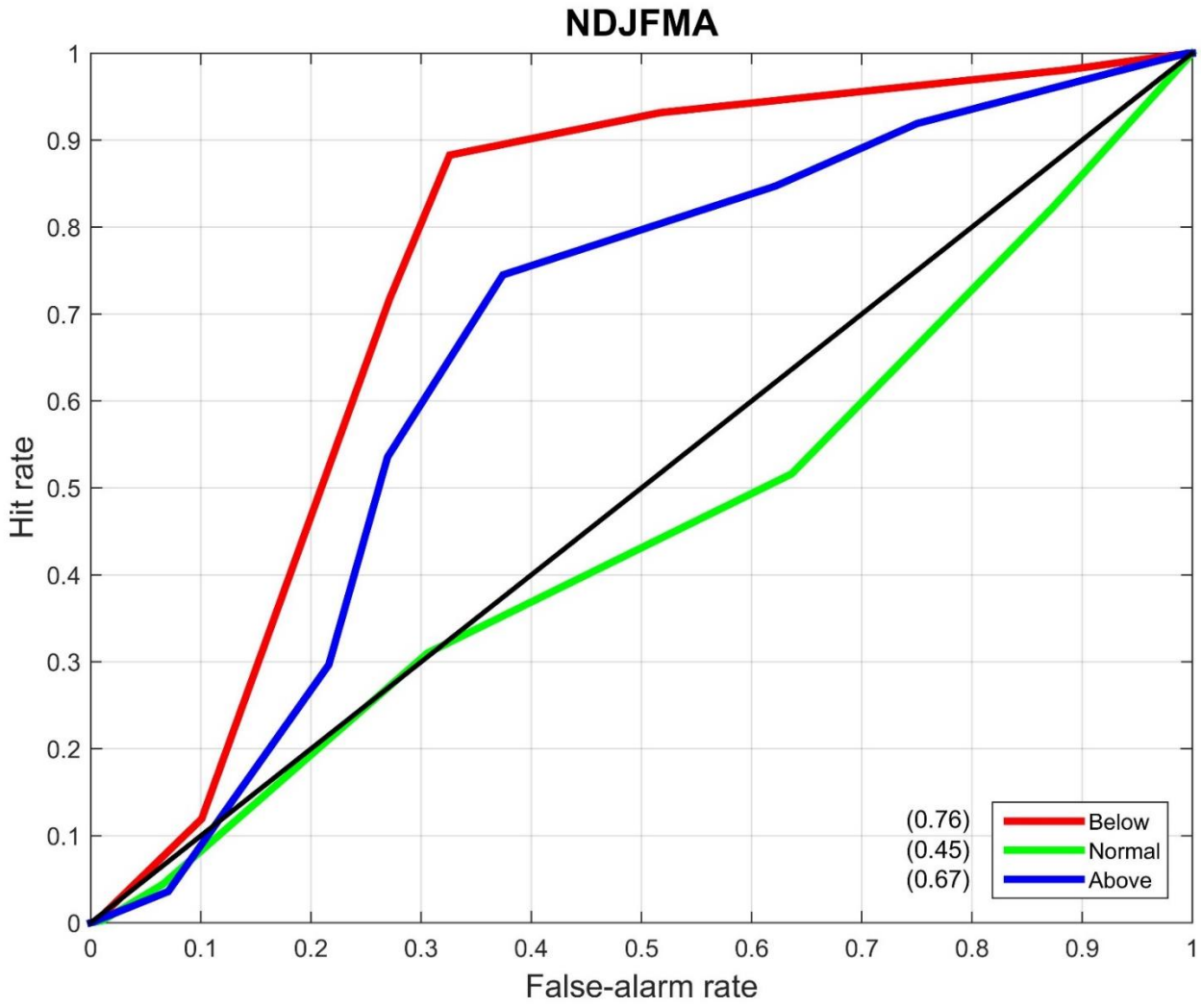

Figure 27: ROC curves obtained by retroactively predicting DMP probabilistically over 12 years (1998/99-2009/10) for the NDJFMA season for above-, below- and near-normal tercile values of the climatological record. The areas underneath the respective curves are shown in parenthesis on the Figure. The x axis shows False-alarm rate, while the y axis shows Hit rate.

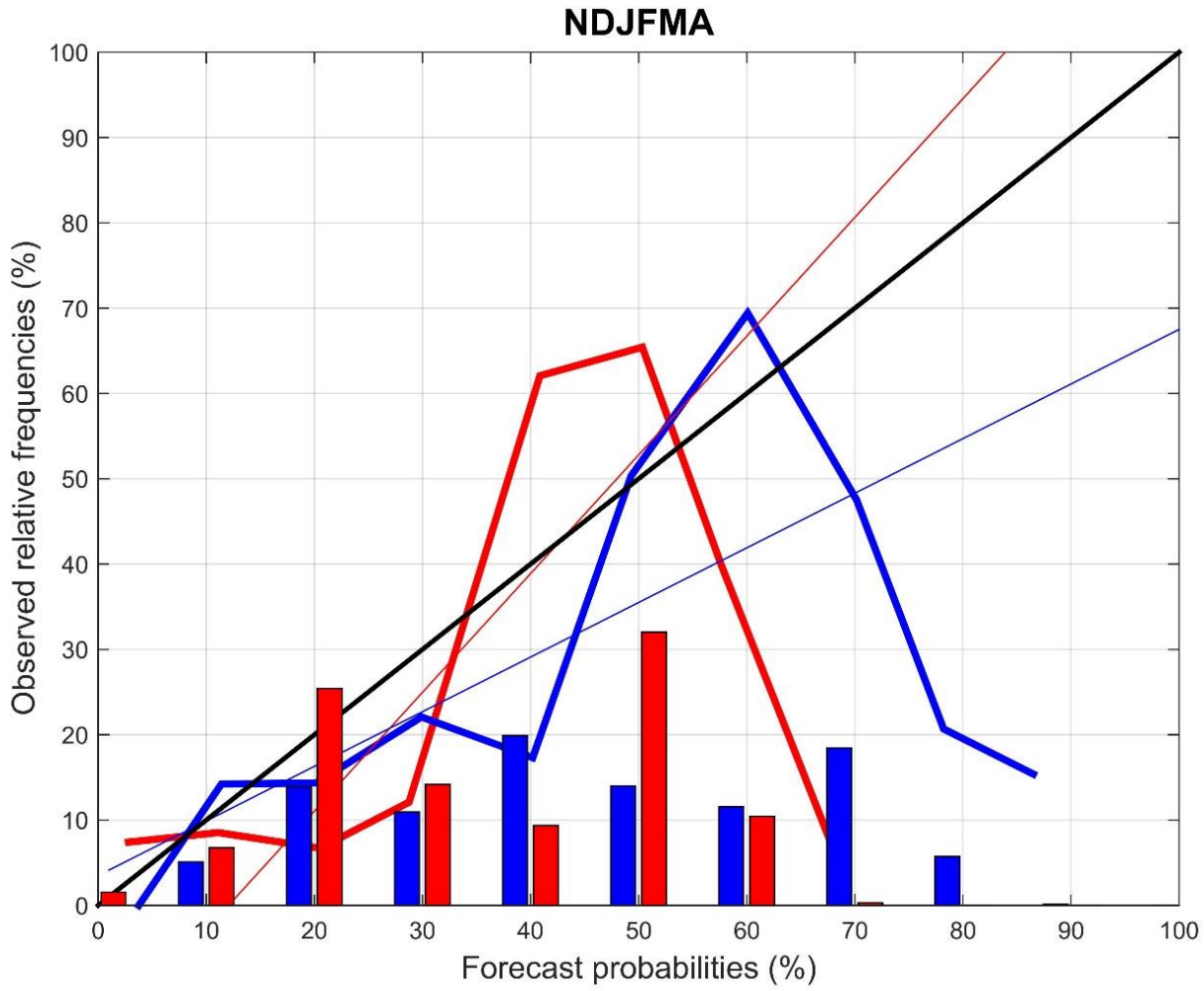

Figure 28: Reliability diagram and frequency histogram for above- (66th tercile) and below- (33rd tercile) normal DMP values for NDJFMA obtained by downscaling the coupled model's low level circulation. The thick blue (red) curve and the blue (red) bars represent high (low) DMP category. The thin blue (red) line is the weighted least squares regression line of the high (low) DMP reliability curve.

The ROC scores are summarized in a table format for better comparison and to show that NDJFMA indeed shows improved results as a whole season compared to the four 3-month seasons (Table 2). The ROC scores confirm that the CGCM model successfully discriminates below- and above- normal DMP seasons, albeit it is only for a short climatological record. Figure 29 shows a typical time series of good correlation between hindcasts and observations for the 12-year period (e.g. Wilks, 2011). It should be noted however that it is a challenging task to use short data sets in verification tests (Landman *et al*., 2014).

Table 2: Summary of ROC scores comparing the four 3-month seasons to the whole season.

Period	Season	Below-normal	Near-normal	Above-normal
3-month season	NDJ	0.58	0.47	0.55
	DJF	0.72	0.45	0.61
	JFM	0.66	0.47	0.56
	FMA	0.78	0.45	0.70
Whole season	NDJFMA	0.76	0.45	0.67

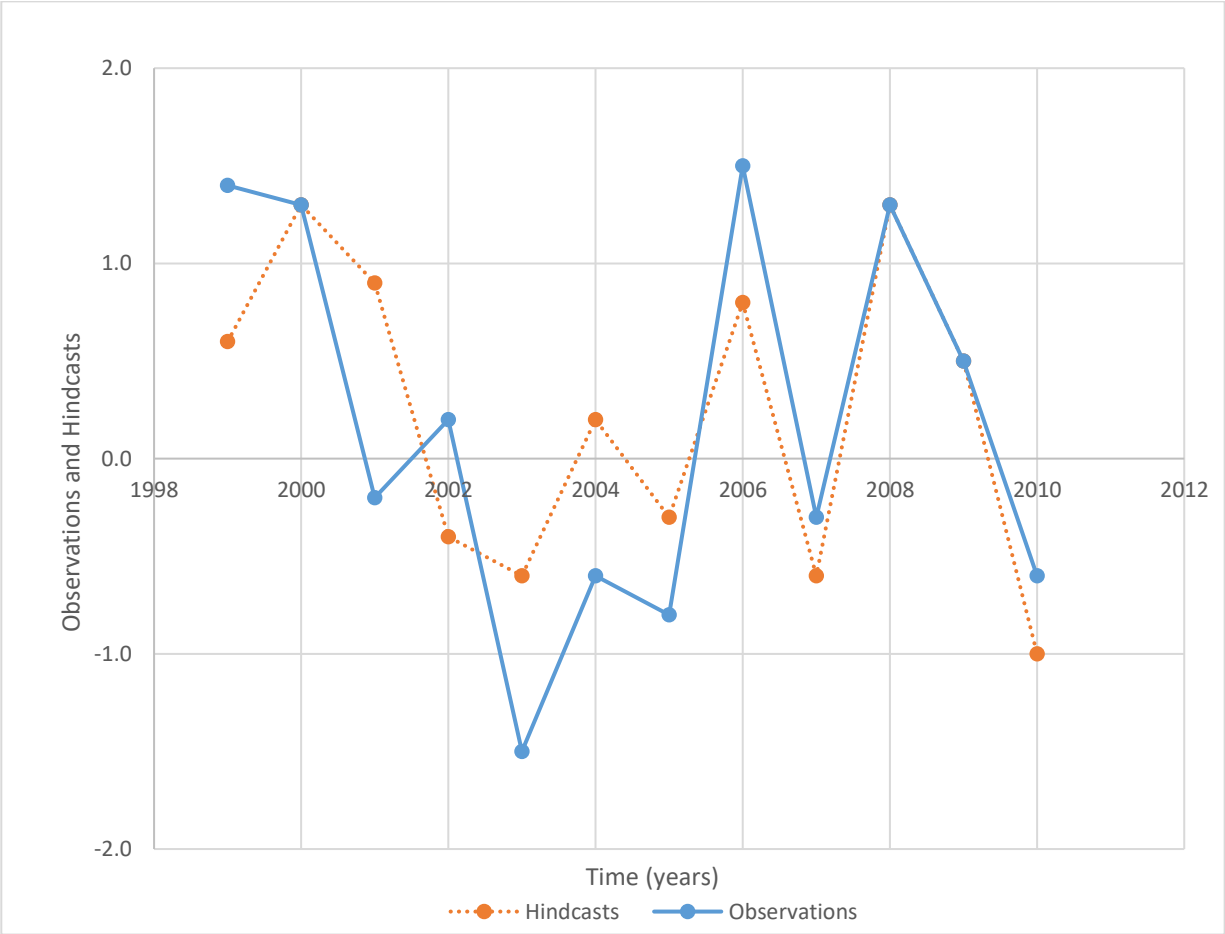

Figure 29: Time series showing a good correlation between observations and hindcasts over the 12-year training period.

4.2 MODIS NPP data analysis

A comparison between the DMP dataset product and MODIS NPP is made in order to validate the prospect of using SPOT-VEGETATION data in this study. DMP and NPP are directly related, however the units of measurement differ, it should be noted that for the sake of better comparison, units of measurement are customized in this study. DMP is generally lower than NPP and sometimes NPP could be twice as much as DMP. A time series graph (Figure 30), shows a positive correlation between NPP and DMP, giving confidence in the use of DMP data in the current study.

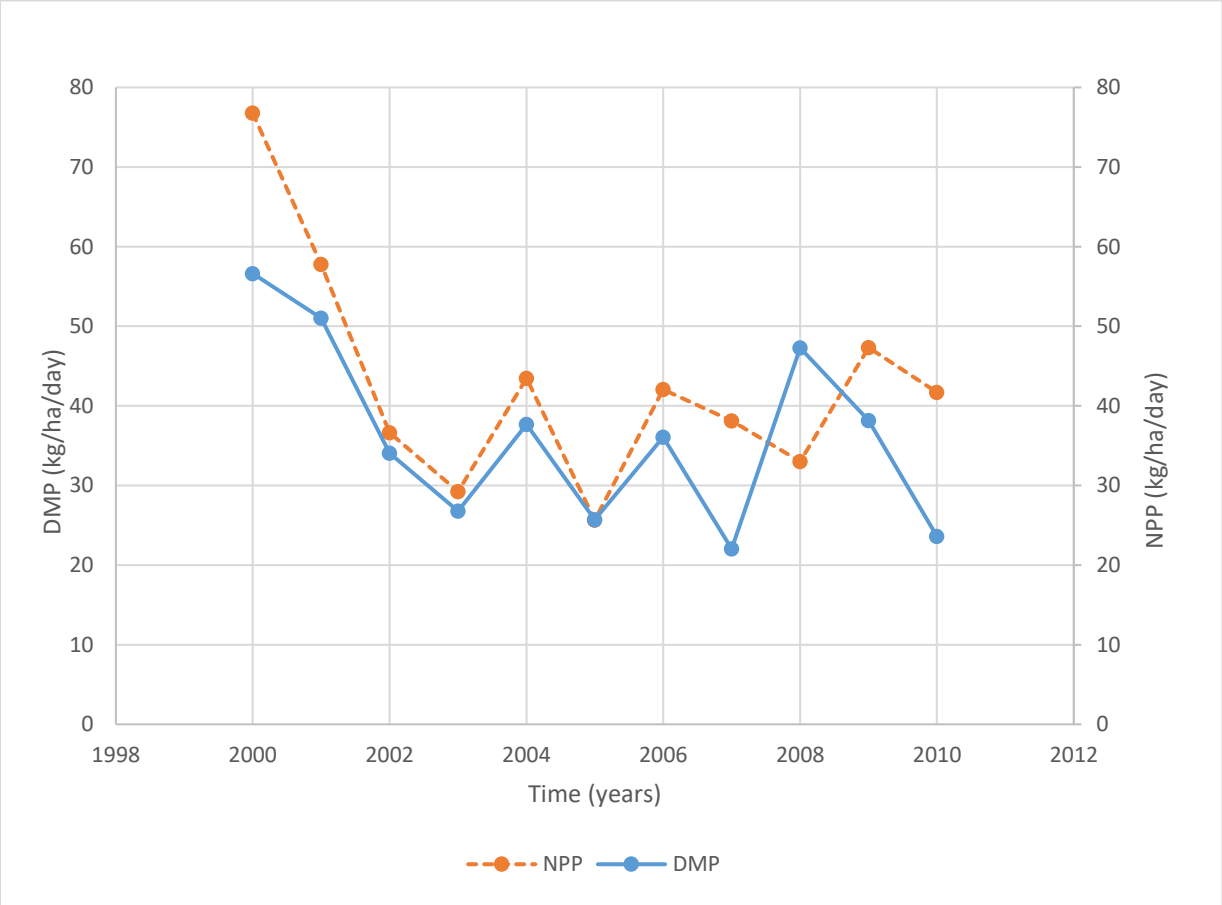

Figure 30: Time series showing a positive correlation between DMP and NPP for 11 years (2000-2010).

4.3 Ground truth data and EO data analysis

4.3.1 Ground truth data

The relationship between DMP and field data in each specific site is analyzed for 12 years (1998/99-2009/10) using linear regression (Figure 31). The R^2 value of 0.75 shows a positive and high correlation between these two variables. This positive correlation shows that DMP may be used as a representative of grass biomass in this research.

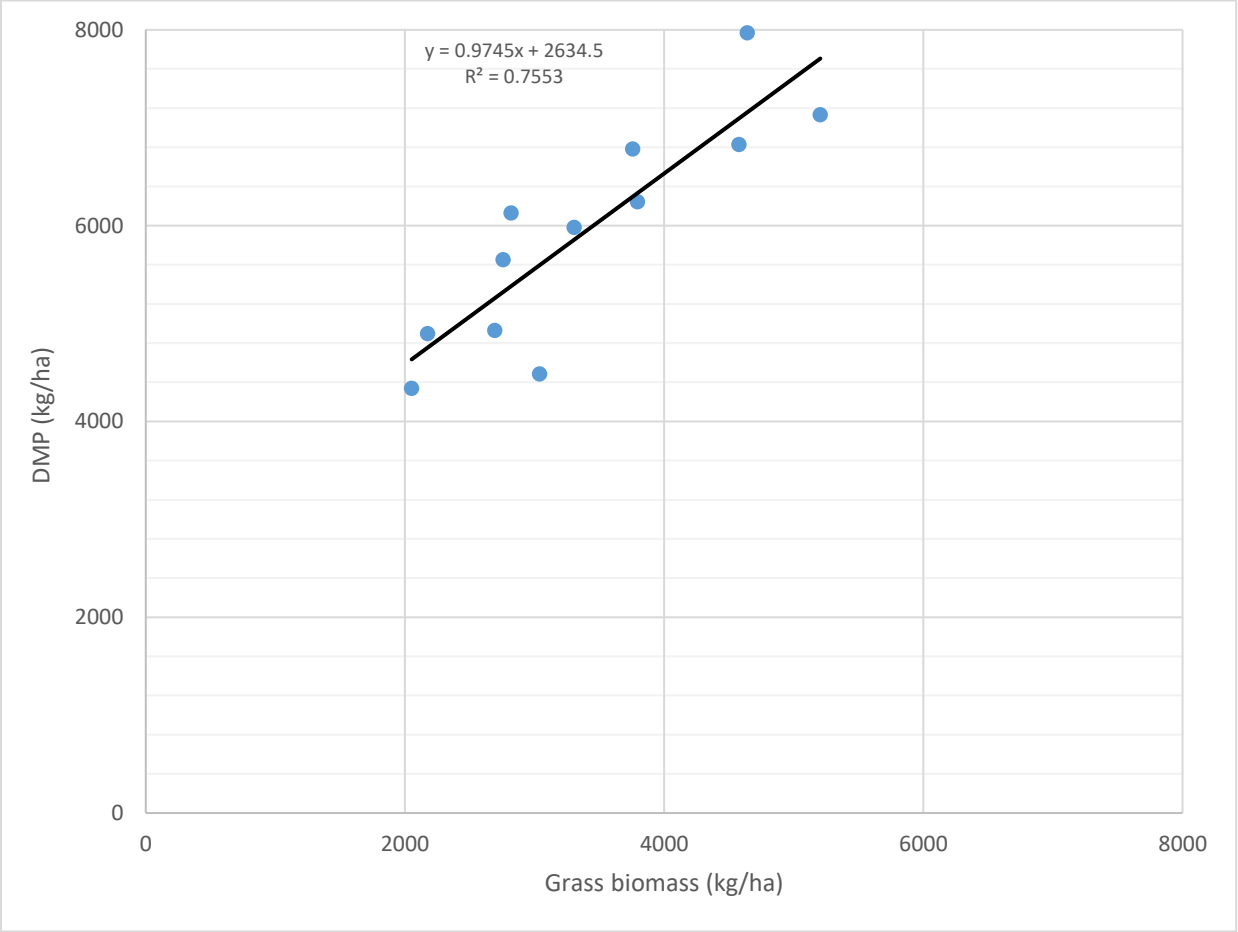

Figure 31: Relationship between average NDJFMA DMP and grass biomass for all veld types (n=12). The x-axis shows grass biomass while the y-axis shows DMP.

4.3.2 Vegetation map of 2009 product analysis

The vegetation map of 2009 – the most recent available product at the time of this study – is used to stratify the grass biomass and DMP data into various biomes and veld types. Linear regression graphs are used to explore the relationship between grass biomass and DMP in each respective veld type (Figures 32-37). The results show positive high correlations between average grass biomass and DMP for some veld types. Figure 32 shows a positive correlation with an R^2 value of 0.82 in the Mopane veld type. The Mopane veld type lies in the eastern parts of the Limpopo Province (mostly in the KNP) where wildlife grazing is prevalent. This veld type contains high grass biomass as the area is a natural habitat and therefore consists of natural vegetation for the various types of wildlife that are conserved in the park.

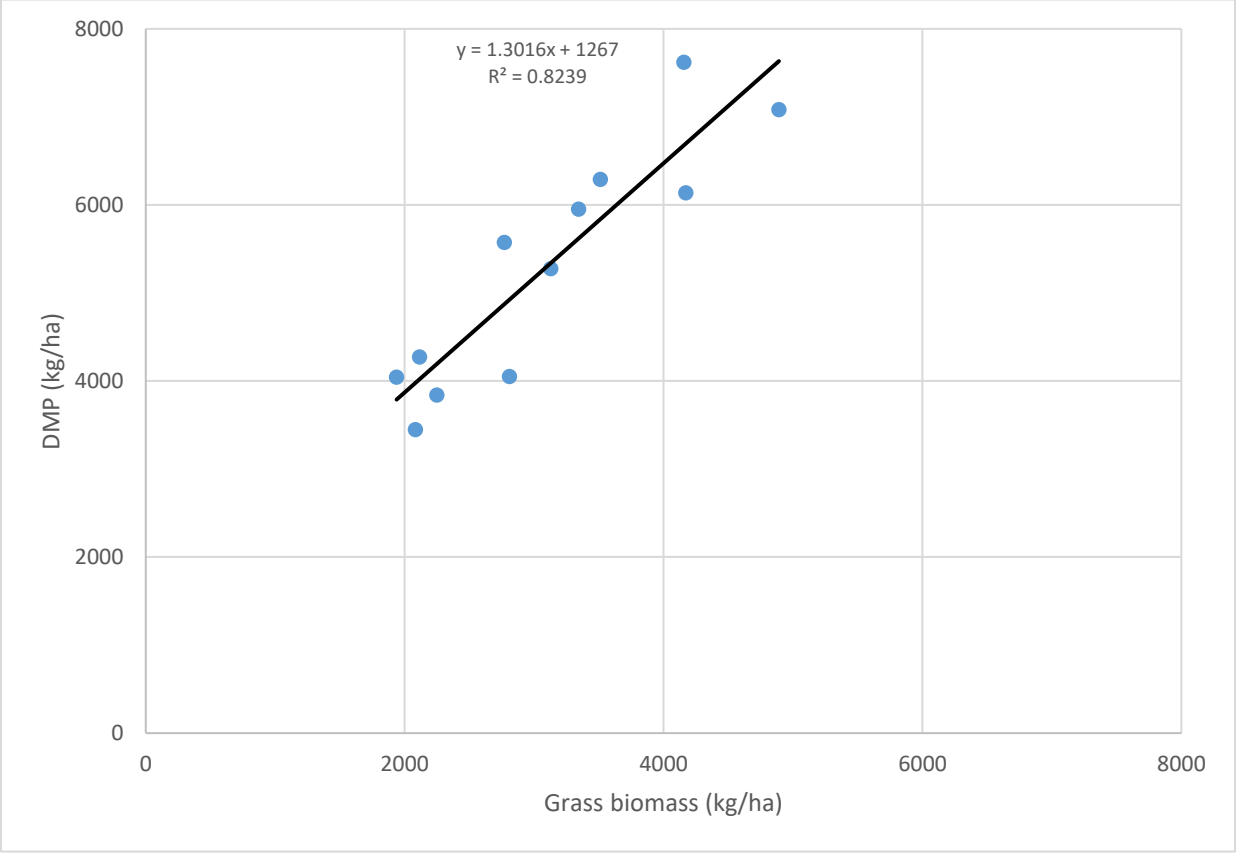

Figure 32: Relationship between average NDJFMA DMP and grass biomass for Mopane veld type (n=12). The x-axis shows grass biomass while the y-axis shows DMP.

The Lowveld shows a positive R^2 value of 0.41 (Figure 33) and is located in the south eastern parts of the province.

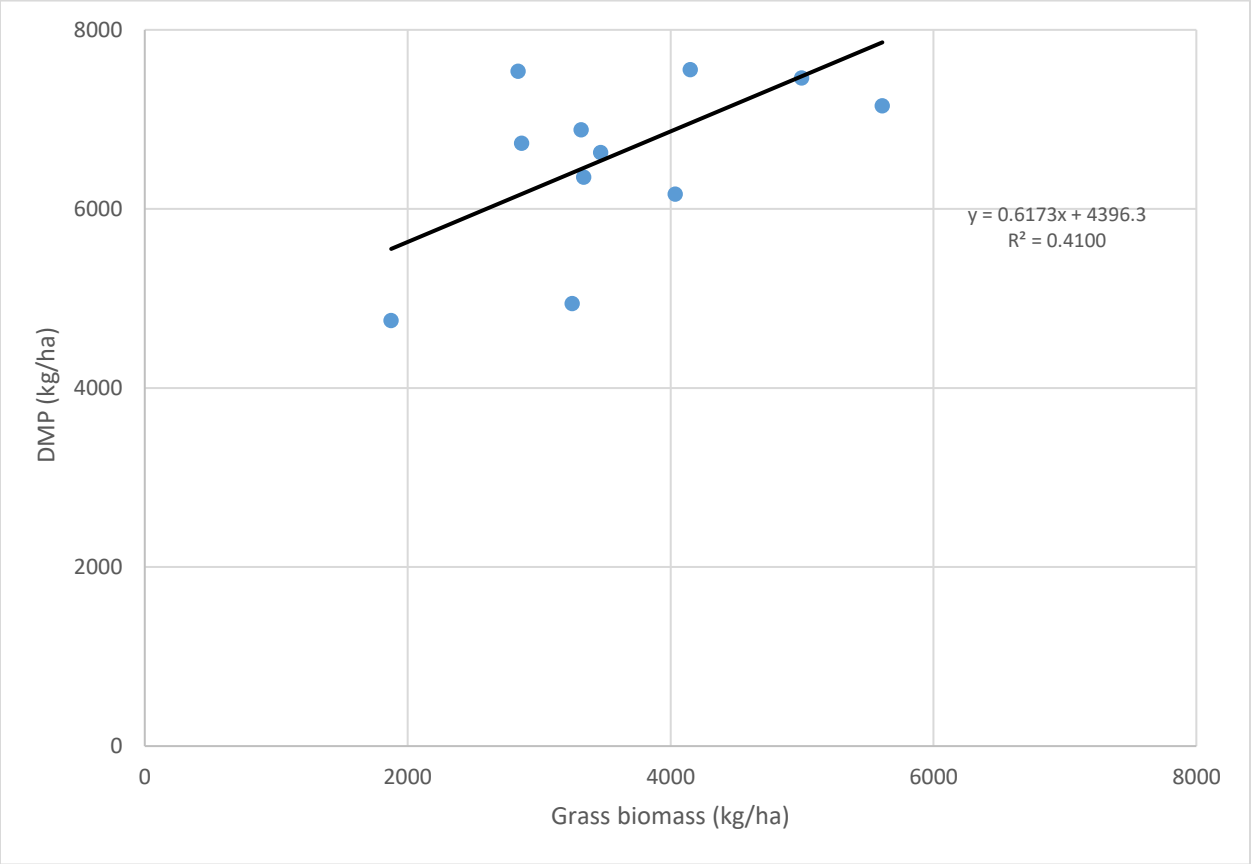

Figure 33: Relationship between average NDJFMA DMP and grass biomass for Lowveld veld type (n=11). The x-axis shows grass biomass while the y-axis shows DMP.

Figure 34 shows a low R^2 of 0.0001 for the Alluvial vegetation veld type. This shows that the DMP cannot distinguish the differences in grass biomass for this veld type. The Alluvial veld type is characterized by low grass biomass, as it is found on the northern borders of the Limpopo Province characterized by dry and warm conditions.

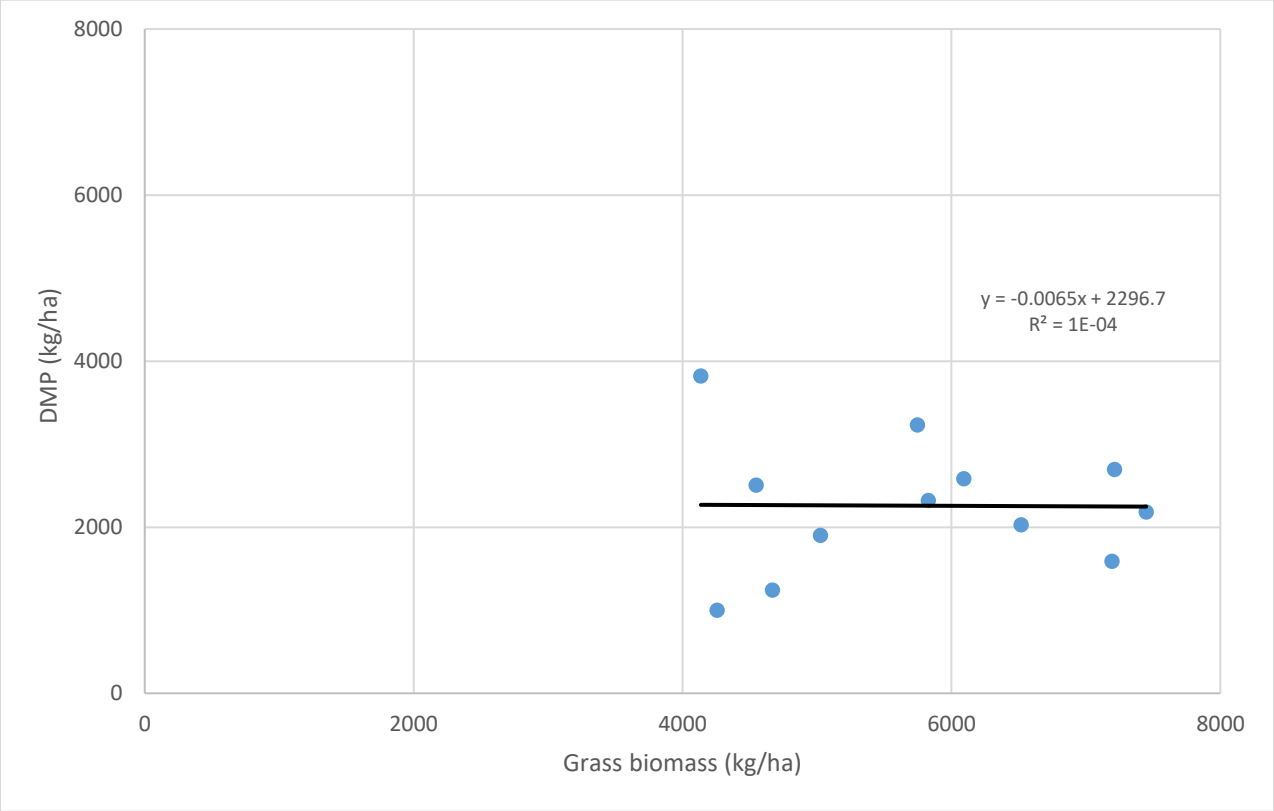

Figure 34: Relationship between average NDJFMA DMP and grass biomass for Alluvial veld type (n=12). The x-axis shows grass biomass while the y-axis shows DMP.

The Zonal and Intrazonal veld type is characterized by high grass biomass, therefore a high R^2 value of 0.70 (Figure 35).

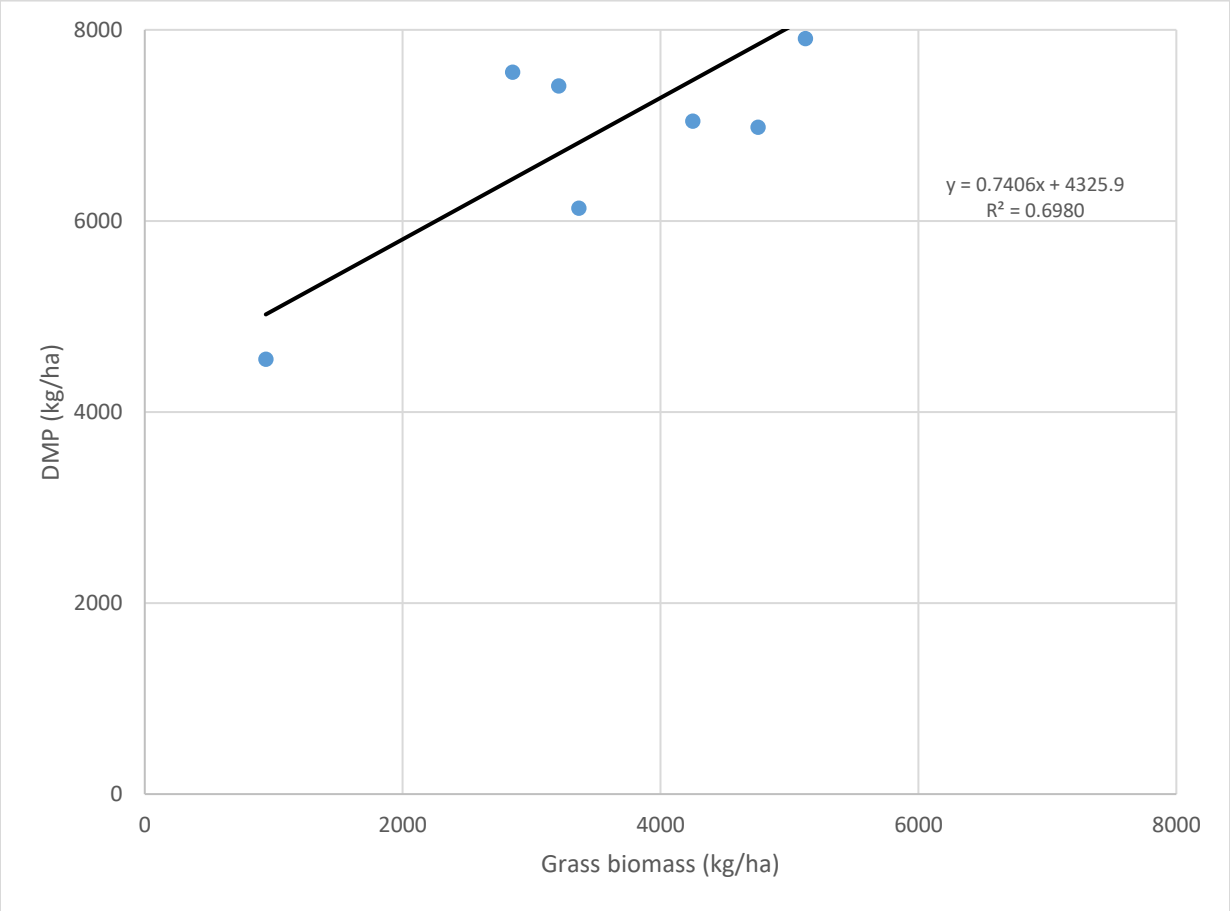

Figure 35: Relationship between average NDJFMA DMP and grass biomass for Zonal and Intrazonal veld type (n=7). The x-axis shows grass biomass while the y-axis shows DMP.

Figure 36 shows a positive R^2 value of 0.05, which is low. The Central bushveld type is characterized by woody vegetation where the Savanna shrubs are dominant. The low correlation between grass biomass and DMP could be affected by the high tree density in the area. The quality of RS imagery is possibly also negatively affected because this veld type lies in a mountainous region. Therefore, DMP should be used with caution for the central bushveld veld type as a representation.

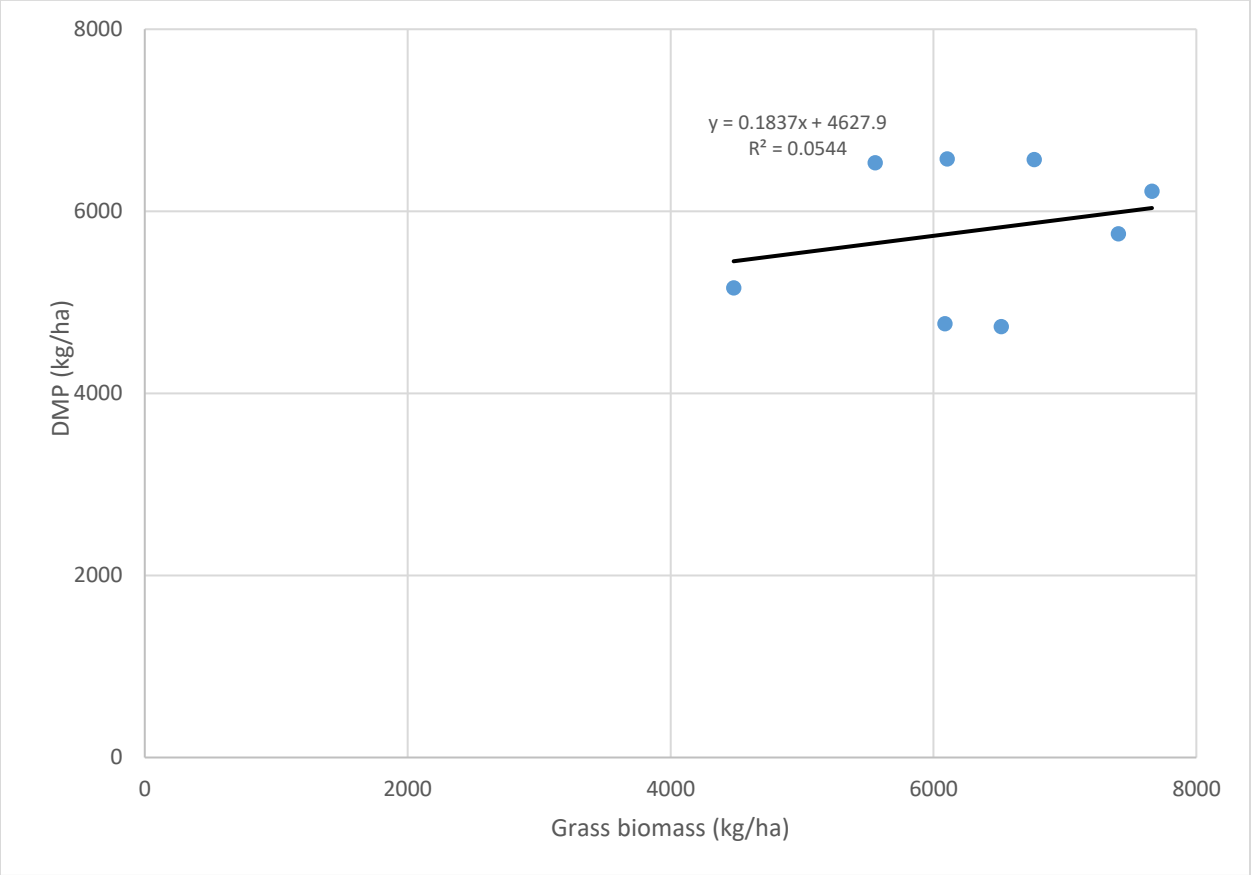

Figure 36: Relationship between average NDJFMA DMP and grass biomass for Central bushveld veld type (n=8). The x-axis shows grass biomass while the y-axis shows DMP.

The Azonal veld type shows a positively good relationship between grass biomass and DMP with R^2 value of 0.76 (Figure 37).

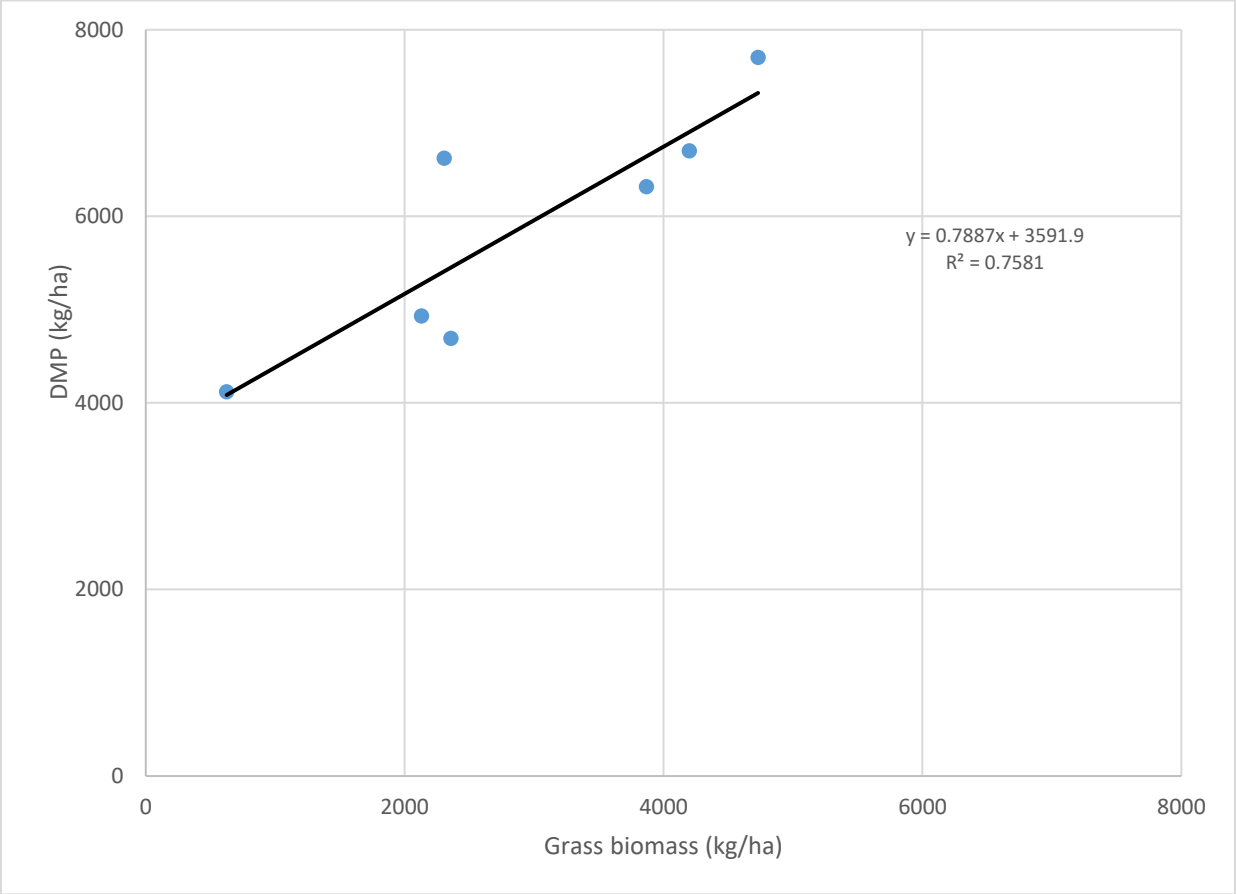

Figure 37: Relationship between average NDJFMA DMP and grass biomass for Azonal veld type (n=7). The x-axis shows grass biomass while the y-axis shows DMP.

4.3.3 Tree density product of 2003 analysis

The tree density product is used as a sublayer to obtain equations per respective veld type. Figures 38-43 show the linear relationship between DMP and grass biomass per tree density category.

In the Mopane veld type (Figure 38), a positive slope is seen in all tree density classes. Grass biomass and DMP show a good relationship. The latter could be attributed to low tree density in this veld type, thus no shadowing effect and less disturbance of the DMP signal. positive R^2 of 0.23 is seen in the medium tree density class, while a low R^2 of 0.09 is seen in the extremely high tree density. The Lowveld has a positive slope in all the classes (Figure 39). The highest R^2 value of 0.27 is seen in the low tree density class and the lowest R^2 value of 0.14 is seen at the high tree density class. Figure 40 shows the alluvial veld type, whereby a negative slope is seen in the 3 density classes. The highest R^2 of 0.15 is seen in the extremely high tree density class.

The Zonal and Intrazonal veld type (Figure 41) shows a positive slope in the 3 tree density classes. The highest R^2 value of 0.77 is seen in the high tree density class, while the lowest R^2 value of 0.41 is seen in the extremely high tree density class. For the Central bushveld type (Figure 42), very limited ground truthing data are available, thereby affecting the results. However, Central bushveld shows a negative slope for low tree density with an R^2 value of 0.01 and a positive slope for medium tree density class with an R^2 value of 0.11.

The Azonal veld type shows a positive slope for extremely high tree density with a high R^2 value of 0.76. (Figure 43). Tree density affects grass biomass growth (and DMP imagery). The graphs below show the relationship between grass biomass and DMP within each veld type, and these relationships differ, some show high R^2 values and others show low R^2 values.

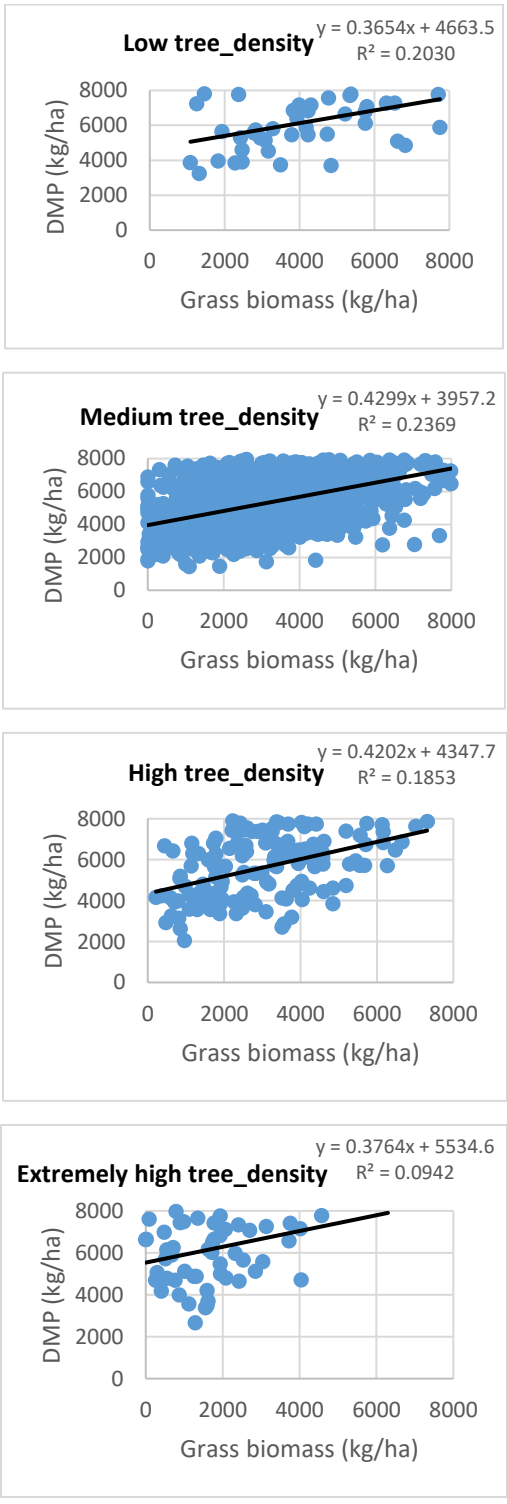

Figure 38: Relationship between grass biomass points and NDJFMA DMP from 1998/99-2009/10 according to various tree density classes for the Mopane veld type. The x-axis shows grass biomass while the y-axis shows DMP.

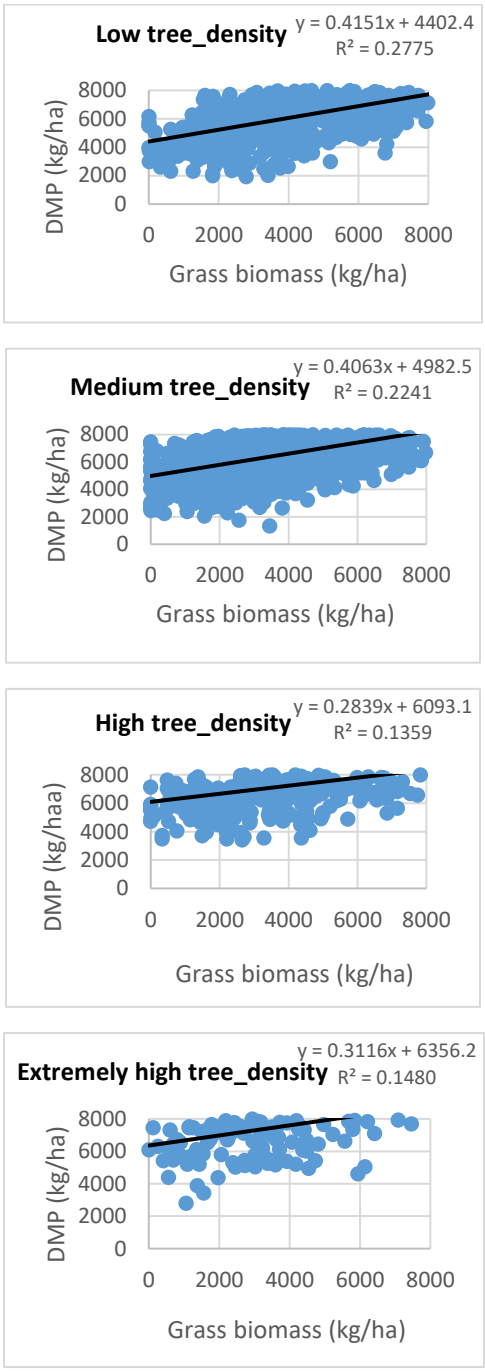

Figure 39: Relationship between grass biomass points and NDJFMA DMP from 1998/99-2009/10 according to various tree density classes for the Lowveld veld type. The x-axis shows grass biomass while the y-axis shows DMP.

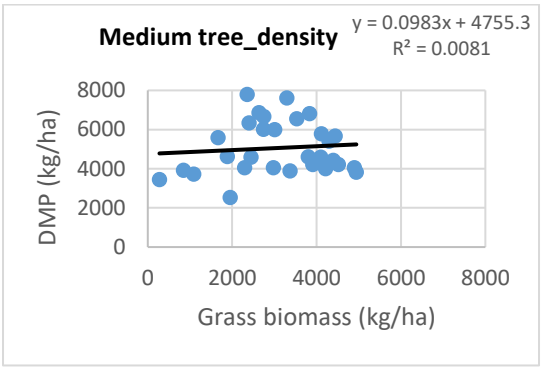

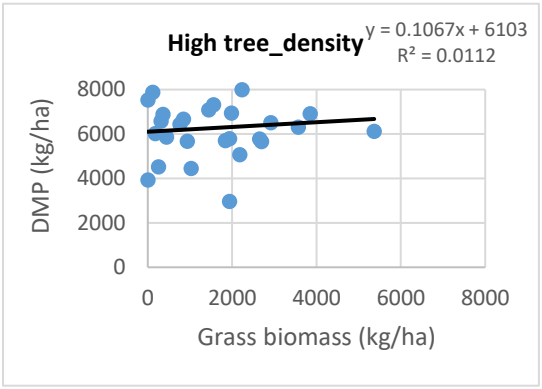

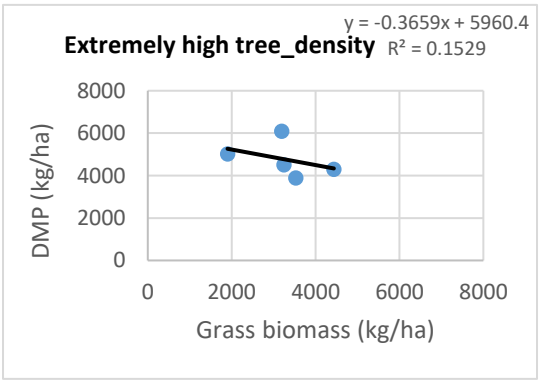

Figure 40: Relationship between grass biomass points and NDJFMA DMP from 1998/99-2009/10 according to various tree density classes for the Alluvial veld type. The x-axis shows grass biomass while the y-axis shows DMP.

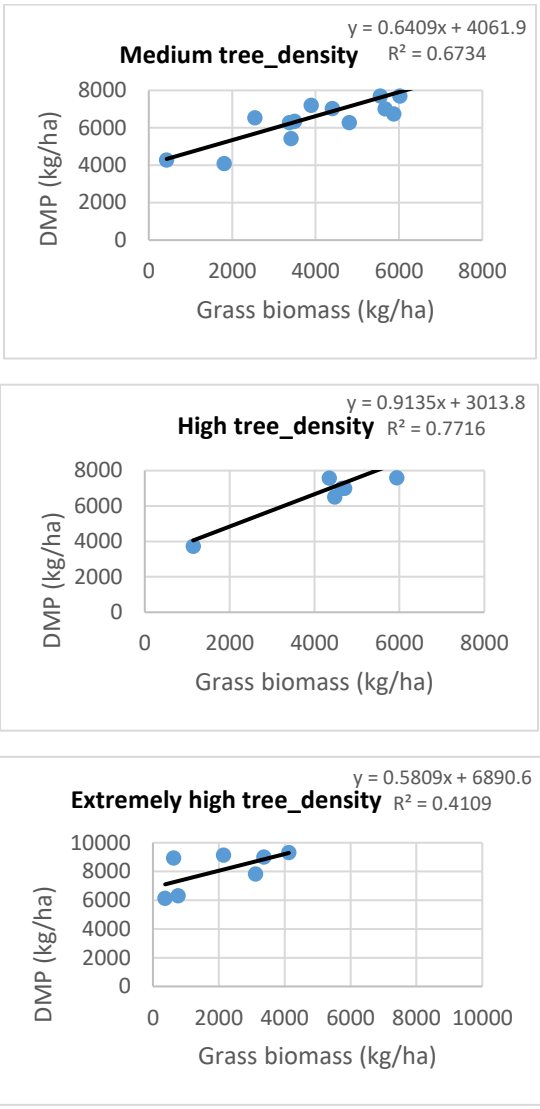

Figure 41: Relationship between grass biomass points and NDJFMA DMP from 1998/99-2009/10 according to various tree density classes for the Zonal and Intrazonal veld type. The x-axis shows grass biomass while the y-axis shows DMP.

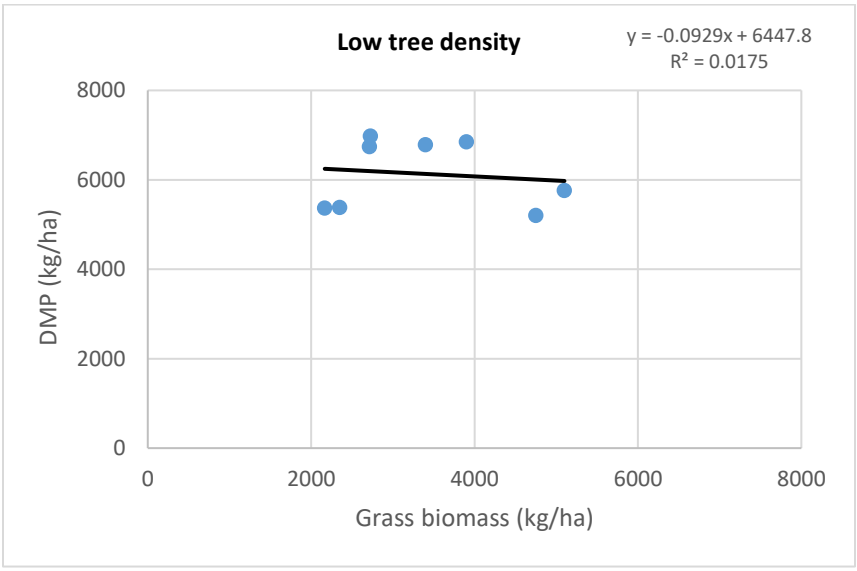

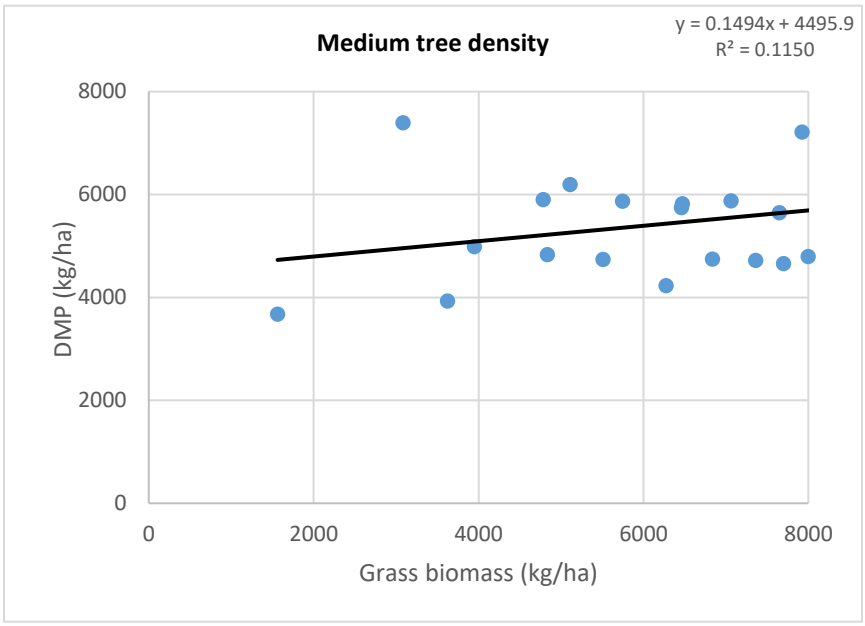

Figure 42: Relationship between grass biomass points and NDJFMA DMP from 1998/99-2009/10 according to various tree density classes for the Central bushveld veld type.

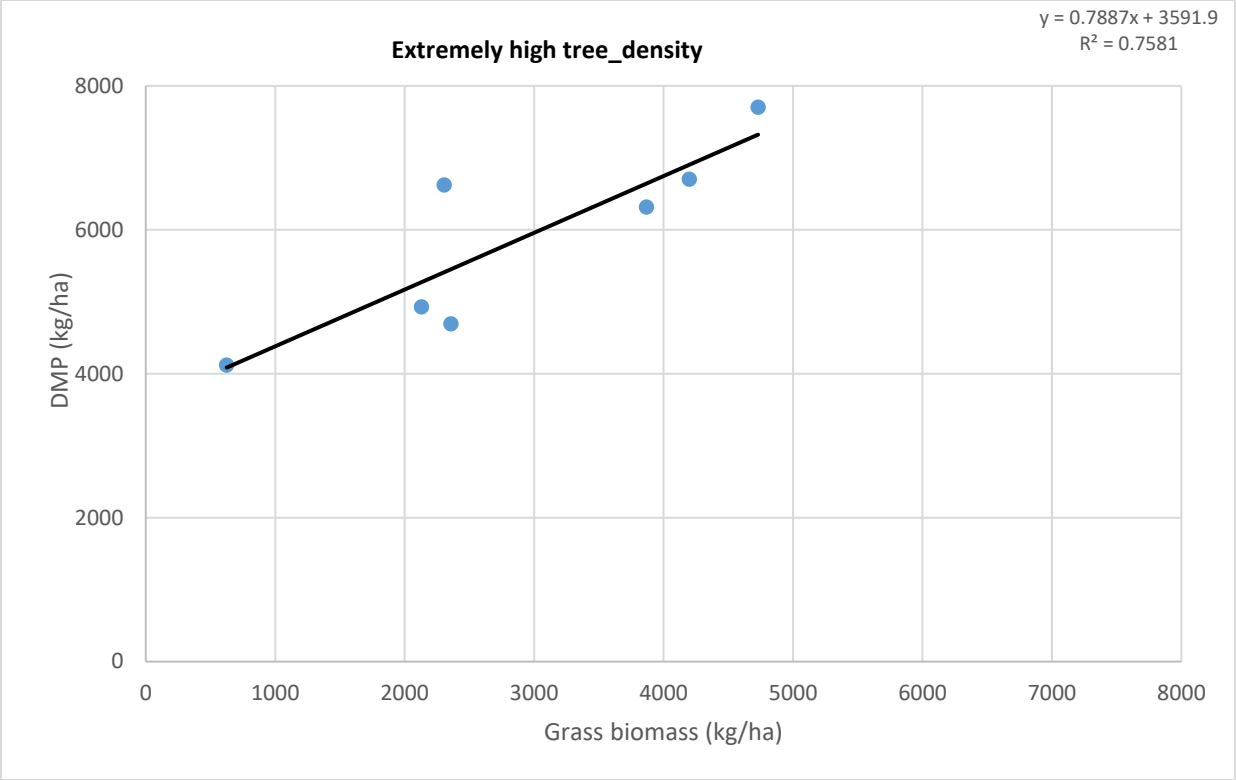

Figure 43: Relationship between grass biomass points and NDJFMA DMP from 1998/99-2009/10 according to various tree density classes for the Azonal veld. The x-axis shows grass biomass while the y-axis shows DMP.

4.4. Estimation of GC

Grass biomass is first estimated using the ERDAS software by building models. There is a strong relationship between rainfall and natural vegetation production hence these maps are interpreted relative to the influence of rainfall. The maps for 1998/99, 1999/00 and 2007/08 show high grass biomass in the Limpopo Province, a result of high rainfall during these years. Dry years such as 2002/03 and 2009/10 show very low grass biomass values. High correlation between field data and maximum DMP over the period of available data clearly indicates, that there is a strong relationship between biomass and GC. Figure 44 shows the output maps from ERDAS software which are later finalized in ArcMap.

Simplified GC maps for 1998/99-2009/10 are calculated (Figure 45). These maps show estimated GC in the Limpopo Province based on the relationship between GC and DMP, neglecting inputs such as palatability. It should be noted that good years are less than 2.0 ha/LSU and bad years are greater than 2.5 ha/LSU. The years with high GC are as follows:1998/99-except the western parts, 1999/00, 2007/08 and 2008/09-except eastern KNP. The years showing low GC are: 2002/03 (large areas in the north), 2003/04 (small areas), 2004/05, 2006/07 (north and east) and 2009/10 (all areas). Overall GC values are high for the Limpopo Province. El Niño years include 2002/03 and 2009/10, whilst La Niña years include 1998/99, 1999/00, 2000/01 and 2007/08. The following years: 2000/01, 2001/02, 2003/04, 2004/05, 2006/07 and 2008/09 are categorized as neutral years according to Oceanic Niño Index (ONI) table

(http://www.cpc.ncep.noaa.gov/products/analysis_monitoring/ensostuff/ensoyears.shtml). It is further emphasized that the dry (wet) years correspond with El Niño (La Niña) years.

The positive bias in the GC estimate may be related to the collection of grass biomass data using the Disc Pasture Meter method from the Kruger National Park – as the grass may include remnants of the previous growing season (Morgenthal, 2015: Personal communication). Furthermore, the period (1998/99-2009/10) during which the GC estimate is made for the current study is characterized by higher rainfall than the periods (reference to the 2005/1993) during which the earlier estimates were made. Moreover, the current study, is more focused on identifying potential deviations before summer than calculating the actual long-term mean – which may additionally be obtained over and above the current average estimate.

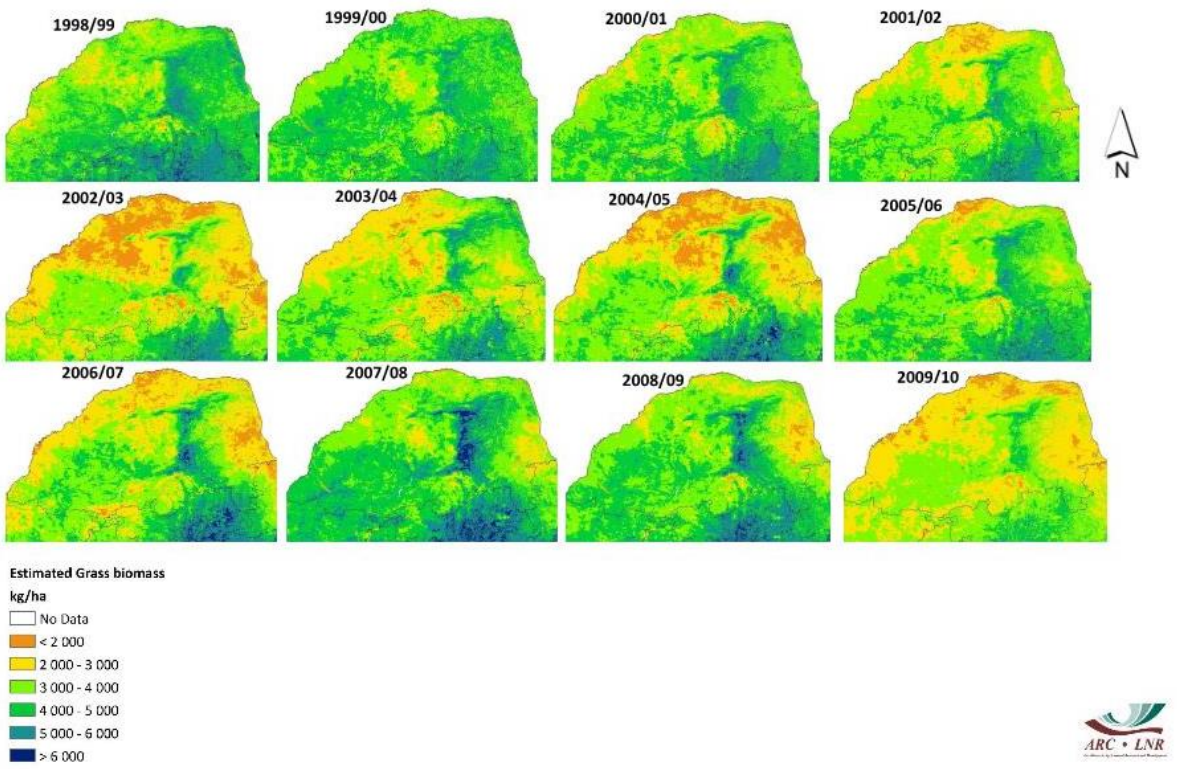

Figure 44: Grass biomass estimates per season for the 12-year period, 1998/99-2009/10 in the Limpopo Province.

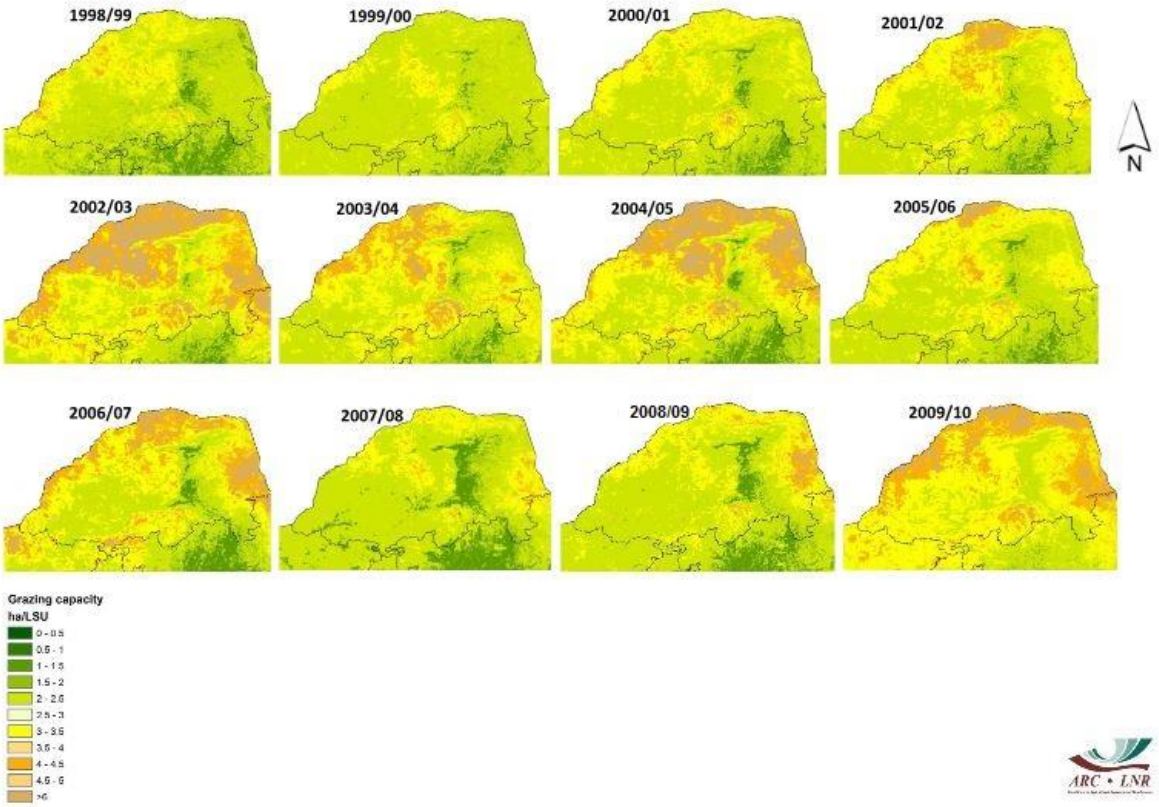

Figure 45: GC maps per season for the 12-year period,1998/99-2009/10 in the Limpopo Province.

Figure 46 shows that the coupled model's geopotential heights (850 hPa) predict GC over the Limpopo Province. These positive results therefore prove the prospect of updating the CC product monthly during the growing season in the Limpopo Province.

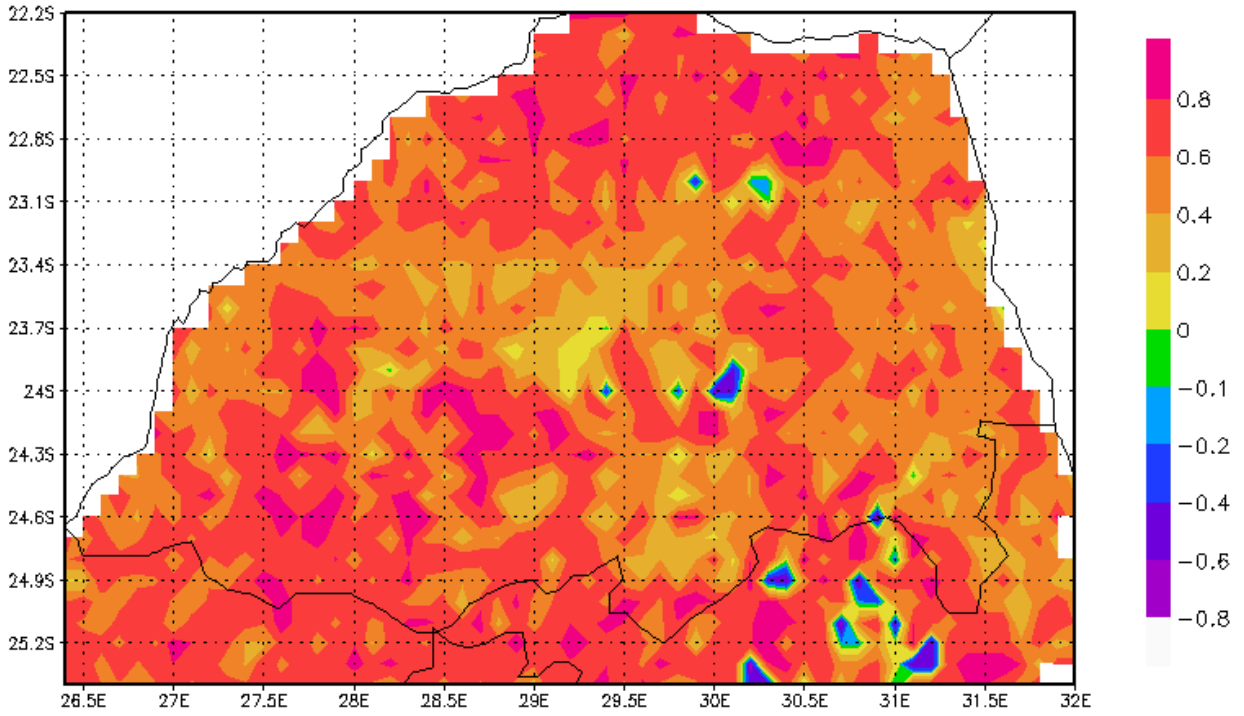

Figure 46: Spearman's rank correlations for the coupled model DJF 850 hPa geopotential heights downscaled to NDJFMA GC values over the Limpopo Province spanning the 12-year period.

The ROC diagram (Figure 47) shows both above- and below-normal ROC scores of 0.67, therefore there are high chances of above- and below-normal GC events occurring. ROC scores for near-normal GC conditions show a small chance of near-normal events occurring. Therefore, again the coupled DJF model shows good discrimination of the above- and below-normal GC seasons, but its discrimination of the near-normal GC seasons is poor.

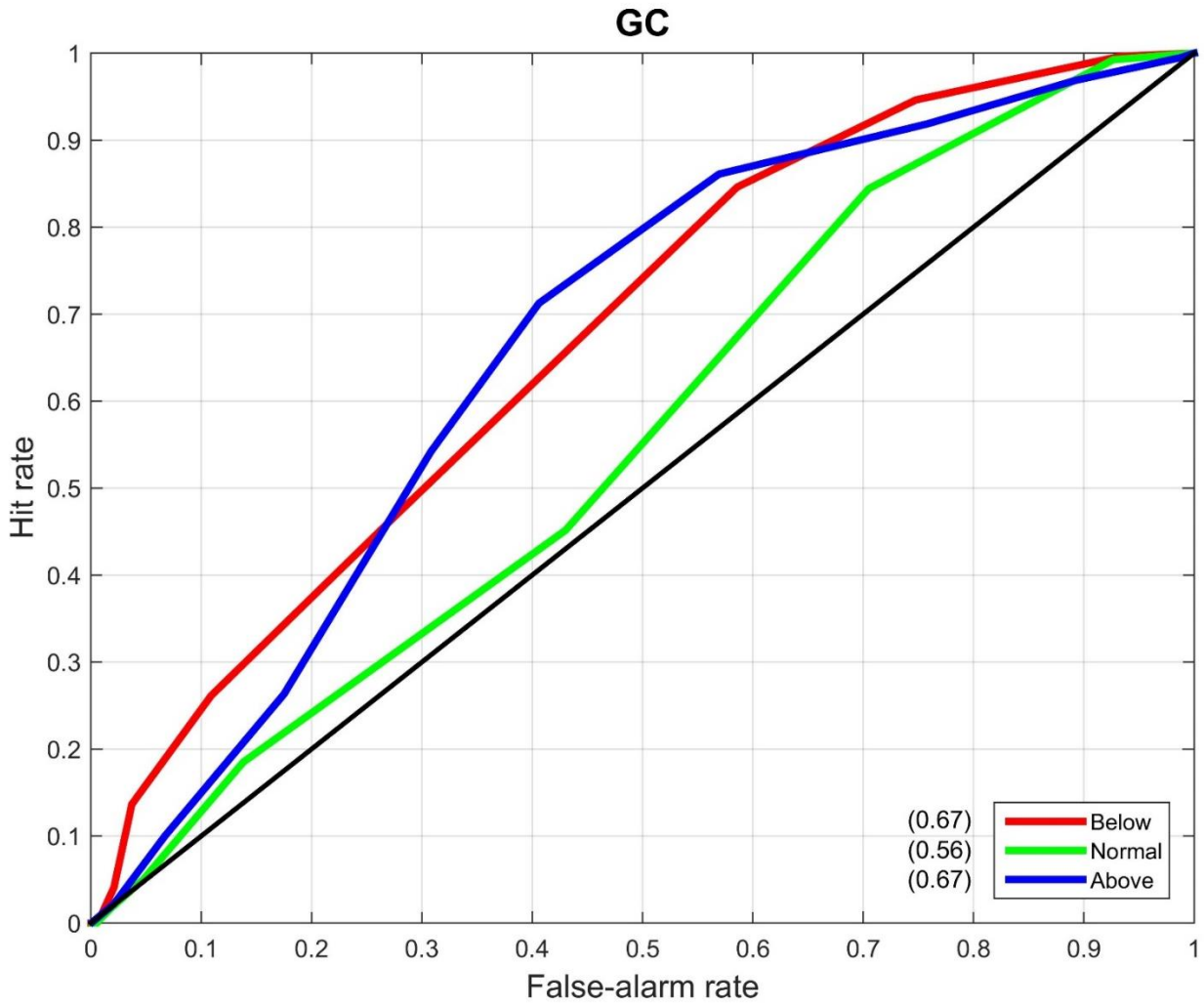

Figure 47: ROC curves obtained by retroactively predicting GC probabilistically over 12 years (1998/99–2009/10) for the NDJFMA season for above-, below- and near-normal tercile values of the climatological record. The areas underneath the respective curves are shown in parenthesis on the Figure. The x axis shows False-alarm rate, while the y axis shows Hit rate.

The reliability diagram (Figure 48) shows that during NDJFMA, the high GC regression line lies above the diagonal line showing underconfidence (56%), with a small portion (between 57-100%) showing over-confidence. However, the low GC regression line lies below the diagonal line which means that the forecasts are over-confident. The forecast probabilities for high GC seasons show higher reliability in the forecasts than those for low GC seasons during NDJFMA.

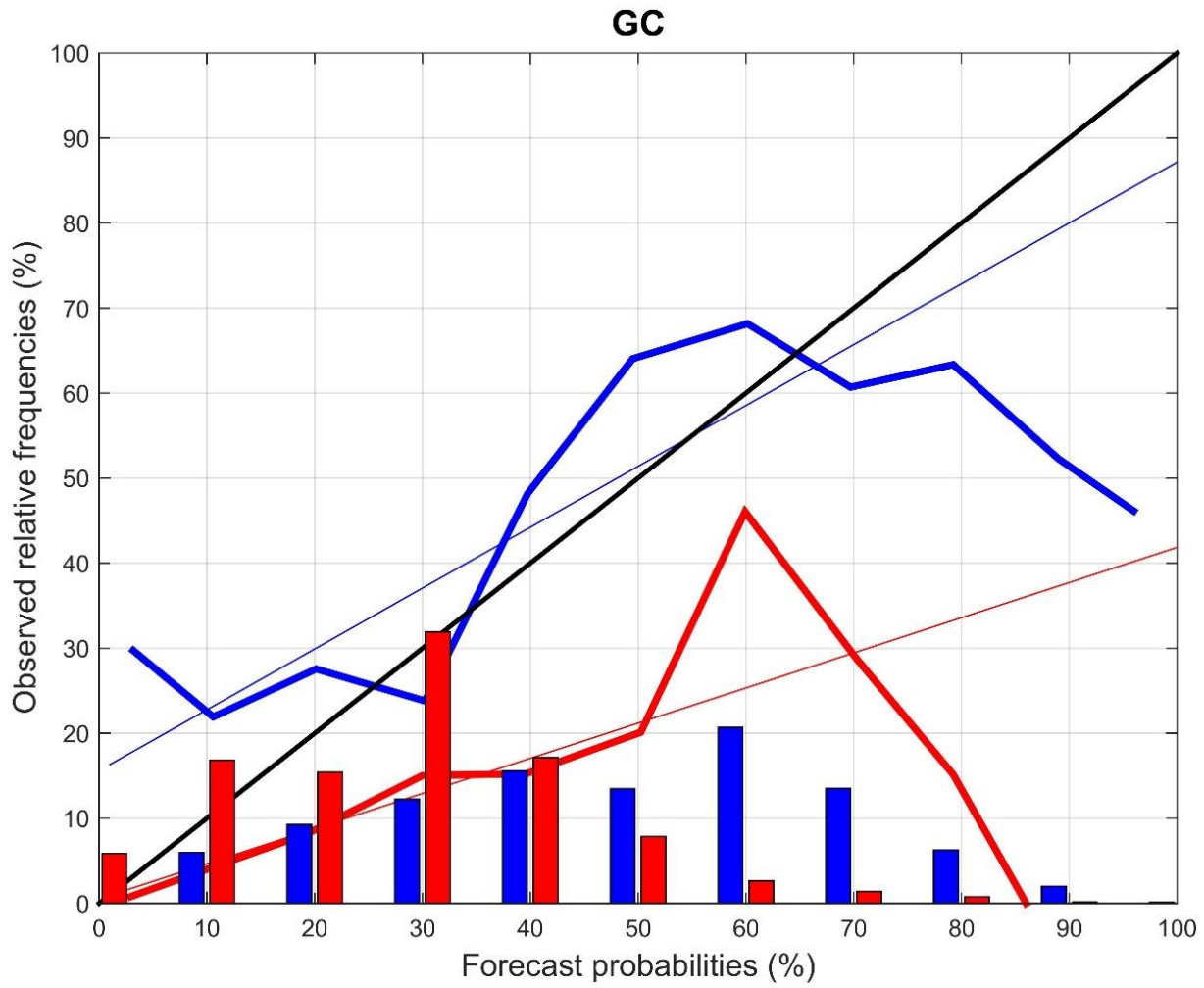

Figure 48: Reliability diagram and frequency histogram for above- (66th tercile) and below- (33rd tercile) normal GC values for NDJFMA obtained by downscaling the coupled model's low level circulation. The thick blue (red) curve and the blue (red) bars represent high (low) GC category. The thin blue (red) line is the weighted least squares regression line of the high (low) GC reliability curve.

4.5 Synopsis

This chapter shows results for all the products, data, and tools that are used to estimate GC in this dissertation. The CPT tool is used to run tests by analyzing correlation between the SPOT-VEGETATION DMP and coupled model rainfall or geopotential heights (850 hPa) data. The initial test is run using coupled model rainfall and DMP data where a positive correlation is found. Other variables are explored as predictors, namely coupled model low level circulation (850 hPa) data. Largely positive correlations are seen between coupled model rainfall and DMP as well as low level circulation and DMP for the central part of the Province. Four rainfall seasons are chosen after several tests are run using CPT namely; NDJ, DJF, JFM and FMA. Of these four 3-month seasons, DJF low level circulation season is shown to best predict the four DMP seasons i.e. NDJ, DJF, JFM and FMA. Verification tests are carried out using the ROC and reliability diagrams. The ROC diagrams show good skill in predicting NDJFMA DMP (and GC) by using DJF low level circulation data for the above- and below-normal DMP (and GC) seasons. A cumulative value for all the four 3-month seasons is also tested as a predictand, ultimately showing DJF low level circulation data to be the best predictor of NDJFMA DMP. Reliability diagrams show that the low DMP seasons are underconfident for the NDJ and JFM seasons, while over-confidence is shown for the DJF and FMA seasons, however for the NDJFMA season; underconfidence is seen for the high GC season while over-confidence is seen for the low GC seasons. Therefore, forecasts for both above- and below-normal conditions can be given out with confidence to farmers along with guidelines for grazing livestock.

Ground truth data are used in ArcMap along with EOS data to analyze the relationship between grass biomass and DMP data. Linear regressions are calculated giving a positive R^2 value of 0.75. The vegetation map product of 2009 product is used to stratify the field data into 6 veld types in the Limpopo Province as follows: Mopane, Lowveld, Azonal, Alluvial, Zonal and Intrazonal and Central bushveld type. Subsequently, the tree density product is used to categorize the data into low, medium, high tree density and extremely high tree density in order to obtain equations per respective veld type. These equations would enable the estimation of CC per veld type with simplicity as GC differs in the different veld types. In the ERDAS software, GC is estimated for the 12-year period (1998/99-2009/10). The last crucial step towards GC is estimating grass biomass by building GIS models. Further, GC is estimated using an equation expressed in ha/LSU and maps are subsequently drawn showing vegetation in different rainfall seasons spanning the 12-year period.

CHAPTER 5

CONCLUSIONS AND RECOMMENDATIONS

Livestock farming and ranching operations comprise a significant component of economic activity in the Limpopo Province with most of the farmers relying on rainfall for irrigation of livestock fodder. This semi-arid area experiences erratic summer rainfall, with a large effect on grass production. Mid-summer characteristics are a good estimate of how the entire rainfall season may behave for Limpopo Province. During dry years, grass production decreases, affecting livestock farming negatively (e.g. condition, morbidity, and probabilities for mortality) and sometimes necessitating the culling of animals, which has major impacts on rural livelihoods.

The motivation to have done this study in the first place is to assist the Limpopo Department of Agriculture (DOA) with management of rangelands and controlling of grazing on pastures by giving spatial and temporal guidelines on a seasonal to inter-annual basis. Seasonal forecasts (compiled from coupled global circulation model output) are employed to analyze the predictability of DMP over the Limpopo Province. These models can produce probabilistic forecasts for favourable or unfavourable grazing in order to advise farmers regarding the availability of pasture in the up-coming season.

It is crucial to have an estimate of GC and to know the deviation from the capacity prior to and during a growing season. The processes involved in this study take into account parameters that influence forage production and its availability. Such information provided to all relevant parties can guide good management practices, supporting proactive adaptive management and provide alternatives in the decision making process. Where seasonal forecasts display sufficient skill, an opportunity is presented where monitoring data can be used in conjunction with such forecasts to make assumptions regarding expected deviations from a long-term mean GC.

In the CPT tool, CCA is used to run tests between the SPOT-VEGETATION DMP and coupled model rainfall data. The CCA is used to analyze correlation between these variables. The results show a positive correlation between coupled model rainfall and DMP data. Improved positive results are seen between coupled model low level circulation (850 hPa) data and DMP data. The following rainfall seasons: NDJ, DJF, JFM and FMA are chosen after several tests, however, DJF low level circulation is selected as the best predictor of the NDJFMA DMP season. ROC and reliability diagrams are used for forecast verification and the results show that CGCM has skill discriminating above- and below-normal GC seasons. Reliability of the probability forecasts is good, showing underconfidence for high GC and over-confidence for low GC seasons and thus

these results can be used to warn farmers of approaching high GC conditions usually characterized by wet (La Niña) seasons. Overall verification results show that forecasts can be issued out to the Limpopo Province farmers for both high and low GC conditions, however, low GC forecasts should be given with great caution.

The ground truth data are used to analyze the relationship between grass biomass and DMP data per veld type. A high R^2 value is seen when DMP is correlated with grass biomass for all the years and veld types combined and this shows a positive relationship between DMP and ground truth data. The following veld types; Mopane, Lowveld, Azonal, Alluvial, Zonal and Intrazonal and Central bushveld are delineated with the use of the vegetation map. The tree density product (in conjunction with the vegetation map) is used to obtain equations per respective veld type and this is achieved by categorizing the data into 4 classes, namely low, medium, high tree density and extremely high tree density. These classes are related to biomass because when there is low tree density, it is expected that grass biomass will be high as a result of less shading effects.

Finally, GC is estimated for the 12-year period (1998/99-2009/10) using ERDAS software where GC maps are drawn showing vegetation – mainly positive values – in different rainfall seasons spanning the 12-year period. The high positive GC values are attributed to the Disc Pasture Meter method (which is used to collect field data) because it focuses on grass length measurements, therefore this method can overestimate as it may include remnants from previous growing seasons. However, the CC anomalies are forecast for each year per growing season, which proves to give positive results.

The results further show that the DMP product can, with certain assumptions, be used as a proxy for grass biomass. In future, work will be done on a large scale where a GC product will be estimated for the SADC region using the same approach that is used in the current study. The main objectives of the current study (to update current CC products and create deviation maps from CC for several historical years with relevant data) have been achieved. The deviation from CC, as derived in this thesis, will play an important role in providing practical advice to livestock farmers in the Limpopo Province of South Africa.

A recent scenario would be the current 2015/16 strong El Niño, characterized by drought and heat stress conditions, that has negatively impacted the agricultural sector across South Africa with the following provinces: KwaZulu-Natal, North West, Free State, Limpopo and the Northern Cape classified as disaster areas (Department of Water and Sanitation Drought report, 2015). The costs for drought relief are an imminent setback to the country's finances, especially for the above

mentioned provinces. However, if the described CC system had been in place prior to the 2015/16 El Niño drought, agricultural advisories could have guided livestock farmers with precautionary measures and alternate management options to minimize loss and damage, as well as finding cost effective means of obtaining supplementary feed for livestock as well as reducing the size of livestock herds. CC would have been estimated by substituting the relevant inputs to estimate GC. The CC maps can as a result of this research be produced operationally and updated during a growing season.

The need for tailored forecasting in the agricultural sector should not be overlooked. The use of these forecasts with grazing management options can potentially assist in controlling overgrazing, resulting in sustainable veld maintenance. The ARC-ISCW is involved in the quarterly meeting of the National Agrometeorological Committee where, various monitoring and early-warning products and messages are assembled and combined into an advisory that is distributed through the Provincial DOA to the extension service structure.

This study is relevant in the Limpopo Province, however the uptake of modelling and seasonal forecasts by farmers and decision makers remains challenging. More effort needs to be channeled towards reaching out to farmers and communities by providing interactive training sessions focusing on seasonal forecasts and their use in agricultural production. Indigenous methods of weather forecasting and GC estimations are also interesting topics to investigate e.g. Zuma-Netshiukhwi *et al.* (2013). However, unavailability of documentation with regards to empirical methods, their implementation, results and/or verification remains a challenge. Finally, the technique may be improved by working from a more detailed baseline CC product.

For future studies, more field data (30 years or more) should be acquired, together with relevant satellite data, to allow for an optimal correlation time period. More field data could potentially yield improved results as there would be more data to be used for verification tests. Species composition is also a necessary branch to explore. Livestock graze on grasses according to palatability, hence more detailed maps would estimate GC considering those aspects. Skill in forecasting deviations from a simplified GC estimate is demonstrated. The estimates may be improved by taking such elements into account in future work, and serve to produce an updated new GC map, which can be used as the baseline for estimating current and expected deviations prior to and during future growing seasons.

Dry matter eaten by grazers and browsers could also be tackled separately in future studies, as the former feed on grass while the latter feed on twigs, shrubs and leaves from trees. This project

demonstrates the development of a tailored forecast, an avenue that should be explored in enhancing relevance of forecasts in agricultural production. Data analysis forms a crucial part of any research project. There are important factors to consider as far as data analysis is concerned and these include:

- Study area boundaries
- Biophysical factors
- Data sources
- Field data collection methods
- Instrumentation and calibration
- Tools and software packages
- Data quality control and model specifications
- Metadata

If attention is given to these factors mentioned above, all modelling work can be carried out more efficiently towards finding solutions that will benefit farmers and pastoralists in southern Africa.

REFERENCES

ACOCKS, J.P.H. (1988) Veld Types of South Africa. 3rd Edition. Memoirs of the Botanical Survey of South Africa **57**, 1-146. Government Printer, Pretoria.

ANYAMBA, A., TUCKER, C.J. and EASTMAN, J.R. (2001) NDVI anomaly patterns over Africa during the 1997/98 ENSO warm event. *International Journal of Remote Sensing* **22**, 1847-1859.

ARCHER, E.R.M. (2004) Beyond the "climate versus grazing" impasse: Using remote sensing to investigate the effects of grazing system choice on vegetation cover in the eastern Karoo. *Journal of Arid Environments* **57**, 381-408.

AZZALI, S. and MENENTI, M. (2000) Mapping vegetation-soil-climate complexes in southern Africa using temporal Fourier analysis of NOAA-AVHRR NDVI data. *International Journal of Remote Sensing* **21**, 973-996.

BARET, F. and GUYOT, G. (1991) Potentials and Limits of Vegetation Indices for LAI and APAR Assessment. *Remote Sensing of Environment* **35**, 161-173.

BARNSTON, A.G., LI, S., MASON, S.J., DEWITT, D.G., GODDARD, L. and GONG, X. (2010) Verification of the first 11 years or IRI's seasonal climate forecasts. *Journal of Applied Meteorology and Climatology* **49**, 493–520.

BARNSTON, A.G., TIPPET, M.K., L'HEUREUX, M.L., LI, S. and DEWITT, D.G. (2012) Skill of real-time seasonal ENSO model predictions during 2002-11: Is our capability increasing? *American Meteorological Society* **93**, 631-651.

BARTALEV, S.A., BELWARD, A.S., ERCHOV, D.V. and ISAEV, A.S. (2003) A new SPOT4-VEGETATION derived land cover map of Northern Eurasia. *International Journal of Remote Sensing* **24**, 1977-1982.

BECKER-RESHEF, I., VERMOTE, E. and JUSTICE, C. (2010) A generalized regression-based model for forecasting winter wheat yields in Kansas and Ukraine using MODIS data. *Remote Sensing of Environment* **114**, 1312-1323.

BENEDETTI, R. and ROSSINI, P. (1993) On the use of NDVI profiles as a tool for agricultural statistics: The case study of Wheat yield estimate and forecast in Emilia Romagna. *Remote Sensing of Environment* **45**, 311-326.

BEYE, G., NDIONE, J.A., NDIAYE, D.S., BA, T. and KA, A. (2007) Using remote sensing and GIS for agricultural and rangeland monitoring in Senegal. Poster, Centere de Suivi Ecoloque (CSE).

BUCKLE, C. (1996) Weather and Climate in Africa. Addison Wesley Longman, England.

CALVAO, T. and PALMEIRIM, J.M. (2004) Mapping Mediterranean scrub with satellite imagery: Biomass estimation and spectral behavior. *International Journal of Remote Sensing* **25**, 1-14.

CLIMATE PREDICTABILITY TOOL (CPT version 14.7.4 software). International Research Institute for Climate and Society. Available from: http://iri.columbia.edu/. [Accessed 10 March 2014].

De LEEUW P.N. and TOTHILL, J.C. (1990) The concept of rangeland carrying capacity in sub-Saharan Africa - myth or reality. *Pastoral Development Network* **29b**, 1-18.

DEPARTMENT OF AGRICULTURE, FORESTRY AND FISHERIES. THE CONSERVATION OF AGRICULTURAL RESOURCES ACT 43 OF 1983. Grazing capacity potential map (1993)

DEPARTMENT OF WATER AND SANITATION DROUGHT REPORT (2015). The October 2015 report on drought conditions across the country.

Available from: http://intranet.dwa.gov.za/what'snew. [Accessed 17 August 2016].

DI, L., RUNDQUIST, D.C. and HAN, L. (1994) Modeling relationships between NDVI and precipitation during vegetative growth cycles. *International Journal of Remote Sensing* **15**, 2121-2136.

DU, M., KAWASHIMA, S., YONEMURA, S., ZHANG, X. and CHEN, S. (2004) Mutual influence between human activities and climate change in the Tibetan Plateau during recent years. *Global and Planetary Change* **41**, 241-249.

Earth Resources Data Analysis System–IMAGINE (ERDAS version 14.00) software. Available from: http://www.hexagongeospatial.com/. [Accessed 26 August 2014].

ENDELEO Project (2009). Available from the VITO website: http://endeleo.vgt.vito.be. [Accessed 16 August 2015].

ENGELBRECHT, F.A., LANDMAN, W.A., ENGELBRECHT, C.J., LANDMAN, S., BOPAPE, M.M., ROUX, B., MCGREGOR, J.L. and THATCHEN, M. (2011) Multi-scale climate modelling over Southern Africa using a variable-resolution global model. *Water SA* **37**, 647-658.

EVANS, J. and GEERKEN, R. (2004) Discrimination between climate and human-induced dryland degradation. *Journal of Arid Environments* **57**, 535-554.

FLOMBAUM, P. and SALA, O.E. (2007) A non-destructive and rapid method to estimate biomass and aboveground net primary production in arid environments. *Journal of Arid Environments* **69**, 352-358.

FRASER, R.H., LI, Z. and LANDRY, R. (2000) SPOT VEGETATION for characterizing Boreal Forest Fires. *International Journal of Remote Sensing* **21**, 3525-3532.

FROST, C. (2006) Using spatial rainfall and products from the MODIS sensor to improve an existing Maize yield estimation system. M.Sc. Thesis, University of Witwatersrand, Johannesburg.

FUNK, C. and BUDDE, M.E. (2009) Phenologically-tuned MODIS NDVI-based production anomaly estimates for Zimbabwe. *Remote Sensing of Environment* **113**, 115-125.

GALLO, K.P. and DAUGHTRY, C.S.T. (1987) Differences in Vegetation Indices for Simulated Landsat-5 MSS and TM, NOAA-9 AVHRR and SPOT-1 Sensor Systems. *Remote Sensing of Environment* **23**, 439-452.

GIBSON, D.J.D. (2006) Land degradation in the Limpopo Province, South Africa. M.Sc. Thesis, University of Witwatersrand, Johannesburg.

GODDARD, L., AITCHELLOUCHE, Y., BAETHGEN, W., DETTINGER, M., GRAHAM, R., HAYMAN, P., KADI, M., MARTÍNEZ, R., MEINKE, H. and CONRAD, E. (2010) Providing seasonal-to-interannual climate information for risk management and decision-making. *Procedia Environmental Sciences* **1**, 81-101.

GODDARD, L., BAETHGEN, W.E., BHOJWANI, H. and ROBERTSON, A.W. (2014) The International Research Institute for Climate & Society: why, what and how. *Earth Perspectives*, doi: 10.1186/2194-6434-1-10.

GOODCHILD, M.F. (1994) Integrating GIS and remote sensing for vegetation analysis and modeling: methodological issues. *Journal of Vegetation Science* **5**, 615-626.

GOETZ, S.J., PRINCE, S.D., GOWARD, S.N., THAWLEY, M.M. and SMALL, J. (1999) Satellite remote sensing of primary production: An improved production efficiency modelling approach. *Ecological modelling* **122**, 239-255.

GUEVARA, J.C., GRÜNWALDT, E.G., ESTEVES, O.R., BISIGATO, A.J., BLANCO, L.J., BIURRUN, F.N., FERRANDO, C.A., CHIRINO, C.C., MORICI, E., FERNÁNDEZ, B., ALLEGRETTI, L.I. and PASSERA, C.B. (2009) Range and livestock production in the Monte Desert, Argentina. *Journal of Arid Environments* **73**, 228-237.

HAIGH, T., TAKLE, E., ANDRESEN, J., WIDHALM, M., CARLTON, J.S. and ANGEL, J. (2015) Mapping the decision points and climate information use of agricultural producers across the U.S. Corn Belt. *Climate Risk Management* **7**, 20-30.

HAMILL, T.M. (1997) Reliability diagrams for multicategory probabilistic forecasts. *Weather and Forecasting* **12**, 736–741.

HAN, L., TSUNEKAWA, A., TSUBO, M. and ZHOU, W. (2013) An enhanced dust index for Asian dust detection with MODIS images. *International Journal of Remote Sensing* **34**, 6484-6495.

HANSEN, M.C., TOWNSHEND, J.R.G., CARROLL, M., DIMICELI, C. and SOHLBERG, R.A. (2003) Global percent tree cover at a spatial resolution of 500 Meters: First results of the MODIS vegetation continuous fields algorithm. *Earth Interactions* **7**, 1-15.

HANSON, C.L., MORRIS, R.P. and WIGHT, J.R. (1983) Using precipitation to predict range Herbage production in southwestern Idaho. *Journal of Range Management* **36**, 766-770.

HAYES, M.J. and DECKER, W.L. (1998) Using satellite and real-time weather data to predict maize production. *International Journal of Biometeorology* **42**, 10-15.

HAYWARD, M.W., O'BRIEN, J., and KERLEY, G.I.H. (2007) Carrying capacity of large African predators: Predictions and tests. *Biological Conservation* **139**, 219-229.

HOFFMAN, M.T., TODD, S., NTSHONA, Z. and TURNER, S. (1999) Land degradation in South Africa. Unpublished Final report. National Botanical Institute, Cape Town.

HUNT, E.R., EVERITT, J.H., RITCHIE, J.C., MORAN, M.S., BOOTH, D.T., ANDERSON, G.L., CLARK, P.E. and SEYFRIED, M.S. (2003) Applications and research using remote sensing for rangeland management. *Journal of Photogrammetric Engineering and Remote Sensing* **69**, 675-693.

JIANLONG, L., TIANGANG, L. and QUANGONG, C. (1998) Estimating grassland yields using remote sensing and GIS technologies in China. *New Zealand Journal of Agricultural Research* **41**, 31-38.

JOSHI, C., De LEEUW, J. and VAN DUREN, I.C. (2004) Remote sensing and GIS applications for mapping and spatial modelling of invasive species. Proceedings of *International Society for Photogrammetry and Remote Sensing* **35**, B7.

KAMTHONKIAT, D., HONDA, K., TURRAL, H., TRIPATHI, N.K. and WUWONGSE, V. (2005) Discrimination of irrigated and rainfed rice in a tropical agricultural system using SPOT VEGETATION NDVI and rainfall data. *International Journal of Remote Sensing* **26**, 2527-2547.

KAWABATA, A., ICHII, K. and YAMAGUCHI, Y. (2001) Global monitoring of interannual changes in vegetation activities using NDVI and its relationship to temperature and rainfall. *International Journal of Remote Sensing* **22**, 1377-1382.

KURTZ, D.B., SCHELLBERG, J. and BRAUN, M. (2010) Ground and satellite based assessment of rangeland management in sub-tropical Argentina. *Applied Geography* **30**, 210-220.

LAMB, D.W. (2000) The use of qualitative airborne multispectral imaging for managing agricultural crops-a case study in south-eastern Australia. *Australian Journal of Experimental Agriculture* **40**, 725-738.

LANDMAN, W. (2014) How the International Research Institute for Climate and Society has contributed towards seasonal climate forecast modelling and operations in South Africa. *Earth Perspectives* **1:22**, 1-13.

LANDMAN, W.A. and BERAKI, A. (2012) Multi-model forecast skill for mid-summer rainfall over southern Africa. *International Journal of Climatology* **32**, 303-314.

LANDMAN, W.A., BERAKI, A., DEWITT, D. and LÖTTER, D. (2014) SST prediction methodologies and verification considerations for dynamical mid-summer rainfall forecasts for South Africa. *Water SA*, **40**, 615-622.

LANDMAN, W.A., DEWITT, D., LEE, D., BERAKI, A. and LÖTTER, D. (2012) Seasonal Rainfall Prediction Skill over South Africa: One-versus Two-Tiered Forecasting Systems. *American Meteorological Society* **27**, 489-501.

LANDMAN, W.A., KGATUKE, M., MBEDZI, M., BERAKI, A., BARTMAN, A. and du PIESANE, A. (2009) Performance comparison of some dynamical and empirical downscaling methods for

South Africa from a seasonal climate modelling perspective. *International Journal of Climatology* **29**, 1535-1549.

LECONTE, R. and BRISSETTE, F. (2004) Mapping near-surface soil moisture with RADARSAT1 synthetic aperture radar data. *Water Resources Research* **40**, 1-13.

MAP OF LIMPOPO PROVINCE. MEASURE Evaluation.

Available from http://www.mapsharing.org.za/. [Accessed 16 July 2014].

LUPO, F., REGINSTER, I. and LAMBIN, E.F. (2001) Monitoring land-cover changes in West Africa with SPOT Vegetation: impact of natural disasters in 1998-1999. *International Journal of Remote Sensing* **22**, 2633-2639.

MALHERBE, J., LANDMAN, W.A., OLIEVIER, C., SAKUMA, H. and LUO, J-J. (2014) Seasonal forecasts of the SINTEX-F coupled model applied to maize yield and streamflow estimates over north-eastern South Africa. *Meteorological Applications* **21**, 733-742.

MALHERBE, J. (2015) Product development envisaged by the ARC for the MESA project. Slideshow. Agricultural Research Council-Institute for Climate, Soil and Water, Pretoria. South Africa.

MARLETTO, V., ZINONI, F., CRISCULO, L., FONTANA, G., MARCHESI, MORGILLO, A., Van SOETENDAEL, M., CEOTTO, E. and ANDERSEN, U. (2004) Evaluation of downscaled DEMETER multi-model ensemble seasonal hindcasts in a northern Italy location by means of a model of wheat growth and soil water balance. *Tellus* **57A**, 488-497.

MARSH, S.S., WALSH, J.L., LEE, C.T., BECK, L.R. and HUTCHINSON, C.F. (1992) Comparison of multi-temporal NOAA-AVHRR and SPOT-XS satellite data for mapping land-cover dynamics in the west African Sahel. *International Journal of Remote Sensing* **13**, 2997-3016.

MASON, S.J., GODDARD, L., GRAHAM, N.E., YULAEVA, E., SUN, L. and ARKIN, P.A. (1999) The IRI Seasonal Climate Prediction System and the 1997/98 El Niño Event. *Bulletin of the American Meteorological Society* **80**, 1853-1873.

MASON, S.J. and GRAHAM, N.E. (1999) Conditional probabilities, relative operating characteristics, and relative operating levels. *Weather and Forecasting* **14**, 713–725.

MASON, S.J. and GRAHAM, N.E. (2002) Areas beneath the relative operating characteristics (ROC) and levels (ROL) curves: Statistical significance and interpretation. *Quartely Journal of the Royal Meteorological Society* **128**, 2145–2166.

MKHABELA, M.S., MKHABELA, M.S. and MASHININI, N.N. (2005) Early maize yield forecasting in the four agro-ecological regions of Swaziland using NDVI data derived from NOAA's AVHRR. *Agricultural and Forest Meteorology* **129**, 1-9.

MKHABELA, M.S., BULLOK, P., RAJ, S., WANG, S. and YANG, Y. (2011) Crop yield forecasting on the Canadian Prairies using MODIS NDVI data. *Agricultural and Forest Meteorology* **151**, 385-393.

Moderate Resolution Imaging Spectroradiometer Net Primary Productivity (MODIS NPP) Available from MODIS website http://modis.gsfc.nasa.gov/data/dataprod/dataproducts. Accessed [23 March 2015].

MOELETSI, M.E., MELLAART, E.A.R., MPANDELI, N.S. and HAMANDAWANA, H. (2013) The use of rainfall forecasts as a decision guide for small scale farming in Limpopo Province, South Africa. *Journal of Agricultural Education and Extension* **19**, 133-145.

MONTÈS, N. (2009) A non-destructive method to estimate biomass in arid environments: A comment on Flombaum and Sala (2007). *Journal of Arid Environments* **73**, 599-601.

MORAN, M.S., INOUE, Y. and BARNES, E.M. (1997) Opportunities and limitations for image-based remote sensing in precision crop management. *Remote Sensing of Environment* **61**, 319-346.

MORGENTHAL, T.L., NEWBY, T. SMITH, H.J.C. and PRETORIUS, D.J. (2004) Development and refinement of a Grazing Capacity Map for South Africa using NOAA (AVHHR) satellite derived data. Final Report No. GW/A/2004/66. Department of Agriculture, Pretoria, South Africa.

MORGENTHAL, T.L. (2015) Personal communication: Discussions on reasons for high (positive) grazing capacity values in the Limpopo Province. Department of Agriculture, Pretoria, South Africa.

MURPHY, A.H. (1970) Predicted forage yield based on fall precipitation in California annual grasslands. *Journal of Range Management* **23**, 363-365.

MURPHY, A.H. (1993) What is a good forecast? An essay on the nature and goodness in weather forecasting. *American Meteorological Society* **8**, 281-293.

MYNENI, R.B., HOFFMAN, S., KNYAZIKHIN, Y., PRIVETTE, J.L., GLASSY, J., TIAN, Y., WANG, Y., SONG, X., ZHANG, Y., SMITH, G.R., LOTSCH, A., FRIEDL, M., MORISETTE, J.T., VOTAVA, P., NEMANI, R.R. and RUNNING, S.W. (2002) Global products of vegetation leaf area and

fraction absorbed PAR from year one of MODIS data. *Remote Sensing of Environment* **83**, 214-231.

NICHOLSON, S.E., DAVENPORT, M.L. and MALO, A.R. (1990) A comparison of the vegetation response to rainfall in the Sahel and east Africa, using Normalized Difference Vegetation Index from NOAA AVHRR. *Climatic Change* **17**, 209-241.

NICHOLSON, S.E., TUCKER, C.J. and BA, M.B. (1998) Desertification, drought, and vegetation: An example from the West African Sahel. *American Meteorological Society* **79**, 815-829.

NUTINI, F., STROPPIANA, D., BOSCHETTI, M., BRIVIO, P.A., BARTHOLOME, E. and BEYE, G. (2011) Evaluation of remotely sensed DMP product using multi-year field measurements of biomass in West Africa. Proceedings of SPIE 8174, *Remote Sensing for Agriculture, Ecosystems and Hydrology* **13***,* doi: 10.1117/12.898906.

PACHAVO, G. and MURWIRA, A. (2013) Land-use and land tenure explain spatial and temporal patterns in terrestrial net primary productivity (NPP) in Southern Africa. *Geocarto International*, doi: 10.1080/10106049.2013.837101.

PALMER, A.R. and BENNETT, J.E. (2013) Degradation of communal rangelands in South Africa: Towards an improved understanding to inform policy. *African Journal of Range and Forage Science* **30**, 57-63.

PALMER, A.R. and YUNUSA, I.A.M. (2011) Biomass production, evapotranspiration and water use efficiency of arid rangelands in the Northern Cape, South Africa. *Journal of Arid Environments* **75**, 1223-1227.

PAUDEL, K.P. and ANDERSEN, P. (2010) Assessing rangeland degradation using multi temporal satellite images and grazing pressure surface model in Upper Mustang, Trans Himalaya, Nepal. *Remote Sensing of Environment* **114**, 1845-1855.

PICKUP, G., BASTIN, G.N. and CHEWINGS, V.H. (1994) Remote-sensing-based condition assessment for nonequilibrium rangelands under large scale commercial grazing. *Ecological Applications* **4**, 497-517.

PICKUP, G., BASTIN, G.N. and CHEWINGS, V.H. (1998) Identifying trends in land degradation in non-equilibrium rangelands. *Journal of Applied Ecology* **35**, 365-377.

PRASAD, A. K., CHAI, L., SINGH, R. P. and KAFATOS, M. (2006) Crop yield estimation model for Iowa using remote sensing and surface parameters. *International Journal of Applied Earth Observation and Geoinformation* **8**, 26-33.

REYNOLDS, C.A., YITAYEW, M., SLACK, D.C., HUTCHINSON, C.F., HUETE, A. N. and PETERSEN, M.S. (2000) Estimating crop yields and production by integrating the FAO Crop Specific Water Balance model with real-time satellite data and ground-based ancillary data. *International Journal of Remote Sensing* **21**, 3487-3508.

RICHARD, Y. and POCCARD, L. (1998) A statistical study of NDVI sensitivity to seasonal and interannual rainfall variations in Southern Africa. *International Journal of Remote Sensing* **19**, 2907-2920.

ROBERTSON, A.W., BELL, M., COUSIN, R., CURTIS, A. and LI, S. (2013) Online tools for assessing the climatology and predictability of rainfall and temperature in the Indo-Gangetic plains based on observed datasets and seasonal forecast models. CGIAR Research Program on Climate Change, Agriculture and Food Security (CCAFS). Cali, Colombia: Working paper no. **27**, 1-24.

ROCKSTROM, J., KAUMBUTHO, P., MWALLEY, J., NZABI, A.W., TEMESGEN, M., MAWENYA, L., BARRON, J., MUTUA, J. and DAMGAARD-LARSEN, S. (2009) Conservation farming strategies in East and Southern Africa: Yields and rain water productivity from on-farm action research. *Soil and Tillage Research* **103**, 23-32.

ROE, E.M. (1997) Viewpoint: On rangeland carrying capacity. *Journal of Range Management* **50**, 467-472.

SCHULZE, R.S. and McGEE, O.S. (1978) Climatic indices and classifications in relation to the biogeography of southern Africa. *Biogeography and Ecology of Southern Africa* **31**, 19-52.

SEMENOV, M.A. and STRATONOVITCH, P. (2010) Use of multi-model ensembles from global climate models for assessment of climate change impacts. *Climate Research* **41**, 1-14.

SHIFTLET, T.N. and DIETZ, H.E. (1974) Relationship between precipitation and annual rangeland herbage production in southeastern Kansas. *Journal of Range Management* **27**, 272-276.

SILESHI, G., AKINNIFESI, F.K., AJAYI, O.C. and PLACE, F. (2008) Meta-analysis of maize yield response to woody and herbaceous legumes in sub-Saharan Africa. *Plant and Soil* **307**, 1-19.

SIVAKUMAR, M.V.K. (2006) Climate prediction and agriculture: Current status and future challenges. *Climate Research* **33**, 3-7.

SMOLIAK, S. (1956) Influence of climatic conditions on forage production of shortgrass rangeland. *Journal of Range Management* **9**, 89-91.

SMOLIAK, S. (1986) Influence of climatic conditions on production of Stipa-Bouteloua Prairie over a 50-year period. *Journal of Range Management* **39**, 100-103.

SPOT-VEGETAION DMP Available from PROBA-V website: http://proba-v.vgt.vito.be/. [Accessed 24 January 2014].

STROEBEL, A., SWANEPOEL, F.J.C., NTHAKHENI, N.D., NESAMVUNI, A.E. and TAYLOR, G. (2008) Benefits obtained from cattle by smallholder farmers: A case study of Limpopo Province, South Africa. *Australian Journal of Experimental Agriculture* **48**, 825-828.

TADROSS, M., HEWITSON, B.C. and USMAN, M.T. (2005) Interannual Variability of the Onset of the Maize growing season over South Africa and Zimbabwe. *American Meteorological Society* **18**, 3356-3372.

TADROSS, M., SUAREZ, P., LOTSCH, A., HACHIGONTA, S., MDOKA, M., UNGANAI, L., LUCIO, F., KAMDONYO, D. and MUCHINDA, M. (2009) Growing-season rainfall and scenarios of future change in southeast Africa: Implications for cultivating maize. *Climate Research* **40**, 147-161.

THORNTON, P.K., JONES, P.G., ERICKSEN, P.J. and CHALLINOR, A.J. (2011) Agriculture and food systems in sub-Saharan Africa in a 4°C+ world. *Philosophical Transactions of the Royal Society* **369**, 117-136.

TOWNSHEND, J.R.G. (1986) Analysis of the dynamics of African vegetation using normalized difference vegetation index. *International Journal of Remote Sensing* **7**, 1435-1445.

TOWNSHEND, J.R.G. (1992) Land cover. *International Journal of Remote Sensing* **13**, 1319-1328.

TROCCOLI, A., HARRISON, M., ANDERSON, D.L.T. and MASON, S.J. (2008) Seasonal climate: Forecasting and managing risk. *NATO Science Series on Earth and Environmental Sciences* **82**: Springer.

TROLLOPE, W.S.W., TROLLOPE, L.A. and BOSCH, O.J.H. (1990) Veld and pasture management terminology in southern Africa. *Journal of Grassland Society of Southern Africa* **7**, 52-61.

TSUBO, S., WALKER, S. and OGINDO, H.O. (2005) A simulation model of cereal-legume intercropping systems for semi-arid regions II. Model application. *Field Crops Research* **93**, 23-33.

TUCKER, C.J., PINZON, J.E., BROWN, M.E., SLAYBACK, D.A., PAK, E.W., MAHONEY, R., VERMOTE, E.F. and EL SALEOUS, N. (2005) An extended AVHRR 8-km NDVI dataset compatible with MODIS and SPOT vegetation NDVI data. *International Journal of Remote Sensing* **26**, 4485-4498.

Umlindi Newsletter, 2015. Umlindi report 201502. http://www.arc.agric.za. [Accessed 20 May 2015].

UNGANAI, L.S. and KOGAN, F.N. (1998) Drought monitoring and corn yield estimation in Southern Africa from AVHRR data. *Remote Sensing of Environment* **63**, 219-232.

VAN DEN DOOL, H.M. and TOTH, Z. (1991) Why do forecasts for near normal often fail? *Weather and Forecasting* **6**, 76–85.

VANDERPOST, C., RINGROSE, S., MATHESON, W. and ARNTZEN, J. (2011) Satellite based long term assessment of rangeland condition in semi-arid areas: An example from Botswana. *Journal of Arid Environments* **75**, 383-389.

VAN OUDTSHOORN, F. (1999) Guide to Grasses of Southern Africa Revised edition, Briza publications, Pretoria, South Africa.

VEGETATION MAP OF 2009. Available from South African National Biodiversity Institute (SANBI) website http://bgis.sanbi.org/vegmap/map.asp. [Accessed 16 September 2014].

VERDIN, J., FUNK, C., KLAVER, R. and ROBERTS, D. (1999) Exploring the correlation between Southern Africa NDVI and Pacific sea surface temperatures: Results for the 1998 maize growing season. *International Journal of Remote Sensing* **20**, 2117-2124.

VOGEL, C., KOCH, I. and VAN ZYL, K. (2010) "A Persistent Truth"-reflections on drought management in Southern Africa. *Weather, Climate & Society* **2**, 9-22.

WALKER, N.J. and SCHULZE, R.E. (2006) An assessment of sustainable maize production under different management and climate scenarios for smallholder agro-ecosystems in KwaZulu-Natal, South Africa. *Physics and Chemistry of the Earth* **31**, 995-1002.

WANG, J., RICH, P.M. and PRICE, K.P. (2003) Temporal responses of NDVI to precipitation and temperature in the central Great Plains, USA. *International Journal of Remote Sensing* **24**, 2345-2364.

WARDLOW, B.D., EGBERT, S.L. and KASTENS, J.H. (2007) Analysis of time-series MODIS 250m vegetation index data for crop classification in the U.S. Central Great Plains. *Journal of Remote Sensing of Environment* **108**, 290-310.

WESSELS, K.J., PRINCE, S.D., CARROLL, M. and MALHERBE, J. (2007a) Relevance of rangeland degradation in semiarid northeastern South Africa to the nonequilibrium theory. *Ecological Applications* **17**, 815-827.

WESSELS, K.J., PRINCE, S.D., MALHERBE, J., SMALL, J., FROST, P.E. and VAN ZYL, D. (2007b) Can human-induced land degradation be distinguished from the effects of rainfall variability? A case study in South Africa. *Journal of Arid Environments* **68**, 271-297.

WESSELS, K.J., PRINCE, S.D., ZAMBATIS, N., MACFADYEN, S., FROST, P.E. and VAN ZYL, D. (2006) Relationship between herbaceous biomass and 1 km^2 Advance Very High Resolution Radiometer (AVHRR) NDVI in Kruger National Park, South Africa. *International Journal of Remote Sensing* **27**, 951-973.

WESSELS, K.J., VAN DEN BERGH, F. and SCHOLES, R.J. (2012) Limits to detectability of land degradation by trend analysis of vegetation index data. *Remote Sensing of Environment* **125**, 10-22.

WETTERHALL, F., WINSEMIUS, H.C., DUTRA E., WERNER, M. and PAPPENBERGER, E. (2015) Seasonal predictions of agro-meteorological drought indicators for the Limpopo basin. *Hydrology and Earth System Sciences* **19**, 2577-2586.

WIGHT, J.R., CLAYTON, L.H. and WHITMER, D. (1984) Using weather records with a forage production model to forecast range forage production. *Journal of Range Management* **37**, 3-6.

WILKS, D.S. (2006) Statistical Methods in the Atmospheric Sciences, (2nd edn). Academic Press: San Diego, CA.

WILKS, D.S. (2011) Statistical Methods in the Atmospheric Sciences (3rd edn). Academic Press: Amsterdam.

XIA, Y.Q. and SHAO, M.A. (2008) Soil water carrying capacity for vegetation: A hydrological and biogeochemical process model solution. *Ecological Modelling* **124**, 112-124.

XIAO, X., BOLES, S., LIU, J., ZHUANG, D. and LIU, M. (2002) Characterization of forest types in Northeastern China, using multi-temporal SPOT-4 VEGETATION sensor data. *Remote Sensing of Environment* **82**, 335-348.

XIAO, X., HOLLINGER, D., ABER, J., GOLTZ, M., DAVIDSON, E.A., ZHANG, Q. and MOORE III, B. (2004) Satellite-based modeling of gross primary production in an evergreen needleleaf forest. *Remote Sensing of Environment* **89**, 519-534.

XIE, Y., ZONGYAO, S. and YU, M. (2008) Remote sensing imagery in vegetation mapping: a review. *Journal of Plant Ecology* **1**, 9-23.

YOU, L., WOOD, S. and WOOD-SICHRA, U. (2009) Generating plausible crop distribution maps for Sub-Saharan Africa using a spatial disaggregated data fusion and optimization approach. *Agricultural Systems* **99**, 126-140.

ZAMBATIS, N., PJK ZACHARIAS, P.J.K., MORRIS, C.D. AND DERRY, J.F. (2006) Re-evaluation of the disc pasture meter calibration for the Kruger National Park, South Africa. *African Journal of Range and Forage Science* **23(2),** 1-13.

ZHANG, J., DONG, W., FU, C. and WU, L. (2003) The influence of vegetation cover on summer precipitation in China: A statistical analysis of NDVI and Climate Data. *Advances in Atmospheric Sciences* **20**, 1002-1006.

ZIERVOGEL, G., NEW, M., VAN GARDEREN, E.A., MIDGELY, G., TAYLOR, A., HAMANN, R., STUART-HILL, S., MYERS, J. and WARBUTON, M. (2014) Climate change impacts and adaptation in South Africa: Overview. *Wiley Interdisciplinary Reviews Climate Change*. doi:10.1002/wcc.295.

ZIKA, M. (2008) The global loss of net primary production resulting from human-induced soil degradation in dry lands. M.Sc. Thesis, University of Wien, Germany.

ZUMA-NETSHIUKHWI, G., STIGTER, K. and WALKER, S. (2013) Use of traditional weather/climate knowledge by farmers in the south-western Free State of South Africa: Agrometeorological learning by scientists. *Atmopshere* **4**, 383-410; doi:10.3390/atmos4040383.

APPENDIX 1

Stratification of data into various veld types with respect to tree density (%).

ID	Date	Site no	Grass Biomass (kg/ha)	Lon	Lat	NDJFMA DMP (kgDM/ha/day)	Veld types	Group ID	Tree density
436	1999	2407	2997	31.4700	-23.9200	69639	Mopane Bioregion	87	11
135	2000	1121	4939	31.2100	-23.3800	67335	Mopane Bioregion	87	17
27	2005	209	4580	31.3700	-25.4300	91378	Lowveld Bioregion	7	33
366	2009	3503	2448	31.2438	-23.0526	45819	Alluvial Vegetation	23	13
162	2007	2711	5867	31.4633	-22.9903	36448	Mopane Bioregion	87	7
57	2010	1708	4354	31.8313	-24.4241	38051	Lowveld Bioregion	7	0
472	2005	3406	1841	30.9900	-22.6600	40827	Zonal & Intrazonal forests	13	14
436	2006	2802	3869	31.2400	-22.4200	63185	Azonal forests	17	48